

DELTRONIC
SOLUTIONS

Delta 3D Printer

*Sponsored by the Cal Poly IME Department
Sponsor Representative: Dr. Jose Macedo*

June 2015

Supported by:



Senior Project Team:

Ram Santos
rfsantos@calpoly.edu

Justin James
jhjames@calpoly.edu

Taylor Chris
tchris@calpoly.edu

Stephen Marshall
smarsh01@calpoly.edu

Paul Maalouf
pmaalouf@calpoly.edu

Table of Contents

Introduction.....	1
Chapter 1: Background	2
3D Printer Parameters.....	3
Existing “\$50,000 Printers”	4
The Delta Mechanism.....	6
Feed Mechanisms and Extruders	9
Heating and Ventilation	10
Software	11
Chapter 2: Objectives.....	13
Sponsor Needs and Background.....	14
Problem Definition.....	14
Engineering Specifications.....	14
Chapter 3: Management Plan	17
Administrative Roles.....	18
Design Roles.....	18
Chapter 4: Concept Design	20
Overall Concept Design	21
Subsystem Design Process.....	23
Linear Motion System	24
Feed Mechanism and Extruder Head	30
Mechanical Links	34
Rod Ends	35
Structure Frame	37
Preliminary Concept.....	40

Chapter 5: Detail Design	42
Kinematics.....	43
Motor Selection	44
Mechanism Components.....	47
Heated Build Plate.....	50
Top and Bottom Plates	53
Enclosure	54
Extruder	56
Electronics Design.....	57
Thermal Expansion	61
Final Design Summary.....	61
Chapter 6: Manufacturing and Testing Plan	62
Manufacturing Plan.....	63
Testing Plan	64
Chapter 7: Manufacturing Details	66
Individual Components	67
Full Assembly	76
Chapter 8: Design Verification.....	81
Heated Bed Calibration	82
Extruder Testing	83
End Effector Positioning	84
Chapter 9: Conclusion.....	85
Engineering Project Expo	86
Recommendations.....	86
Operator's Manual.....	88

Appendix A: Supporting Analysis	89
Kinematics.....	90
HVAC Systems.....	98
Thermal expansion FEA.....	102
Appendix B: Code Documentation.....	109
Inverse Kinematics MATLAB Script	110
Machine Software	115
Appendix C: Other Figures and Tables	124
QFD House of Quality	125
Preliminary SolidWorks Model.....	126
Gantt Chart	127
Design Verification Plan and Report (DVP&R)	128
Final Budget.....	129
Electronics Wiring Schematic.....	130
Appendix D: Works Cited.....	131
Appendix E: Specification Sheets.....	136
Appendix F: Detail Drawings.....	143
Appendix G: Operator's Manual	151

List of Figures

Figure 1: ORD MH-3000	3
Figure 2: Kossel Mini	4
Figure 3: SeeMeCNC PartDaddy	4
Figure 4: Stratasys Dimension SST 100es	5
Figure 5: BigRep ONE	5
Figure 6: Stratasys Objet 30 Pro.....	5
Figure 7: 3D Systems Projet 3500 HDMax	6
Figure 8: Stratasys Eden 260V	6
Figure 9: Bosch Direct Drive delta robot	8
Figure 10: Rostock MAX v2	8
Figure 11: Simplified, enlarged conceptual diagram of fused deposition modeling	9
Figure 12: Conceptual diagram of the selective laser sintering process	9
Figure 13: Conceptual diagram of the stereolithography process.....	10
Figure 14: Conceptual diagram of the Objet PolyJet printing process	10
Figure 15: MSDS on ABS with fume inhalation passage highlighted	11
Figure 16: 3D printing delamination.....	11
Figure 17: 3D printing software chain.....	12
Figure 18: The mechanical design process	22
Figure 19: Concept model of linear slide and distal feed mechanisms	25
Figure 20: ETL long-travel linear slide by Newmark Systems	26
Figure 21: Ball screw ball recirculation mechanism.....	27
Figure 22: iselAutomation belt-driven slide.....	27
Figure 23: ServoBelt stage mechanism	28
Figure 24: Yaskawa SGT Sigma Trac	28

Figure 25: DGlass 3D proximal-style extruder	32
Figure 26: Distal-style extruder	32
Figure 27: Double-head extruder	33
Figure 28: Carbon fiber tubes and rods.....	35
Figure 29: Cardan joint	36
Figure 30: Traditional ball joint	36
Figure 31: Magnetic ball joints.....	36
Figure 32: Aluminum T-slot extrusion	38
Figure 33: Possible frame shapes for the linear slide mechanism.....	39
Figure 34: Distinction between forward and inverse kinematics.....	43
Figure 35: SolidWorks assembly of Bell-Everman ServoBelt Light linear slide.....	44
Figure 36: Move profile for motor sizing.....	46
Figure 37: SigmaSelect results.....	46
Figure 38: Torque-speed curve for Yaskawa SGMJV-02A*A servomotor	47
Figure 39: 12-cm vertical offset of linear slide.....	48
Figure 40: Configuration of chrome balls on ServoBelt Light carriage.....	48
Figure 41: KD-418 magnetic ball joint.....	49
Figure 42: SolidWorks render of extruder plate.....	50
Figure 43: SolidWorks render of whole extruder subassembly	50
Figure 44: Sketch of one-dimensional heat transfer system for heated build plate	52
Figure 45: Heating pad for build platform	53
Figure 46: Industrial fiberglass insulation.....	53
Figure 47: Bosch 60-mm T-slot extrusion	54
Figure 48: Hole pattern for T-slot and plates.....	54
Figure 49: Yield Lab charcoal filter	55

Figure 50: Micron 3DP "All Metal" extruder.....	56
Figure 51: Data processing from STL files	58
Figure 52: Circuit used to measure thermistor voltage drop	59
Figure 53: Plot of manufacturer data for extruder temperature calibration	60
Figure 54: IME department's hydraulic shear	67
Figure 55: Post-CNC extruder platform	68
Figure 56: Final assembly of extruder platform	68
Figure 57: Haas protective siding.....	69
Figure 58: Ladd Caine aligning the back edge of the underplate	69
Figure 59: Aligning and clamping the aluminum plate	70
Figure 60: Tooling used for the first plate.....	70
Figure 61: Center of plate and edge finder.....	70
Figure 62: The 4" fan holes being end-milled and the L-shaped datum slot.....	71
Figure 63: Fixture for arm assembly	72
Figure 64: Initial soda lime glass bed temperature test	73
Figure 65: Cracked soda lime glass.....	73
Figure 66: Initial orientation of motor.....	75
Figure 67: Repositioned motor.....	75
Figure 68: Yaskawa servomotor power plug	75
Figure 69: Bell-Everman linear slides attached to top and bottom plates	76
Figure 70: 4" ducting as seen from above	77
Figure 71: Ducts and 5" holes into cabinet	77
Figure 72: Fans mounted inside table.....	77
Figure 73: Control system and wiring	78
Figure 74: Loose extruder wiring.....	79

Figure 75: Extruder wiring in shrink tubing	79
Figure 76: Bed leveling mechanism.....	80
Figure 77: Close-up of a Z-bracket and plastic foot used to level the bed	80
Figure 78: Thermocouple wire taped to glass	82
Figure 79: Glass heat loss calibration.....	82
Figure 80: Dial indicator zip-tied to platform.....	84
Figure 81: The team with the final design and poster; from left to right— Stephen Marshall, Taylor Chris, Justin James, Ramon Santos, Paul Maalouf.....	86
Figure 82: Illustration of variable definitions for kinematics equations	91
Figure 83: Effective link definition.....	92
Figure 84: Contour plot of build volume.....	95
Figure 85: Mesh plot of build volume	96

List of Tables

Table 1: Formal engineering specifications.....	15
Table 2: Comparison of proposed specifications with current products	16
Table 3: Pros and cons of the rotational arm and linear slide delta mechanisms	21
Table 4: Pugh matrix for linear motion system selection	25
Table 5: Decision matrix for linear motion system selection	29
Table 6: Decision matrix for feed mechanism selection	31
Table 7: Decision matrix for proximal vs. distal feed mechanism selection	33
Table 8: Decision matrix for single- vs. double-nozzle extruder selection.....	34
Table 9: Pugh matrix for mechanical link selection.....	34
Table 10: Decision matrix for mechanism arm selection	35
Table 11: Decision matrix for joint selection	37
Table 12: Decision matrix for frame material selection	38
Table 13: Decision matrix for structure shape selection.....	39
Table 14: Summary of subsystem design decisions	41
Table 15: Selected final designs	61
Table 16: Key events and deadlines for ME senior design project	63
Table 17: Extruder calibration Trial 1	83
Table 18: Extruder calibration Trial 2	83
Table 19: Variable definitions for kinematics computations.....	90

Introduction

The Delta 3D Printer project is a 2014-2015 Cal Poly ME senior project sponsored by Dr. Jose Macedo, Professor and Department Chair of the Cal Poly IME Department; Yaskawa America, Inc., industry-leading producer of high-quality electronic drives and motors; and more recently Bell-Everman, Inc., producer of high-precision embedded motion systems.

The Delta 3D Printer project was conceived by Dr. Macedo as a collaboration between Cal Poly engineering and Yaskawa America. The servomotors used by the product will be donated by Yaskawa, with permission and guidance from Yaskawa senior development director Dr. Ed Nicolson.

In early December, Bell-Everman became involved with the project, agreeing to donate linear motion systems to establish a relationship with Cal Poly's engineering program. Mike Everman, CTO of Bell-Everman, is the designer of these systems and the main point of contact with this team.

The project follows the ME senior design project course syllabus and guidelines, under the direction of lab advisor Dr. Peter Schuster.

The Concept

Dr. Macedo created the project in order to obtain a 3D printer for the Cal Poly IME Department, collaborate with industry, and provide a valuable project to Cal Poly students. It was pitched to the fall 2014 ME senior project class alongside over 30 other projects.

The goal of the project, as specified by Dr. Macedo, is to design, build, and test a 3D printer for the IME Department that:

- Utilizes the delta robot mechanism
- Runs on Yaskawa servomotors
- Has performance comparable to that of 3D printers at or around \$50,000 in price
- Remains modifiable by future Cal Poly students and faculty

The Team

The team is named Deltronic Solutions and consists of the following five members:

- Ram Santos (ME)
- Justin James (ME)
- Taylor Chris (ME)
- Stephen Marshall (ME)
- Paul Maalouf (CPE)

The original team consisted of only the four ME students, as selected by the senior project advisors. During winter 2015, a computer engineering major was added to take the lead on the electronics and software elements of the project, due to unanticipated difficulty in those areas.

The Plan

As of the writing of this report, our work on this project is completed. The printer has been assembled and tested and was exhibited at the Cal Poly College of Engineering Project Expo on May 29, 2015.

This report is a year-long cumulative effort, whose purpose is to provide a detailed account of the design process from beginning to end, as well as to make recommendations for improvements to the machine to be made in the future.

CHAPTER 1: BACKGROUND

Introduction

The concept of additive manufacturing has existed since the early 1990s. In the past few years, however, interest in 3D printing as a method for fabricating high-performance mechanical parts has dramatically increased.

With sufficient developments in additive manufacturing technology, 3D printing may replace other methods such as casting for certain types of low-volume production.

3D Printer Parameters

A wide variety of 3D printers has become available on the market for home and industrial use. These printers vary greatly in accuracy, speed, print volume, print material, kinematics, and price.

Because our goal is to be competitive with \$50,000 printers, our first task was to quantify, with engineering specifications, what a “\$50,000 printer” is. Because the expected use of our 3D printer is to print plastic parts, we focused our research on 3D printers that use fused-deposition modeling to print plastic.

After examining alternatives, we've found that accuracy, speed, and build volume are the critical parameters in our product's value.

Accuracy

Of the printers we examined, the Stratasys Eden 260V has the greatest accuracy, at 20 μm in its high-accuracy setting (Stratasys). Other high-end printers from Stratasys, 3D Systems, and BigRep have accuracies of 25 to 100 μm .

The accuracy of a printer appears to be greatly affected by its material and print speed. Next

we will discuss typical print speeds for 3D printers in this price range.

Speed

Most high-end printer companies fail to specify the print speed of their printers, so we were only able to find useful speed data for some of our competition.

The Stratasys Objet 30 Pro is capable of printing at volumetric speeds of up to 112 cm^3/h (Newman). This printer will be discussed in further detail later in this section.

The highest linear print speed we encountered was that of the ORD MH-3000 printer, shown in Figure 1. It is allegedly capable of printing at 500 mm/s (3ders.org). However, we speculate that this listed speed is not the actual print speed but instead the maximum translational speed while not printing.

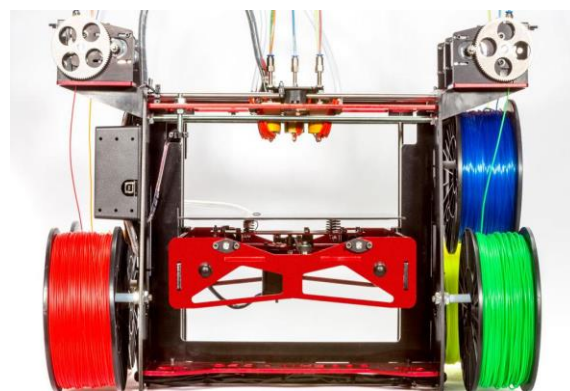


Figure 1: ORD MH-3000

(Source: ORD)

Print volume

Print volume varies most drastically of all specifications since there is a wide range of products that can be 3D printed. There is correlation between printer size and cost. However, printers with very large build volumes typically sacrifice accuracy. Even a

very small printer can be valued at \$50,000 if it is sufficiently fast or accurate or if it has other unique capabilities

It is therefore impossible to specify, with a single range of values, what the print volume of a \$50,000 3D printer is. We will instead discuss two existing printers with very different print volumes, not to set a target for our product, but to communicate how diverse the competition is.

The Kossel Mini, pictured in Figure 2, has a $6.7'' \times 6.7'' \times 9.4''$ build volume. The Kossel Mini is a hobbyist's tabletop 3D printer, whose components can be bought as a do-it-yourself kit for under \$100. This type of printer could be used to build small plastic toys, for example.



Figure 2: Kossel Mini
(Source: RepRap)

The PartDaddy, by SeeMeeCNC, is shown in Figure 3. It is 15 feet tall and has a build volume of $4' \times 4' \times 10'$. While not very precise, such a printer could be used to construct an entire piece of furniture in a single print. For

that application, precision is less important, as products can be shaped afterward.



Figure 3: SeeMeeCNC PartDaddy
(Source: DIY 3D Printing)

Existing “\$50,000 Printers”

Based on the above parameters, we chose five 3D printers to best define a \$50,000 printer:

- Stratasys Dimension SST 1200es
- BigRep ONE
- Stratasys Objet 30 Pro
- 3D Systems Projet 3500 HDMax
- Stratasys Eden 260V

These printers' prices range from \$36,500 to \$91,250. While this is a wide range, there are few printers on the market with prices on that order of magnitude.

Printers in this range tend to be more specialized, and their specifications vary greatly. Comparison between these printers indicates the sensitivity of price to variations in individual parameters. We synthesized the characteristics of these machines to develop our own parameters, which are specified later

in this report. The five chosen printers are described in detail below, in order of increasing price.

Stratasys Dimension SST 1200es

The Stratasys Dimension SST, pictured in Figure 4, is the cheapest of the five, valued at \$36,500 (MCAD).



*Figure 4: Stratasys Dimension SST 1200es
(Source: Stratasys)*

The Dimension SST has a print volume of $10'' \times 10'' \times 12''$. It has two main settings, one for speed and one for accuracy. The accuracy setting allows for a layer thickness of 178 μm and a print accuracy of 200 μm (Stratasys). Compared to the other printers we chose, the Dimension SST has inferior speed and accuracy. However, its ease of use and ability to print in a variety of colors are desirable characteristics.

BigRep ONE

The BigRep ONE, pictured in Figure 5, is priced at \$39,000. This printer is massive, with its build envelope outlined in the picture.



*Figure 5: BigRep ONE
(Source: BigRep)*

In inches, the volume is $41.7'' \times 42.1'' \times 43.5''$, making the BigRep ONE's print volume the largest of the five (3ders). It can also print very fast, at 150 mm/s . The BigRep ONE's 100- μm layer thickness and 100- μm accuracy are actually better than those of the smaller Dimension SST above, but the BigRep ONE is still inaccurate relative to others at this price. However, its large build envelope is its selling point and compensates well for its weaknesses in high-volume applications.



*Figure 6: Stratasys Objet 30 Pro
(Source: Stratasys)*

Stratasys Objet 30 Pro

The Stratasys Objet 30 Pro has the price the closest to \$50,000, with a price tag of \$42,900. It is shown in Figure 6.

The Object 30 Pro is capable of printing 28- μm layers and is accurate to 100 μm . It is a relatively compact printer, with a build volume of only 11.6" \times 7.6" \times 5.9" (MCAD). However, its small layer thickness allows for good surface finish. As previously mentioned, the Objet 30 Pro has the highest listed volumetric print rate, 112 cm^3/h , out of the printers we examined.

3D Systems Projet 3500 HDMax

The 3D Systems Projet 3500 HDMax, pictured in Figure 7, has a selling price of \$69,500. Although it is not apparent in the photo, the printer stands nearly six feet tall.



Figure 7: 3D Systems Projet 3500 HDMax
(Source: Aniwa)

The Projet 3500 HDMax has a build volume of 11.75" \times 7.3" \times 8", which is comparable to that of the Objet 30 Pro described above. Its relatively high price is due to its very high accuracy. It can print in three different layer thicknesses: 16 μm , 29 μm , and 36 μm . When set to a 16- μm layer thickness, the Projet 3500

HDMax is able to reach a printing accuracy as high as within 25 μm (Aniwa).

Stratasys Eden 260V

The Eden 260V is the third and most expensive Stratasys model we chose for comparison. It is shown in Figure 8 and costs \$91,250.

The Eden 260V's 20- μm accuracy makes it the most accurate of the five printers. It is able to print in either 16- μm layers or 30- μm layers (MCAD) and has a 10" \times 10" \times 7.9" print volume. The Eden 260V's specifications are very comparable to those of the Projet 3500 HDMax discussed above.



Figure 8: Stratasys Eden 260V
(Source: Stratasys)

The Delta Mechanism

The delta robot mechanism has been used for many applications since the 1980s, most notably for assembly line pick-and-place robots. More recently the delta mechanism has been used for 3D printers.

It is a sponsor-specified requirement that we use the delta robot mechanism in our design. Although we are not considering using a Cartesian mechanism, we will explain some important differences between these two main printing mechanisms.

Cartesian vs. delta

Each of the five printers discussed above employs a Cartesian mechanism. This means that the motions, or degrees of freedom, that determine the position of its end effector are along three orthogonal axes X , Y , and Z . Each of these motions is actuated by its own motor.

Figure 5, in the “Existing \$50,000 Printers” section above, shows how three Cartesian axes can define the position of the end effector. The four-sided horizontal carriage moves up the Z axis along the corners of the frame to position the print head vertically. A horizontal bar slides along the carriage, while the print head itself slides along this bar. This positions the print head in the horizontal XY plane.

One variation of this mechanism is one in which the print bed itself moves in the Z direction instead of the print head. This allows the XY carriage to remain stationary and can reduce the inertia of the system.

Cartesian mechanisms are *serial mechanisms*, meaning that the moving parts are connected in series with each other. The X and Y axes themselves do not remain stationary when the Z position changes, nor are they independent from each other. Each motion depends on the previous, and there is a lot of moving mass.

Because of their high amount of moving mass, Cartesian printers require more powerful motors to accelerate the mechanism’s inertia. One advantage of Cartesian robots, however, is that their kinematics are much simpler than those of delta robots. This means it is easier to program and can obtain higher accuracies more easily.

In contrast, the delta robot mechanism is a *parallel mechanism*. This means that each

motion occurs completely independently from the others. The delta mechanism uses three rigid arms to constrain its end effector to move in pure translation in 3D space. That is, it can move freely around the build envelope but cannot rotate. The lack of rotation is important because the print head must always be parallel to the work table for sufficient accuracy.

The delta robot is popular because it can attain higher speeds and larger movements while requiring very small motor inputs due to little inertia. The primary disadvantage of the delta mechanism is that its kinematics are complex, depending on trigonometric functions. It is therefore difficult to control its movements accurately. Even a task as simple as moving horizontally along the print bed requires input from all three motors.

There are two typical delta robot designs, the rotational arm mechanism and the linear slide mechanism. Each design is explained in further detail.

Rotational arm mechanism

The original delta robot used the rotational arm mechanism. It was invented in the early 1980s but did not see industrial use until the late 1990s. A modern example of a rotational arm delta robot, the Bosch Direct Drive robot, is shown in Figure 9.

The rotational arm mechanism uses three arms, each consisting of two links connected by an elbow joint. The three top links are attached to the top of the frame and directly actuated by a motor. The three bottom links are pinned to the tool and usually consist of two slender rods each. The tool is therefore pinned to six rods instead of three, which keep it parallel to the work surface. The Bosch Direct Drive delta robot is pictured in Figure 8.

Although it is not a 3D printer, it is an example of a rotational arm delta robot.



Figure 9: Bosch Direct Drive delta robot
(Source: RobAid)

The rotational arm variant is widely used in production line settings because the entire mechanism can be connected to the frame directly above the workspace.

The robot is typically not as powerful as the linear slide robot and is used mostly for picking and placing light objects. Due to direct actuation by the motors, the rotational arm mechanism is capable of faster speeds than the linear slide mechanism.

The kinematics governing the exact placement of the end effector are much more complex than those of the linear slide robot. Due to the circular-arc path taken by the elbow joint, its accuracy and speed vary with height. This mechanism is difficult to keep level, especially near the top of the build envelope. This is not a problem for pick-and-place robots but is a drawback for path-dependent operations such as 3D printing.

Linear slide mechanism

A newer variant of the delta robot employs the linear slide mechanism. One example of a

linear slide delta robot is the Rostock MAX v2, pictured in Figure 10.

This mechanism also uses two pairs of three rigid rods to move the tool around in space. However, these rods are not connected to another bar. Instead, they are connected to collars which slide along the three columns in the frame. Each collar's position is controlled by a separate motor.



Figure 10: Rostock MAX v2
(Source: SeeMeCNC)

The motors of the linear slide mechanism can be positioned at the bottom of the structure, helping to avoid top heavy design. This variant is also more powerful than the rotational arm mechanism and therefore able to move more mass. Because the links are not directly actuated, rotary motor motion must be transformed into linear motion, introducing a source of inaccuracy. The linear slide mechanism has always been more popular than the rotational arm mechanism in the 3D printing industry. This is due to superiority in path-dependent operations, independence of accuracy and speed on Z position, and relative ease of assembly.

Feed Mechanisms and Extruders

The term “3D printing” encompasses a wide variety of processes used to rapidly produce detailed parts from raw materials like plastic, metal, and even composites. The most common feed mechanisms are as follows:

- Fused-deposition modeling (FDM)
- Selective laser sintering (SLS)
- Stereolithography (SLA)
- PolyJet

Fused-deposition modeling is by far the most common method used in plastic-extruding 3D printers and the method most compatible with the delta mechanism. We will describe the other processes as well, albeit in less detail.

Fused-deposition modeling

Fused-deposition modeling (FDM) superheats and extrudes a plastic filament, typically acrylonitrile butadiene styrene (ABS) or polylactic acid (PLA). A diagram of the FDM process is shown in Figure 11.

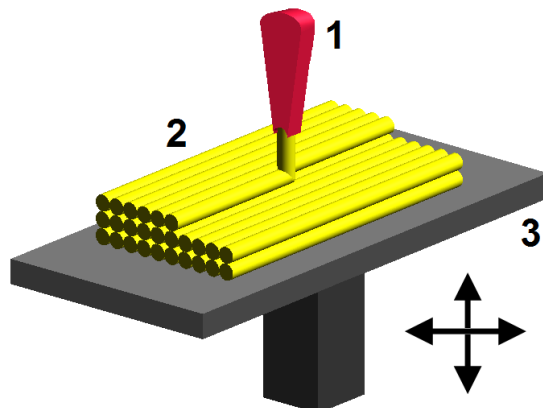


Figure 11: Simplified, enlarged conceptual diagram of fused deposition modeling
(Source: Wikipedia)

The plastic filament is driven through a heat exchanger using a powered gearing system. The melted plastic is then pushed through a nozzle, from which it flows onto a flat platform, or bed. The nozzle's motion parallel to the bed determines the shape of each layer. To form the next layer, either the nozzle is raised or the bed is lowered.

Different materials must be heated to different temperatures. For example, ABS is printed at about 215 °F, and PLA at about 170 °F.

Most nozzles accept 1.75-mm or 3-mm filament as input, since these are the most common sizes of ABS and PLA filament. Outputs vary more but are commonly in the range of 0.2 mm to 0.5 mm.

Selective laser sintering

Selective laser sintering (SLS) uses a fine powder as input instead of a spool of filament. It is the method typically used in the additive manufacturing of metal parts. The SLS process is shown in Figure 12.

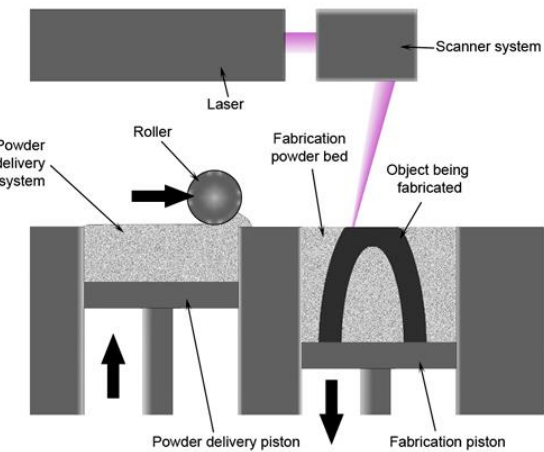
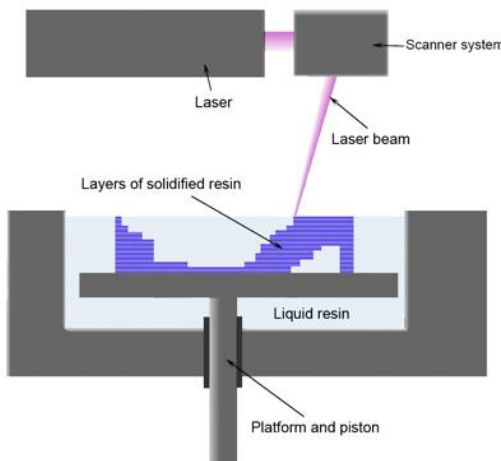


Figure 12: Conceptual diagram of the selective laser sintering process
(Source: Wikipedia)

First, a roller spreads a thin layer of powder across the bed. Then, a powerful laser melts regions of powder to form a layer of fused material. A scanning system focuses the laser to melt only a thin layer of material. The bed is then lowered and another layer of powder is rolled on top.

Stereolithography

Stereolithography (SLA) utilizes a bath of liquid photocurable resin. The SLA process is illustrated in Figure 13.



*Figure 13: Conceptual diagram of the stereolithography process
(Source: Wikipedia)*

A piston with a flat horizontal surface sits in the resin to support the structure being built. A laser or high-power UV light source is focused on certain regions, hardening it to form a layer of the product. The piston is then lowered to form the next layer.

PolyJet

PolyJet is the method employed by Stratasys Objet 3D printers. This technology is very similar to inkjet printing. Instead of ink, the jets spray photocurable resin. The layers are

cured one at a time in succession. A diagram of a PolyJet spray is shown in Figure 14.

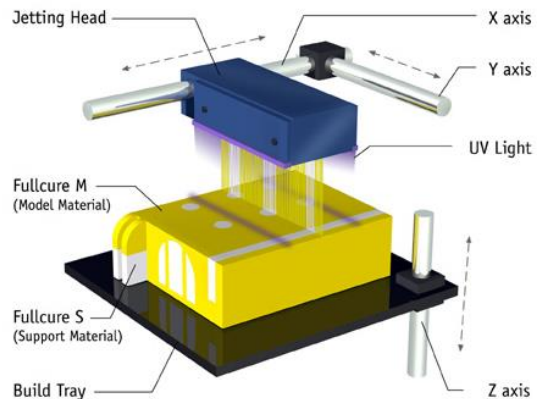


*Figure 14: Conceptual diagram of the Objet PolyJet printing process
(Source: Proto3000)*

Heating and Ventilation

Since many 3D printers print in plastic that produces toxic fumes when heated, they must be properly enclosed and possibly even ventilated to prevent harm. Because they must be able to melt the plastic, extrude it, and keep it hot, there is a lot of heat created within the enclosure. Regulation of the temperature within the enclosure is then important for both positioning and extrusion. This section discusses various problems that are related to thermal considerations.

Toxic fume ventilation

Some plastics release harmful fumes when melted. The most common plastic used in 3D printers is ABS, which expels acrylonitrile fumes during printing. These fumes carry an unpleasant odor and can be harmful at close proximity, as seen in Figure 15. Thus ABS printers are often enclosed, and the fumes are vented out. PLA, on the other hand, is harmless when melted and requires no enclosure.

HAZARDS IDENTIFICATION

Emergency Overview:

Solid pellets with slight or no odor. Spilled pellets create slipping hazard. Can burn in a fire creating dense toxic smoke. Molten plastic can cause severe thermal burns. Fumes produced during melt processing may cause eye, skin and respiratory tract irritation. Secondary operations, such as grinding, sanding or sawing, can produce dust which may present a respiratory hazard. Product in pellet form is unlikely to cause irritation.

Chronic/Carcinogenicity:

None of the components present in this material are listed by IARC, NTP, OSHA, or ACGIA as a carcinogen.

Figure 15: MSDS on ABS with fume inhalation passage highlighted

(Source: Edinburg Plastics)

Heated build plate

A common issue in 3D printing is the peeling of a part from the surface on which it is printed. This is caused by local cooling of the bottom layers of the printed part. The result is deformed and/or delaminated parts, as seen in Figure 16.

This is unacceptable performance for a high-end 3D printer. The most common solution to this issue is to use a build plate that is heated externally. There are no fully assembled heated build plates available in the size for our build volume. Thus, we will have to assemble one ourselves.

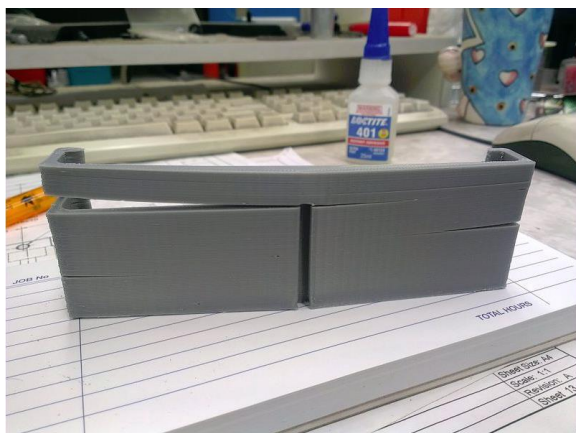


Figure 16: 3D printing delamination
(Source: RepRap)

Again, this problem arises when printing in ABS but not when printing in PLA. This is because the softening temperature of ABS is higher than that of PLA.

Temperature regulation

Adding heat to the system via the extruder, the motors, and possibly the heated build plate can lead to high temperatures throughout the enclosure. This can compromise some of the electronics contained inside and create pockets of thermal expansion, decreasing overall accuracy.

Software

The software involved in the 3D printing process is comprised of two basic parts. First, a slicer program converts a CAD model, typically an STL file, into machine G-code. Next, control software converts G-code into electrical pulses that move the motors. This process is outlined in Figure 17.

3D printers have varying degrees of software integration. Some are fully integrated, which means they can receive STL files and simply print the parts. The slicing and positional control is done internally. Others may require

carrying out intermediate steps on a separate device, such as a laptop or tablet.

Slicer software

Most 3D printer models under \$1,000 use open-source slicer software that is available for download on the Internet. The most widely used program to convert STL files to G-code is Slic3r. This software has options for speed, temperature, and feed control (Slic3r). There are similar programs such as Skeinforge, Cura, and Kisslicer, which are all available for free download online (Edutech).

Control software

Unlike slicer software, control software is usually designed for each specific printer

configuration and mechanism. Such software can be programmed onto a programmable logic controller (PLC) or a microcontroller. One way this can be achieved is by using Yaskawa's MotionWorks software, which is based on the industry standard IEC 61131 programming languages for PLCs.

There are open-source options for control software as well. The most popular of these is Repetier-Host, which was developed for the RepRap printing platform. There are also programs that combine the slicing and control software. Netfabb is one such package that is available for free online (Edutech). Higher-end printers make use of proprietary software that is integrated into the machine.

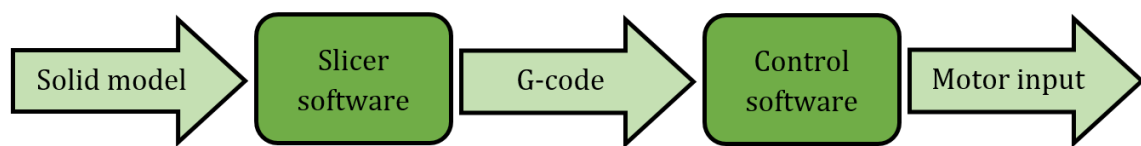


Figure 17: 3D printing software chain

CHAPTER 2: OBJECTIVES

Introduction

In this section we will explain in detail what the problem is and justify the need for this project. We will then explain how we converted the project requirements into quantifiable engineering specifications.

Sponsor Needs and Background

Cal Poly's IME department in the past has utilized two rapid prototype machines that were loaned. Now both machines' loans have expired, and the IME department lacks a 3D printer. It needs a cost-effective way to obtain another rapid prototype machine for educational use.

Dr. Macedo saw several opportunities in creating this project. First, it would be a great project and educational tool for us, the Cal Poly students who would have the privilege to work on it. Second, it would supply the IME department, not only with something that it can use and modify, but something that is homemade, by and for Cal Poly students. Third, it would provide a means to strengthen the connection between Cal Poly's IME department and Yaskawa, which recently sponsored the Automatic Foosball Table senior project.

Problem Definition

The Cal Poly IME Department currently lacks 3D printers. Dr. Macedo, head of the IME department, seeks to acquire a 3D printer, so that students and faculty can benefit from and modify it in the future.

Yaskawa America, Inc., is willing to donate electronic components because it would like

to have a good relationship with Cal Poly and its engineering departments.

By the end of this academic year, the IME department will have a functioning 3D printer on campus that will be modifiable by future students and faculty.

As per Dr. Macedo's request, we must employ the delta robot mechanism to manufacture parts from commercially available plastic. The IME department has provided a budget of approximately \$5000.

Engineering Specifications

The sponsor's desires are broad and must be quantified. This section outlines the process by which we translate Dr. Macedo's needs into formal engineering specifications.

Quality Function Deployment

To refine our goals, we use Quality Function Deployment (QFD), a method used to quantify customer requirements, evaluate existing products, determine specifications, and assess the importance of each objective. The process is represented graphically by a chart known as a "house of quality." Our house of quality is shown in Appendix A.

In Table 1 we have tabulated all of the engineering specifications determined from QFD. "Risk" is a measure of how critical a particular parameter is. Risk is labeled as H for high, M for medium, and L for low. "Compliance" indicates how a particular parameter can be evaluated. Results in this category are labeled A for analysis, I for inspection, T for testing, and S for similarity to existing products. We believe the most important of these factors are cost, print speed, accuracy, and build volume.

Table 1: Formal engineering specifications

Spec.	Parameter	Requirement or Target	Tolerance	Risk	Compliance
1	Print speed	500 mm/s	Min	H	A, T, S
2	Accuracy	25 μm	$\pm 5 \mu\text{m}$	H	T
3	Non-toxicity	Vents acrylonitrile fumes	N/A	H	S
4	Machine footprint	3 m \times 3m \times 2.4 m	Max	L	A, I
5	Delta mechanism	Uses delta mechanism	N/A	L	I, S
6	Total budget	\$5,000	Max	H	A
7	Open-source	All except firmware	N/A	L	A, S
8	Input file type	STL files	N/A	L	S
9	Print material cost	\$35/kg	Max	L	A, S
10	Build volume	30 cm \times 30 cm \times 30 cm	Min	H	A, I, T, S
11	No. of colors	1	Min	L	A, S
13	Custom parts	As few as possible	N/A	L	S
14	Layer thickness	30 μm	$\pm 10 \mu\text{m}$	M	S, T
15	Software cost	\$0	Max	M	A, S

Comparison of Key Specifications

Here we have formally selected our target specifications, which we have determined based on the information listed above, shown, summarizes the specifications of the five printers we discussed above and compares them with our proposed criteria.

We chose our targets ambitiously, aiming for the higher-performance end of the range in each category. Our product will be comparable to the Projet 3500 HDMax and Eden 260V in terms of layer thickness and accuracy. It will have a high volumetric print rate and be able to print a one-square-foot cube.

Table 2: Comparison of proposed specifications with current products

Printer	Cost	Speed (mm/s)	Layer Thickness (μm)	Accuracy (μm)	Build Volume (cm^3)
Dimension SST 1200es	\$36,500	—	178	200	$25 \times 25 \times 30$
BigRep ONE	\$39,000	150	100	100	$115 \times 100 \times 118$
Objet 30 Pro	\$42,900	—	28	100	$29 \times 19 \times 15$
Projet 3500 HDMax	\$69,500	—	16-36	25	$30 \times 19 \times 20$
Eden 260V	\$91,250	—	16-30	20	$25 \times 25 \times 20$
Proposed Project	\$5,000 + Donations	500	30	25	$30 \times 30 \times 30$

CHAPTER 3:

MANAGEMENT PLAN

Introduction

This section details how the team functions internally. We list each critical role, which team member is responsible for playing it, and what duties that member must fulfill. Each member is able to delegate his responsibilities to other members at his discretion.

Administrative Roles

These are roles not directly related to the design of the product. They are necessary to ensure that the group is organized, remains on par with the course syllabus, and adheres to the requirements imposed by the department and project sponsors.

Communications Officer

- Ram Santos

Ram is the main point of contact between the project team and the project sponsor, Dr. Macedo. Ram facilitates meetings with him and with lab advisor Dr. Schuster. Ram submits status reports to Dr. Schuster prior to weekly meetings.

Ram has delegated communications tasks to Justin, who is the liaison with sponsors Ed Nicolson from Yaskawa and Mike Everman from Bell-Everman.

Treasurer

- Taylor Chris

Taylor manages the team's funds. He allocates the funds for build materials and travel as necessary and reviews part orders before they are made. Taylor will prepare the budget for the final design.

Secretary

- Ram Santos

Ram maintains an information repository for the team. Most of this information is saved on Google Drive, in a folder shared with the rest of the team. Ram takes detailed notes during interactions with advisors and sponsors.

Ram is the last person to review and edit the team's documents and outgoing emails. He assembles and formats the team's reports to ensure that they look professional and are free of grammatical errors.

Design Roles

These are the subsystem design tasks. These are assigned based on each member's interests and abilities.

Structural Design

- Ram Santos
- Taylor Chris

Ram ensures the structural integrity of the robot. He will perform material selection and size mechanical parts for sufficient strength and stiffness and for satisfaction of the build volume requirements.

Taylor is responsible for designing some of elements in the frame of the robot and communicates with third-party machine shops to ensure our frame's cost-efficiency and precision.

Electronics and Software

- Paul Maalouf
- Stephen Marshall

Stephen and Paul design the electronics that control the robot. They will use any resources at their disposal to become knowledgeable about, and proficient with, the software packages necessary. Stephen and Paul will communicate with certain contacts who have done previous work in this field and decide what hardware is most suitable for this design. They will test and calibrate motion systems and document their work with detailed diagrams of system architecture and software.

Motor Implementation

- Justin James

Justin selects appropriate Yaskawa motors using mechanism inertia calculations, motor specifications, and recommendations from Yaskawa engineers.

Extruder Mechanism

- Stephen Marshall

Stephen does relevant research on plastic extrusion mechanisms and uses it to select and implement the feed mechanism and the extrusion head. He will be especially aware of the limitations of plastic extruders and be able to make recommendations for ways to improve the system.

Manufacturing

- Taylor Chris
- Justin James

Justin and Taylor will ensure the design's manufacturability at a low cost. They will select the most effective ways to manufacture the robot so that it is within tolerance.

Thermal Systems

- Justin James

Justin will design the systems by which our machine heats the parts being built, keeps its electronics cool, and vents toxic fumes.

CHAPTER 4: CONCEPT DESIGN

Introduction

To complete this project we are following a formal design process, consisting of planning, conceptual design, detail design, and production phases. Currently we have completed conceptual design and are moving on with detail design.

This design process is summarized in Figure 18 on the following page. In the planning phase, we analyzed the problem and divided it into distinct parts. In the conceptual design phase, we generated as many ideas as possible for each subsystem. We then evaluated each design to narrow our focus to one top concept.

In the detail design phase, we will finalize our specifications and order parts. This process will take place until approximately halfway through Winter Quarter. Finally, in the production phase we will assemble and test our final product. This phase leads directly to the Senior Project Expo in Spring Quarter.

Overall Concept Design

The only overall choice that needed to be made before any other was whether we would employ the rotational arm or linear slide mechanism. Because there were only two

choices, we made this decision using a simple list of pros and cons, which have been discussed previously in this report. These pros and cons are summarized in Table 3.

We decided to move forward with the linear slide mechanism. This was a simple choice to make, as it was clear from our research that the rotational arm mechanism is more suited to a different application entirely.

Because 3D printing is a highly path-dependent operation, the linear slide mechanism is superior for our application. The rotational arm mechanism is best left for pick-and-place operations. The other pros and cons are insignificant in comparison.

Our concept generation was accelerated by the fact that our whole-system design was largely prescribed by our sponsor. The printer must deposit material precisely and employ the delta mechanism. There was no need to develop creative alternatives.

Most components in a delta 3D printer can be designed or selected independently from one another. For example, our choice of print head does not depend on whether we use the rotational arm or linear slide mechanism, or vice versa.

Table 3: Pros and cons of the rotational arm and linear slide delta mechanisms

Mechanism	Rotational Arm	Linear Slide
Pros	<ul style="list-style-type: none">• Links are directly actuated• Low inertia	<ul style="list-style-type: none">• Good path precision• Simple assembly
Cons	<ul style="list-style-type: none">• Poor path precision• Difficult to assemble	<ul style="list-style-type: none">• Requires linear motion system• High inertia

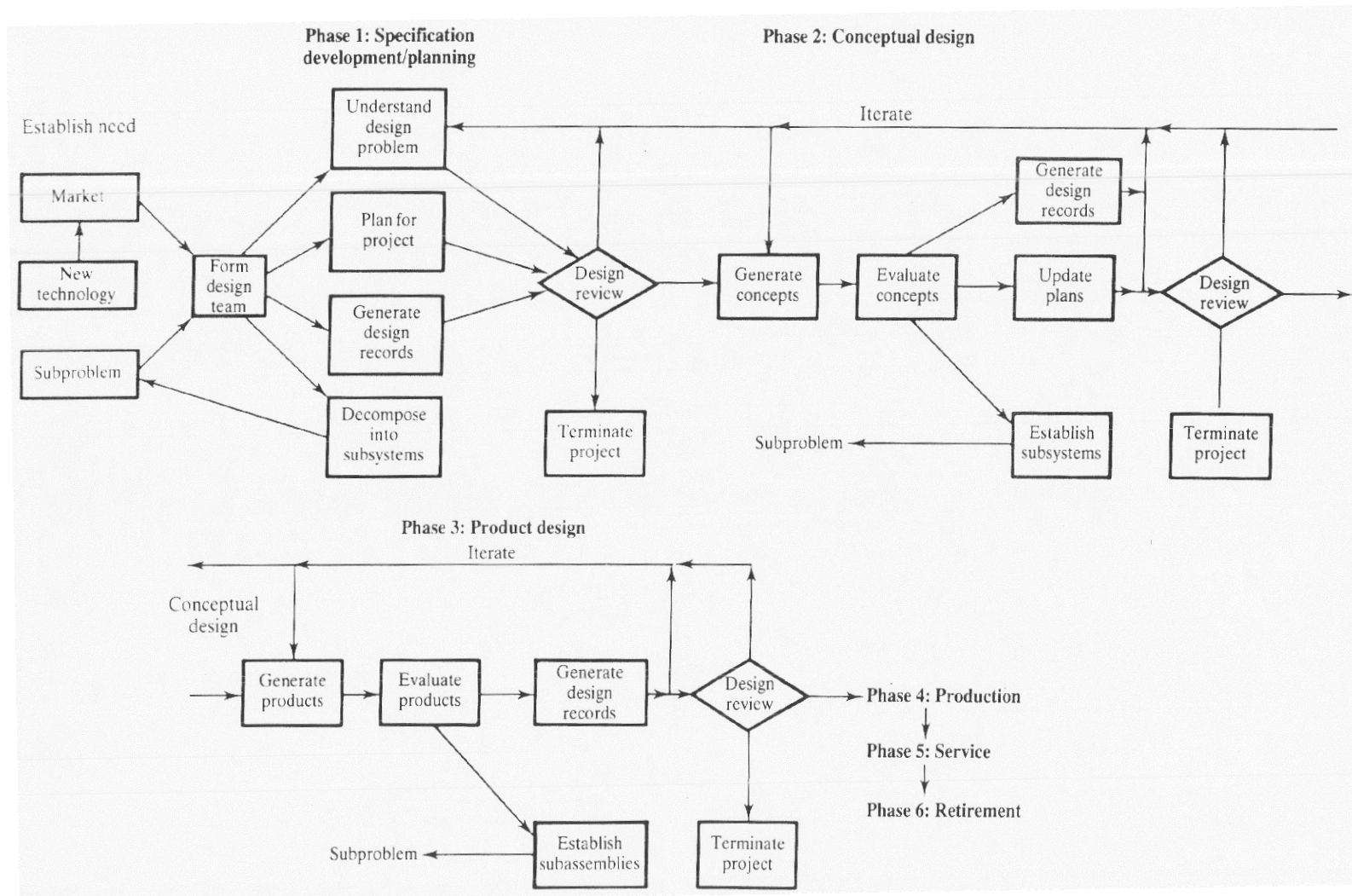


Figure 18: The mechanical design process
(Source: Ullman 1992)

Furthermore, because our product requires such high levels of precision, no component will be built from scratch. With the resources we have at our disposal, we cannot reliably manufacture any single subsystem without introducing more error than is allowed by our project requirements.

Therefore, instead of first choosing an overall design and then designing or selecting each component, we restricted our ideation process to the subsystem level. We did not develop multiple whole-system concepts. Our top concept would simply be the combination of the top choices for each subsystem.

Subsystem Design Process

There are five independent subsystems in a linear slide delta 3D printer that require a selection process:

- Linear motion system
- Feed mechanism and extruder head
- Mechanical links
- Joints
- Mechanical frame

Here we will describe the different techniques employed in the ideation and selection of subsystem designs.

Ideation techniques

Each subsystem underwent different forms of concept generation. We primarily used the following techniques:

- Brainstorming
- Brainwriting
- Concept modeling
- Comparison with existing products

Each of these methods is described in detail below. We did not use all of these for each subsystem design.

Brainstorming

This is the classic idea-generating technique, in which each team member simply states ideas out loud as they form. Possible solutions are formed quickly as they build upon one another. While this process is an easy one to execute, it can be limiting because team members are not thinking independently from each other. They are influenced by what has already been said.

Brainwriting

In brainwriting, each member begins with his own sheet of paper and writes down as many concepts as he can conceive that will perform the needed function. This is done in silence for several minutes, after which each paper is rotated to another member of the team. That member then builds upon the ideas on the page or is inspired to generate new ones. This process is repeated in silence until each member receives the paper he started with. This method is effective because it forces each member to form ideas independently and yields many ideas in a short period of time.

Concept modeling

Concept modeling involves building a crude physical model of the product or one of its subsystems. The model is not expected to have full functionality or even closely resemble the final product. It simply simulates one or several of the functions of the design. While this does not generate many new concepts, it can illustrate what is meant by a particular suggestion or fuel alternative solutions.

Comparison with existing products

The above are effective methods for producing creative solutions to problems. However, because we are not inventing anything new for our product, most of our ideas were facilitated by, or simply taken from, extensive research on existing products. The list of top concepts for each function was simply the pool of solutions we found in similar products.

Selection techniques

To narrow down ideas, we employed the same two methods for each subsystem design, the Pugh matrix and the weighted decision matrix.

Pugh matrix

A Pugh matrix is a table that simply rates each concept's performance for each requirement, relative to one concept that is chosen as the datum. There is no weighting to the criteria, and the relative performance of each design is indicated only by a plus sign indicating superiority, a minus sign indicating inferiority, or an S for "the same."

Pugh matrices are a rudimentary method for evaluating designs, since there is no weighting to indicate the relative importance of the requirements. Constructing Pugh matrices requires only an elementary understanding of the viability of each design. They are capable of eliminating ideas that are weaker in all aspects than the others, but to make final decisions a weighted decision matrix is more appropriate. These are explained below.

Weighted decision matrix

Weighted decision matrices are structurally similar to Pugh matrices, but two important differences make them effective for choosing final designs. First, each criterion is assigned a

fractional weight indicating how sensitive the final decision is to that parameter. Second, performance is scored absolutely, from 0 to 100%, instead of relative to a datum.

Forming decision matrices requires more comprehensive knowledge of the benefits and drawbacks of each option than Pugh matrices do. Therefore, extensive research is typically done on each concept before a matrix can be completed. This intermediate research is far more detailed than the background research shown earlier in this report.

Linear Motion System

The linear motion system is how linear movements are obtained from a servomotor that produces rotary motion. This subsystem's design was the most difficult to select and thus has the most extensive design process.

Ideation

We used two main ideation methods for the linear motion system, brainwriting and concept modeling.

Most of the initial ideas were fueled by research, which lead to bias toward certain mainstream solutions. While brainwriting resulted in many unorthodox concepts, most unnecessarily complex or required too much design from scratch.

After brainwriting we built a concept model. We constructed a wooden frame and built the mechanism using foamcore board, straws, and Lego Technic parts. The concept model can be seen in Figure 19. This did not result in any new ideas, it highlighted the difficulty of assembling and aligning a delta mechanism.



Figure 19: Concept model of linear slide and distal feed mechanisms

Pugh matrix

Common sense narrowed our pool to 11 ideas. At this point we constructed a Pugh matrix, which can be seen in Table 4.

From the results of the Pugh matrix, we were able to eliminate all but five choices:

- Lead screw
- Ball screw
- Timing belt
- Bell-Everman ServoBelt
- Linear servomotor

Research

With a target accuracy of $30 \mu\text{m}$, every part of the assembly must be implemented almost perfectly. A single element being slightly out of place could compromise our product's ability to meet its accuracy requirement.

We consequently restricted our research to products in which the entire linear motion subsystem is preassembled. Buying individual components and interfacing them would lead to a mechanism that is too inaccurate to justify its own cost. Outsourcing the assembly of this subsystem will save design time and reduce stacking of tolerances.

Table 4: Pugh matrix for linear motion system selection

Concept \ Criterion	1 Linear servomotor	2 Belt and rotary servo	3 Hydraulic pistons	4 Chain and rotary servo	5 Pneumatic cylinder	6 Accordion mechanism	7 Lead screw and rotary servo	8 Ball screw and rotary servo	9 Gears and rotary servo	10 Pulley-cable system	11 Counterweight
Accuracy	S	-	-	-	-	+	S	S	-	-	
Backlash	+	S	-	S	-	+	+	+	-	-	
Driver cost	-	S	S	S	+	+	S	S	S	+	
Speed	+	S	S	S	-	+	+	-	-	-	
Material cost	-	-	S	-	+	-	-	-	+	S	
Yaskawa motor	S	-	S	-	-	S	S	S	S	-	
Feasibility	S	S	S	S	-	S	S	-	-	-	
Σ^+	2	0	0	2	4	2	1	1	1	1	
Σ^-	2	3	2	3	5	1	1	3	4	5	
ΣS	3	4	5	4	0	2	4	3	2	1	

The top five concepts are explained below in further detail. Shown are products that include an entire linear motion subsystem instead of just the screws or belts.

Lead screw

The first concept explored further is a linear slide system that utilizes a lead screw and two linear guide shafts. A lead screw functions like a normal screw and has friction in its threads. One example of such an integrated system shown in Figure 20.

The guide shafts are located on each side of the lead screw and run parallel to it. The carriage is connected to the linear guide shafts using a linear bearing. The carriage is driven by the rotation of the lead screw, which is actuated by a motor. An anti-backlash nut allows the lead screw to move the carriage bidirectionally with minimal accuracy loss.

A lead screw system has many advantages. It has high force density, meaning it is capable of moving heavy loads. Because it relies on friction, a lead screw stage can easily self-lock for vertical applications. The elimination of backlash makes lead screw systems capable of accuracies of less than 20 μm . They are also relatively cheap, with an 800-mm stage being priced at about \$1,000.

Although friction can be an asset to lead screw systems, the disadvantages of lead screws are all associated with friction. High energy loss due to friction means a greater torque is necessary to drive the system, lowering its efficiency. Lead screws have low allowable duty cycles due to heat considerations. The increased wear due to friction makes backlash increase over time, decreasing accuracy.



*Figure 20: ETL long-travel linear slide by Newmark Systems
(Source: Newmark)*

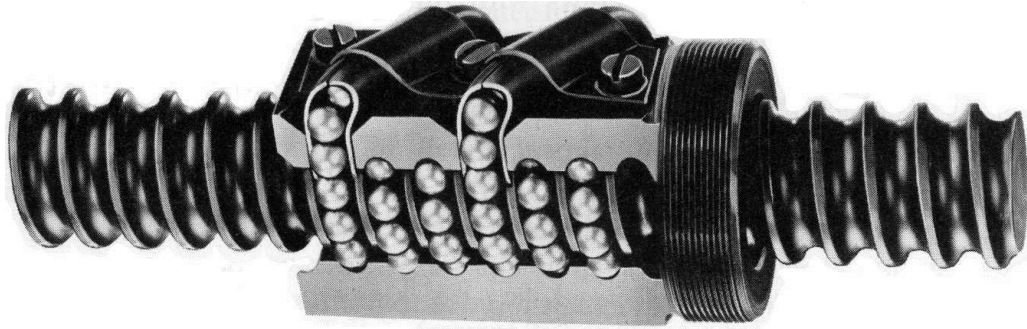


Figure 21: Ball screw ball recirculation mechanism

(Source: MDP)

Ball screw

A ball screw linear stage functions similarly to a lead screw stage. The difference is that a ball screw nut utilizes recirculating balls in order to eliminate the friction seen in lead screws. Figure 21 shows how the balls are recirculated in a ball screw nut. With the nearly perfect fit of the ball bearing in the grooves of the ball screw there is little to no backlash in the system.

Like lead screws, ball screws are able to move heavy loads. Ball screws, however, lack the important disadvantages that lead screws have. The absence of sliding friction results in high efficiency and low wear. Furthermore, high-end ball screws can have accuracies under 1 μm , which do not increase over time.

The main disadvantage of using a ball screw stage is that it is far more expensive than a lead screw stage. An 800-mm stage of the highest accuracy can cost over \$3,000. Purchasing three of these systems for our design would be beyond our budget. Ball screw systems also require frequent lubrication.

Timing belt

A timing belt linear stage system is shown in Figure 22. On the far side of the slide in the figure is a shaft to which a motor can be

connected to move the belt. The carriage is attached to the timing belt and to guide rails that constrain movement to a single axis.

Timing belt systems are capable of higher speeds than lead screw or ball screw systems. They are also designed for longer travel lengths. Consequently, a timing belt system of 800-mm length would be relatively cheap, only \$600 to \$1000 per stage. Another benefit is that timing belts do not need to be lubricated and require very little maintenance.

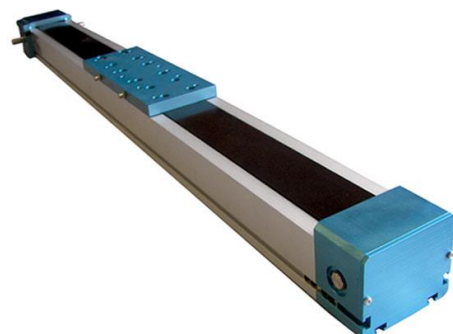


Figure 22: iselAutomation belt-driven slide

(Source: iselAutomation)

A major shortcoming of timing belts is that belts are elastic. This means even high-end timing belt systems can have accuracies as high as 50 μm to 200 μm due to overshoot. Long vibration settling times also reduces

printing speed. Over time, belts can stretch, further reducing accuracy. With a target accuracy of 30 μm , we can only justify using a timing belt system if all other methods are cost-prohibitive.

Bell-Everman ServoBelt

The ServoBelt linear slide is a product exclusive to Bell-Everman, a small embedded motion system company located in Goleta, California. Like timing belt drives, ServoBelt drives move a carriage along guide rails. However, in Bell-Everman's patented belt drive system, the belt runs over the driving pinion and under two idle rollers on each side of the pinion. This mechanism can be seen in Figure 23.

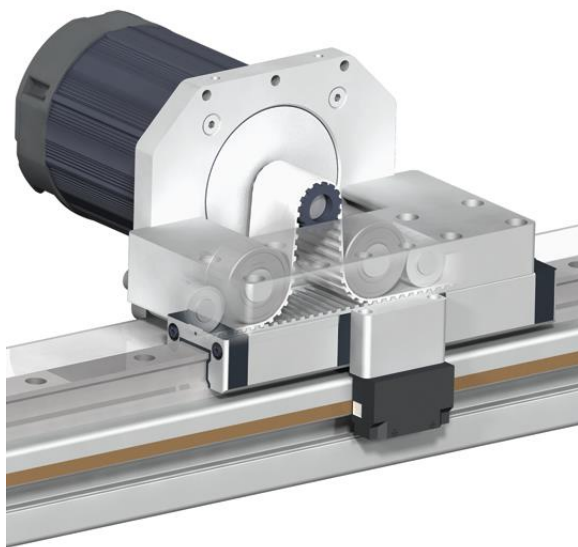


*Figure 23: ServoBelt stage mechanism
(Source: Bell-Everman)*

Tension in the belt is limited to the small segment near the pinion, as the rest of the belt remains stationary. Because the entire belt is not constantly in tension, it is not as susceptible to stretching over time, and positioning error is nearly eliminated.

ServoBelt drives can have accuracies as low as 4 μm , which is significantly lower than any amount attainable by standard timing belt drives. They also require little maintenance and are highly debris-resistant, since the belt teeth are not exposed. ServoBelt drives are very durable, having 50-million-cycle lives with minimal tolerance changes.

As with ball screw systems, the disadvantage of ServoBelt systems is that they may be cost-prohibitive. An 800-mm linear stage costs over \$2,100, not including a linear encoder. With linear encoders and end stops, the stages cost over \$2,800.

Linear servomotor

Unlike other linear motion stages, linear servomotor stages eliminate the mechanical drive train and directly couple the motor to the carriage. The linear servomotor is essentially a rotary servo motor that is redesigned to lie flat on a table or track. These linear motors move linearly using magnets. Because Yaskawa produces linear servomotors, we would be using one of theirs if we decided to use one. A Yaskawa linear servomotor is shown in Figure 24.



*Figure 24: Yaskawa SGT Sigma Trac
(Source: Yaskawa)*

In terms of absolute performance, linear servomotors are the best option available. They can achieve accuracies as low as 0.5 µm, are lightweight and compact, and move extremely fast. Furthermore, since the motor and slide are directly coupled, Yaskawa's built-in vibration suppression technology can virtually eliminate positional overshoot.

The cost of a linear servomotor, however, is several times greater than any alternative, at upwards of \$7,000. While Yaskawa has said they will donate motors and amplifiers, we would have to prove that the increased performance justifies the price.

Decision matrix

Our final decision matrix for the linear motion system is shown in Table 5. The five top concepts were scored on nine criteria.

Accuracy, repeatability, speed, and cost were the most important factors in our decision. The accuracy criterion was given a weight of

15 because, in order to print parts with a 30 micron tolerance, the linear slides need to have very high accuracy. Because our system has a lot of repetitive bidirectional movement, repeatability is critical and was given a weight of 15. Speed was given a weight of 15 because one of our goals is to minimize the print time. Cost is a major factor in our decision since we are given a limited budget. No design will be selected if it is cost-prohibitive.

Durability is important because the machine is to be used by the IME department for years to come, but with performance being our most critical aspect, we gave durability a weight of 5. Maintenance was only given a weight of 5 because the printer will remain functional as long as it is supervised by a technician. We gave ease of implementation a weight of 10 because we do not want to design a printer that we are unable to build and interface properly. Finally, the efficiency criterion was given a 5 because, although it affects motor sizing, it is not nearly as significant as precision and cost.

Table 5: Decision matrix for linear motion system selection

	Accuracy	Repeatability	Durability	Maintenance	Speed	Cost	Ease of Implementation	Efficiency	Overall Satisfaction
Weighting factor	15	15	5	5	15	25	10	5	100
Lead screw	70%	60%	30%	30%	50%	80%	80%	30%	
	10.5	9	1.5	1.5	7.5	20	8	1.5	59.5
Ball screw	90%	100%	80%	60%	70%	20%	50%	80%	
	13.5	15	4	3	10.5	5	5	4	60
Timing belt	20%	10%	40%	70%	90%	100%	70%	70%	
	3	1.5	2	3.5	13.5	25	7	3.5	59
ServoBelt	90%	90%	90%	80%	80%	40%	70%	60%	
	13.5	13.5	4.5	4	12	10	7	3	67.5
Linear motor	100%	100%	100%	80%	100%	0%	70%	100%	
	15	15	5	4	15	0	7	5	66

Final selection

Based on the decision matrix, the best option is the Bell-Everman ServoBelt linear stage. It offers similar performance to that of a ball screw system but with a smaller price tag. It does not perform as well as a linear motor, but the difference is not significant enough to justify paying the higher price.

Although the ServoBelt system is not the most expensive option, purchasing three stages costs at least \$6,300, outside our estimated \$5,000 budget for the product as a whole. However, when we contacted Bell-Everman to request a quote for one of their stages, its president, Tom Maccianti, offered us a better deal. He informed us that Bell-Everman had been looking for a way to “work closely” with Cal Poly engineering students. Bell-Everman is located in Goleta, CA, a short drive south from San Luis Obispo. Mike Everman, co-founder and CTO of the company, is a Cal Poly AERO alumnus. He in particular is interested in giving back to the engineering program here and may advise us on our project in the future.

We shared the requirements of our product with Bell-Everman and asked if we could tour their facility sometime in the next month. The company replied, offering to be a resource for advice and welcoming us to visit. Although the terms of Bell-Everman’s involvement have yet to be determined, Maccianti said that the company may be willing to give us discounts on, or even donate, parts. We will be communicating with Bell-Everman over the next month, working out a deal and possibly visiting their facility.

With Bell-Everman’s eagerness to “pay it forward,” we are less concerned that our choice is cost-prohibitive. If we are given a significant discount, Bell-Everman ServoBelt

linear stages will be indisputably the best choice for our application.

Feed Mechanism and Extruder Head

Deciding on a feed mechanism and extruder head was relatively easy. The nature of our project narrowed our options to a single concept for each and prohibited all others.

It is beyond the scope of our project to invent a new technology by which to extrude plastic. Therefore we did not undergo any formal ideation process for feed mechanisms and print heads.

Because we did not have many concepts to choose from, we also did not form Pugh matrices to narrow down our ideas for this subsystem. Our decisions were made so that we would avoid going beyond the scope of our project and being unable to complete it.

Feed mechanism

The choice of feed mechanism was obvious because our customer requirements make other concepts unusable. Three requirements in particular limited our choices. These are explained below.

First, one of our requirements is to use cheap, commercially available material. The only choice that meets that requirement is FDM. Since FDM uses spools of ABS or PLA, material can be purchased for under \$30 per kilogram. In contrast, SLS uses powders that are not readily available through commercial sources, while SLA and PolyJet use photocurable resin, whose price ranges from \$55 to hundreds of dollars per kilogram.

Second, because our product will be used on campus, potentially by students, it must be easy to use safely. FDM is not as hazardous as other methods. SLS uses high-power lasers and high-voltage sources which are hazardous to work with, while photopolymers used in PolyJet and SLA are corrosive to the skin and can cause eye damage.

Finally, we are required to employ a delta robot mechanism. The only feed mechanism for which a delta robot makes sense is FDM. PolyJet lends itself to, and is more efficient with, a Cartesian coordinate system, and SLS and SLA do not require three-degree-of-freedom mechanisms at all.

FDM is therefore the only logical choice for a feed method. For completeness, we have included a decision matrix in Table 6.

Accuracy was given the largest weight, 25, to reflect the design goal of sub-30- μm accuracy. Layer thickness has a large impact on accuracy, so it was given a weight of 15. Print

head cost was given a weight of 15 because it is the largest drain on our overall budget aside from the linear motion system. Material cost was weighed at 20 to reflect the customer requirement that the device run on cheap, commercially available material.

Print speed was given a weight of 10, although this did not affect the outcome because all choices exceed our speed requirements. Mass was given a weight of 10 because it will impact accuracy and motor sizing, which affects speed. Maintenance will be concern during calibration and testing but was weighed at 5 because it is not critical in meeting our customer requirements.

In the decision matrix we omitted our concerns about safety and incompatibility with the delta mechanism. Instead we assumed that we have the resources necessary to properly implement all the systems safely and within our sponsor's limitations. FDM remains the best choice, largely due to cost.

Table 6: Decision matrix for feed mechanism selection

	Cost of Print Head	Cost of Material	Print Speed	Accuracy	Mass	Layer Thickness	Maintenance	Overall Satisfaction
Weighting factor	15	20	10	25	10	15	5	100
FDM	100% 15	100% 20	100% 10	80% 20	100% 10	50% 7.5	100% 5	87.5
SLS	10% 1.5	10% 2	100% 10	90% 22.5	50% 5	100% 15	80% 4	60
PolyJet	10% 1.5	50% 10	100% 10	100% 25	50% 5	100% 15	80% 4	70.5
SLA	10% 1.5	50% 10	100% 10	100% 25	20% 2	100% 15	80% 4	67.5

Extruder head

Since we have decided to use FDM as our feed method, we must select an appropriate print head. There is a variety of print heads on the market with a wide range of complexity levels. There are two ways in which 3D printer heads typically differ from one another. One is that some use proximal filament feeds, while others use distal feeds. The other is that some heads consist of multiple extruder nozzles.

Proximal vs. distal feed

A proximal feed mechanism is one in which the gears that pull the filament from its spool are located on the print head itself. This can be seen in Figure 25.



*Figure 25: DGlass 3D proximal-style extruder
(Source: DGlass 3D)*

Proximal mechanisms are better than distal mechanisms at controlling the amount of filament that flows through the nozzle. However, this adds weight to the print head, requiring a more powerful motor to move it and possibly increasing positional overshoot.

In a distal, or Bowden, feed mechanism, the gears are located remotely, usually attached to the static frame of the printer. The filament is

fed to the moving print head through a low-friction Teflon tube. A Bowden mechanism is shown in Figure 26. Such a mechanism would be attached to the frame of the printer as in our concept model, which is shown in Figure 19 on page 25.



*Figure 26: Distal-style extruder
(Source: thingiverse)*

Because they have less moving mass, Bowden extruders require less motor torque. However, the plastic filament is put into compression over the length between the gears and the nozzle, which makes it harder to control the flow rate of the plastic.

A decision matrix for this selection is shown in Table 7. As with other subsystems, accuracy is paramount and weighted most heavily. Cost is important, but this choice has a small impact on our overall budget compared to other design choices. The extruder's mass is a large contribution to the overall inertia of the system, but the ServoBelt drives we have selected for linear motion are more than capable of accelerating this mass. Maintenance is not a critical design factor, but it is inconvenient to frequently unjam a print head.

We have selected a proximal print head, since we are primarily concerned with minimizing positional error at all sources.

Table 7: Decision matrix for proximal vs. distal feed mechanism selection

	Cost	Accuracy	Mass	Maintenance	Overall Satisfaction
Weighting factor	25	40	20	15	100
Proximal	50%	100%	20%	80%	
	12.5	40	4	12	68.5
Distal	80%	20%	100%	60%	
	20	16	20	9	65

Single- vs. double-nozzle extruder

Most FDM printers use a single nozzle. However, using multiple nozzles has two key advantages. Figure 27 depicts a dual-head extruder.



Figure 27: Double-head extruder
(Source: Micron 3DP)

First, multi-nozzle extruders enable printing in different colors simultaneously. The ORD MH-3000, in Figure 1 on page 3, has a quintuple-nozzle extruder and can print in five different at once.

Second, printing with at least two nozzles means having the ability to print support

material for parts with internal cavities or overhanging geometries.

Adding a second nozzle would significantly increase the mass of the mechanism and cost twice as much as a single-nozzle extruder. Versatility refers to the number of useful features the extruder possesses. Complexity is critical because we are hesitant about making the design more difficult to implement and control reliably. It would also increase the complexity of our design, especially in terms of control software.

The decision matrix for this selection is shown in Table 8. Versatility and complexity are the two heaviest factors. Mass and cost are relevant but not as important.

We have decided to use a single extruder. While the increased functionality afforded by a dual extruder is valuable, we are afraid of being overly ambitious in our design. It is worth noting that it would be reasonably simple for the single print head to be replaced with a dual print head in the future.

Table 8: Decision matrix for single- vs. double-nozzle extruder selection

	Versatility	System Complexity	Mass	Cost	Overall Satisfaction
Weighting factor	30	40	15	15	100
Single	40%	90%	80%	100%	
		12	36	12	15
Double	90%	50%	40%	50%	
		27	20	6	7.5
					60.5

Final selection

We will be using a proximal-style, single-nozzle FDM extruder head. This is the only choice that satisfies the sponsor requirements without going too far above and beyond them. It is still unknown from whom we will be purchasing this extruder, but we are certain that this is the best choice for our application.

Mechanical Links

Here we will explain our selection process for the pairs of mechanical links that connect the linear stage to the extruder.

As was the case with feed methods, we did not use a formal ideation process. There are only two reasonable choices for materials because of weight considerations. Aluminum and carbon fiber are the only materials worth comparing for low-weight, high-precision applications. The only other choice is whether to use a solid or hollow cross section.

We did narrow down these four choices with a Pugh matrix, followed of course by a decision matrix to make the final decision.

Table 9: Pugh matrix for mechanical link selection

Concept	1	2	3	4
	Carbon Fiber		Aluminum	
Criterion				
DATUM		+	-	S
	Weight	-	-	-
	Strength	+	-	-
	Stiffness	-	+	+
	Cost	2	1	1
	Σ^+	2	3	2
	Σ^-	0	0	1
ΣS				

Table 10: Decision matrix for mechanism arm selection

	Weight	Axial Strength	Transverse Strength	Axial Stiffness	Transverse Stiffness	Cost	Overall Satisfaction
Weighting factor	15	5	5	50	5	10	100
Composite Rod	90% 13.5	100% 5	10% 0.5	100% 50	10% 0.5	70% 7	76.5
Composite Tube	100% 15	80% 4	20% 1	80% 40	20% 1	50% 5	66

Final decision

We will be using solid carbon fiber rods for the mechanical links. Solid rods are superior to hollow tubes in terms of axial strength and stiffness due to their high cross-sectional area. We have not yet decided the size of the rods, but for reference, a 0.250"-diameter, 24"-long, unidirectional, carbon-fiber-vinyl-ester rod costs approximately \$9, approximately 0.2% of our projected budget. Various carbon fiber rods and tubes are shown in Figure 28.



*Figure 28: Carbon fiber tubes and rods
(Source: RCWorld)*

Rod Ends

We also selected joints to connect the carbon fiber rods to the linear slides and to the print head. Although this was not a difficult or expensive decision, it is critical for our project. With such high-precision motors and control

software, we expect our main sources of inaccuracy to be mechanical. Since carbon fiber is extremely stiff, mechanical error will likely occur at joints.

Research

We did not perform a formal ideation process because it would not make sense to invent a new joint for this project, nor could we reliably manufacture such a solution. We briefly researched each concept and used that information to form a decision matrix. A Pugh matrix was unnecessary because only three realistic solutions were found. We examined these joint types in particular:

- Cardan joints
- Ball joints
- Magnetic ball joints

All of these provide the three required degrees of freedom but varying levels of accuracy. Each design is described below.

Cardan joints

A Cardan joint, or U-joint, consists of two U-shaped ends. Each is pinned to a common joint through two holes at 90° to one another. Figure 29 depicts a typical U-joint.



*Figure 29: Cardan joint
(Source: The Green Book)*

U-joints are the most widely used method of achieving this motion because they are the cheapest. However, their high number of moving parts causes backlash, especially when undergoing changes in direction.

Ball joints

A traditional ball joint is shown in Figure 30. Ball joints are more accurate than U-joints due to fewer moving parts but are still prone to backlash because of frictional wear. It is apparent in the figure that a ball joint has a limited range of motion by design.



*Figure 30: Traditional ball joint
(Source: Danuser)*

Magnetic ball joints

Magnetic ball joints function similarly to standard ball joints but rely on magnets, instead of mechanical forces, to remain intact. Some magnetic ball joints are shown in Figure 31.

Magnetic ball joints are superior to traditional ball joints in terms of accuracy, wear, and range of motion, but are the most expensive of the options we considered. Because there is no mechanical holding force, the ball can be separated from its socket. The force required to do this is approximately 1 kilogram-force. We do not expect our device to exert that high a load, but we will conduct simple tests to quantify strength.



*Figure 31: Magnetic ball joints
(Source: Hilan)*

Decision matrix

In Table 11 is a decision matrix for selecting a joint type for our delta mechanism. Accuracy is the most critical factor. Range of motion is the next heaviest criterion and is one main reason the traditional ball joints cannot compete with magnetic ones. Implementation, temperature, durability, and cost are all minor factors, especially since the three options are all acceptable in all of those areas.

Table 11: Decision matrix for joint selection

	Accuracy	Cost	Range of Motion	Ease of Implementation	Temperature Range	Durability	Overall Satisfaction
Weighting factor	40	5	20	15	10	10	100
Cardan	30%	90%	80%	80%	80%	60%	58.5
	12	4.5	16	12	8	6	
Ball	60%	80%	30%	80%	80%	80%	62
	24	4	6	12	8	8	
Magnetic Ball	90%	60%	100%	60%	50%	70%	80
	36	3	20	9	5	7	

Final decision

We have decided to use magnetic ball joints in our design. Again, precision is paramount, so we will not compromise that criterion lightly. All three joint types considered are extremely cheap, so cost had little effect on the decision.

Structure Frame

While many of our subsystem components were independent of each other, the frame material and shape were designed based on the previous subsystem decisions.

The frame must incorporate the three vertical slides, the printing bed, electrical components, and a spool of plastic filament. The spools will be mounted to the top of the frame so that filament can be easily routed into the extruder. The electrical component will be stored under the printing bed so that the product uses less space and is safer to be around.

Frame material

The rigidity and alignment accuracy of the different subsystems is a major concern. Even

with highly accurate joints and electronic components, structural vibrations and misalignments can easily push the precision of our prints beyond the 30-µm tolerances.

Since our delta mechanism relies on three independent linear slides in order to move the extruder, the accurate alignment of these three linear slides is essential to ensure that our control software positioning properly.

To produce a structure machined to such tight tolerances would raise the cost of the printer drastically. Instead, we plan to design a structure that will allow for alignment calibration on the fly.

The frame also has to be extremely adaptable so that future modifications can be made. These design considerations led us to select a material having the following qualities:

- Rigidity
- Alignment adjustability
- Adaptability
- Commercial availability
- Cost

Table 12: Decision matrix for frame material selection

	Rigidity	Alignment Adjustability	Adaptability	Commercial availability	Cost	Overall Satisfaction
Weighting factor	30	30	15	15	10	100
Carbon Fiber Tubing	100% 30	30% 9	40% 6	60% 9	10% 1	55
Aluminum T-slot Extrusions	80% 24	100% 30	100% 15	100% 15	50% 5	89
Circular Steel Tubing	90% 27	80% 24	50% 7.5	100% 15	70% 7	80.5
Rectangular Steel Tubing	90% 27	90% 27	70% 10.5	100% 15	60% 6	85.5

Based on the above criteria we formed the decision matrix seen in Table 12, which evaluates the following material choices:

- Carbon fiber tubing
- Aluminum T-slot extrusions
- Circular steel tubing
- Rectangular steel tubing



*Figure 32: Aluminum T-slot extrusion
(Source: 80/20)*

Aluminum T-slot extrusions received the highest score due to ease of integration of subsystems and the ability to adjust components in the t-slot channels. These

T-slots also allow for seamless integration with Bell-Everman's ServoBelt linear slides, which are designed with built-in T-slot extrusions. The other frame materials require drilling holes in exact positions, not allowing for many adjustments. An aluminum T-slot extrusion can be seen in Figure 32.

Frame shape

Initial design

There are also several choices for the shape of the frame. The frame's shape must take into account ease of assembly, adjustability, structural stability, and amount of frame material used.

The linear slide mechanism requires that our three T-slot extrusion columns be equidistant from the center of the build volume, forming an equilateral triangle. Therefore, the top and bottom of the frame must allow the attachment of the columns in this formation. The sketches shown in Figure 33 show three possible ways to mount the three vertical columns.

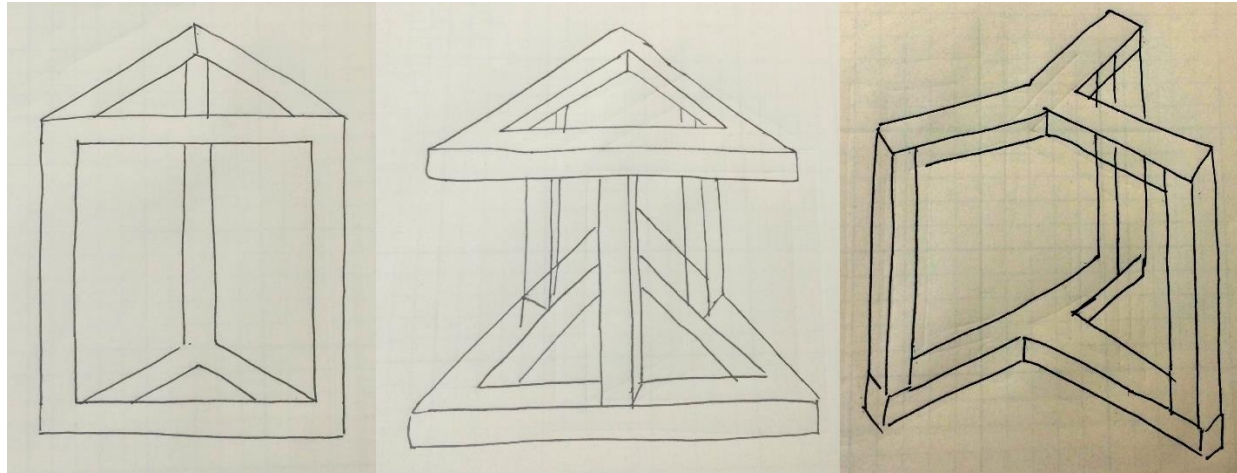


Figure 33: Possible frame shapes for the linear slide mechanism

The leftmost design puts the columns at the corners of a triangular base and is the most common shape among delta 3D printers. It is a simple shape with a good balance of stability and quantity of material used. However, it uses three-way joints at the corners that may be difficult to assemble accurately.

The next design puts the columns at the midpoints of the triangle's sides. It uses only two-way joints and is more easily assembled than the first design. However, it uses more

material and has a larger footprint than the first for any given build volume. It is also less structurally stable, since the column's joints can migrate along the base over time.

The rightmost shape uses the least possible frame material for any given build volume. Instead of using a triangular base, it has a Y-shaped base with bars connecting the triangle's corners to its center. This design is less structurally stable than the other designs and has fewer ways to adjust it.

Table 13: Decision matrix for structure shape selection

	Ease of Assembly	Adjustability	Structural Stability	Material Used	Overall Satisfaction
Weighting factor	15	45	35	5	100
Triangular with Corner Joints	60% 9	90% 40.5	80% 28	90% 4.5	82
Triangular with Midpoint Joints	90% 13.5	90% 40.5	60% 21	20% 1	76
Y-shaped	100% 15	40% 18	50% 17.5	100% 5	55.5

A decision matrix for the frame shapes is shown in Table 13. Adjustability is our most important factor. Misalignments are inevitable, and the end user should be able to recalibrate the printer when necessary. Ease of assembly is not as important because this will only need to be done once. Material used is inconsequential because T-slot extrusion is very inexpensive.

We have chosen the triangular base with corner joints. This provides the best stability without increasing the physical footprint of the machine.

Final design

When discussing with Bell-Everman our application of their ServoBelt Light slides, they informed us that they would construct ServoBelt slides on 60-by-60-mm Bosch aluminum T-slot.

We then revisited the design of the top and bottom of our structure and looked to minimize the number of bolts needed to hold the vertical columns in position. We are able to use the four M8 threaded holes and corner square holes to fasten and align our structure.

In order to best utilize this cross section, and by the recommendation of Bell-Everman on how to interface with their product, we

decided to abandon T-slot as a solution for the top and bottom of the structure.

Instead, we will use aluminum plates to align the T-slot used for the columns. Assembly will be simpler and more precise, since the holes can be drilled into the plate. Precision pins and screws can be inserted into the holes and then into the holes in the columns. To ensure the rigidity and tolerances of the frame, the manufacture of the plates will be outsourced to a professional machine shop.

Preliminary Concept

Our final design will include all of the selections made above. In Table 14 is a summary of our subsystem decisions and how they meet our customer requirements.

Preliminary solid model

In Appendix C is a preliminary SolidWorks model that we have created for the final product. In this model we have omitted the feed mechanism, motors, and other electronics. This model was created primarily to simulate the kinematics of the robot. The parts included in the model are not necessarily the parts that we selected for our design. They are instead similar parts that nonetheless depict our product's function.

Table 14: Summary of subsystem design decisions

Category	Chosen Concept	Reasons	Requirements Met
Linear slide	ServoBelt drive	Cost and accuracy	Accuracy Print speed
Mechanical links	Carbon fiber rods	High rigidity Low inertia	Accuracy
Joints	Magnetic ball	Low backlash	Accuracy
Extruder	Single-head proximal	Simplicity Accuracy	Accuracy Print speed
Frame	Triangular T-slot	Stability Adjustability	Accuracy Build volume

CHAPTER 5: DETAIL DESIGN

Introduction

In this section we document our detail design process. We explain the technical processes we used to make final decisions about part design and selection.

Kinematics

In order to properly use the delta mechanism, we need a mathematical model of the mechanism's kinematics. Specifically, we need a clearly-defined relationship between the positions of the three carriages on their vertical slides and the location of the nozzle from which material is extruded.

The kinematic equations of a robot can be solved in two ways. The *forward kinematics* receive actuator positions as input and output the end effector position. Conversely, the *inverse kinematics* turn end effector positions into actuator positions. This is illustrated by the diagram in Figure 34.

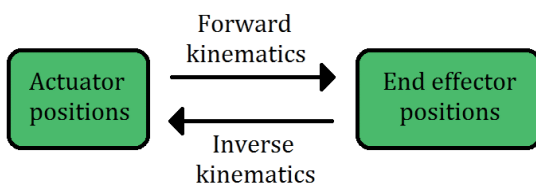


Figure 34: Distinction between forward and inverse kinematics

The forward and inverse kinematics solutions are useful in different ways and, in some cases, require different methods to produce. The applications of the forward and inverse kinematics are described below. The formal derivations are left out of this section but included in Appendix A.

Inverse kinematics

For delta 3D printers, the inverse kinematics are extremely important. 3D printing requires that the extruder nozzle be located at the correct point in space at all times. Because the end effector position is prescribed by the slicer software, we must convert this into positions for the carriages. The inverse kinematics solution is used directly by the robot's control system to position the print head.

The inverse kinematics solution can be used to discern whether any region in space can be reached by the print head. Therefore, it can be used to analytically compute the build volume of the printer and, by extension, the final dimensions of the assembly. A MATLAB script, attached in Appendix B, was used to iteratively size some components in the mechanism. By varying dimensions such as rod length and column spacing, we were able to ensure that the build volume requirements were met.

Visual representations of the build volume of our printer can be seen in Figure 84 and Figure 85 in Appendix A. The output of the script using our final dimensions indicates that inside our theoretical build volume we can fit a cylinder with a 50-cm diameter and a 33-cm height. These values satisfy our goal of being able to print a 30-cm cube. Attaining this build volume requires the following dimensions:

- Linear slide travel length 840 mm
- Linear slide vertical offset 120 mm
- Carbon fiber rod length 460 mm
- Column radial distance 400 mm

Here, "linear slide vertical offset" refers to the height above the bottom aluminum plate at which the carriage begins its travel.

Forward Kinematics

The forward kinematics are less essential than the inverse kinematics. It is possible to program and run a 3D printer using only the inverse kinematics. However, the forward kinematics solution still has utility in calibration of the robot.

The solution of the forward kinematics is more difficult than that of the inverse kinematics. This is related to the fact that a delta mechanism is a parallel mechanism, not a serial mechanism. This distinction is described in detail in Chapter 1.

The solution of the forward kinematics is left out of this report, since it will not be useful until the prototype is built and the control system can use it for error estimation.

Motor Selection

Yaskawa has a vast selection of rotary servomotors. Fortunately they have powerful software tool known as SigmaSelect, available for free download on their website. Also, the engineers at Yaskawa have lots of experience sizing their motors and were willing to help.

SigmaSelect allows us to input the movement profile, loads, masses, inertial properties, and configuration of an application and generates a list of motors whose properties meet the design requirements. First, however, we need to define those design requirements.

Mass properties

The two inertial quantities that SigmaSelect requires as input are “application inertia” and “load mass.” These must be determined by analysis of the moving components in our system. Fortunately, Bell-Everman supplied us with an extremely detailed, configurable SolidWorks model of the ServoBelt Light stage we will be using, shown without proprietary dimensions in Figure 35.

Application inertia

The application inertia is the total mass moment of inertia of all components in the system. The rotating component is the pinion gear that is attached to the motor shaft and meshes with the belt teeth. Its mass moment of inertia was found in the “Mass Properties” tab in SolidWorks.

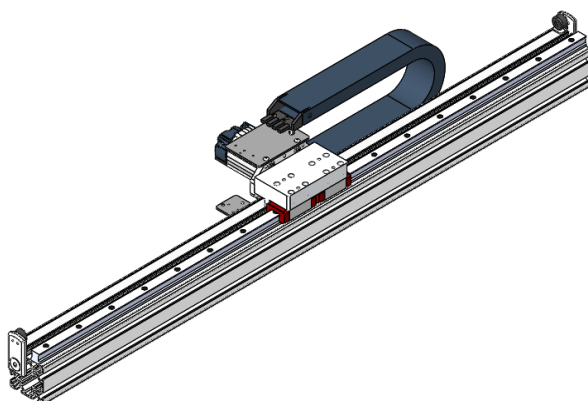


Figure 35: SolidWorks assembly of Bell-Everman ServoBelt Light linear slide

A sanity check was performed as well. We modeled the gear as a cylindrical solid with inner diameter equal to the motor shaft diameter, outer diameter equal to the gear addendum, and density equal to that of steel. This gave us an upper bound on the inertia.

The motor sizing process was performed at this upper bound value, at the lower bound value given by SolidWorks, and at the average of the two values. Fortunately, all three values resulted in the same motor being selected.

The mass of the belt was found in a similar manner. Note that due to the unique design, the moving belt mass is very low—only a few centimeters of the belt are in motion at any given time. This results in the moving belt mass being only 38 grams.

Load mass

Quantifying load mass was trickier. Because the motors are moving their own mass, choosing a more powerful motor could change the inertia the motor had to move. SigmaSelect assumes that the motor is not responsible for moving its own mass. Therefore, this process required an iterative approach.

We estimated the carriage mass as 1kg. For the mass of the remainder of the mechanism, we assumed the worst case, in which one motor carries the entire print head mass of 0.5kg.

We chose a motor mass of 1 kg for the first iteration, resulting in a load mass input of 2.5 kg. For this load mass, SigmaSelect recommended a motor whose mass is 1.5 kg. The calculation was then repeated with a load mass of 3 kg, and the same motor was chosen.

Other input properties

Without testing, it is difficult or impossible to quantify the friction loading applied to the belt. This friction is captured by the “efficiency” value for the mechanism. Instead of analytically determining friction properties, we asked Yaskawa for advice. Yaskawa engineers recommended a value of 0.96 to 0.98 for the efficiency of timing belts. The calculations were performed with a value of 0.96, which is the worst-case scenario.

The “inclination” was set to 90° because the carriage will be moving only vertically. The SigmaSelect software also requested input for counterweights and thrust assistance. Our design, as far as we knew, would have neither.

Move profile

Lastly, SigmaSelect asks for a “move profile.” This is so that it can use the accelerations to calculate the torque required.

The recommended maximum acceleration for many 3D printers is 1000 mm/s² (MakerBot). However, we believe we can safely achieve higher accelerations than this. Nearly all printers on the market use stepper motors, while our device will use servomotors. Our printer will also be much more rigid than the do-it-yourself printers for which the 1000-mm/s² acceleration is recommended. We settled on a target maximum acceleration of 2000 mm/s². This leaves us room to improve upon existing designs.

We then created a simple trapezoidal velocity profile, where the motor starts from rest, then undergoes maximum acceleration, dwells, and then decelerates to rest. This simulates a fast travel along the Z-axis, where the carriages start from rest at the top of their travel and

stop before the end effector hits the base. The movement profile is shown in Figure 36. Position, velocity, acceleration, and estimated torque are respectively shown in the plot as blue, red, green, and orange.

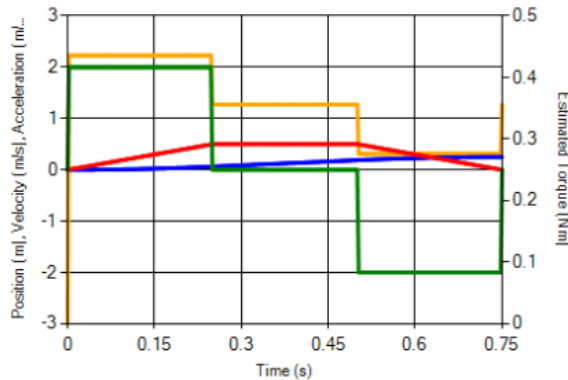


Figure 36: Move profile for motor sizing

Selection

With the application quantities and move profile quantified, the SigmaSelect software gave a list of compatible motors, of which a screenshot is shown in Figure 37. Each motor is given a relative “cost factor,” where a higher value signifies lower cost. From here, we began filtering results.

First, we wanted to avoid overdesigning. We therefore limited the selections to those with torque safety factors between 1 and 10. We also ignored all non-stock parts, since doing so would decrease the lead time and cost.

We also needed to make sure that the motor met our specific requirements. We eliminated all motors that did not have brakes, since we need a brake to prevent the end effector from crashing into the heated build plate when power is cut off.

The next step is looking at inertia matching. Matching the motor inertia to the application inertia more closely results in less overshoot and fewer settling problems. To gauge this we looked at each motor’s “allowable inertia ratio.” The most cost-effective result that met all of the above requirements resulted in a 233% allowable inertia ratio. This would result in significant overshoot, which is not acceptable given our accuracy requirements. The second result, which only cost 7% more, had only 78% of its allowable inertia ratio. Thus, the motor we recommended to Yaskawa was the SGMAV-02A*A.

Part No.	ed	% Peak Speed	Required Peak Speed (RPM)	Allowable Inertia Ratio	% of Allowable Inertia Ratio	Application Inertia Ratio	Cost Factor
SGMAV-C2A*A		7%	415.2	30	233%	69.9	1
SGMAV-02A*A		7%	415.2	30	78%	23.3	1.07
SGMAV-04A*A		7%	415.2	20	83%	16.5	1.22
SGMAV-06A*A		7%	415.2	20	54%	10.8	1.38
SGMAV-08A*A		7%	415.2	20	22%	4.47	1.56
SGMAV-10A*A		7%	415.2	10	30%	2.95	1.73
SGM JV-02A*A		7%	415.2	15	87%	13	1.07

Figure 37: SigmaSelect results

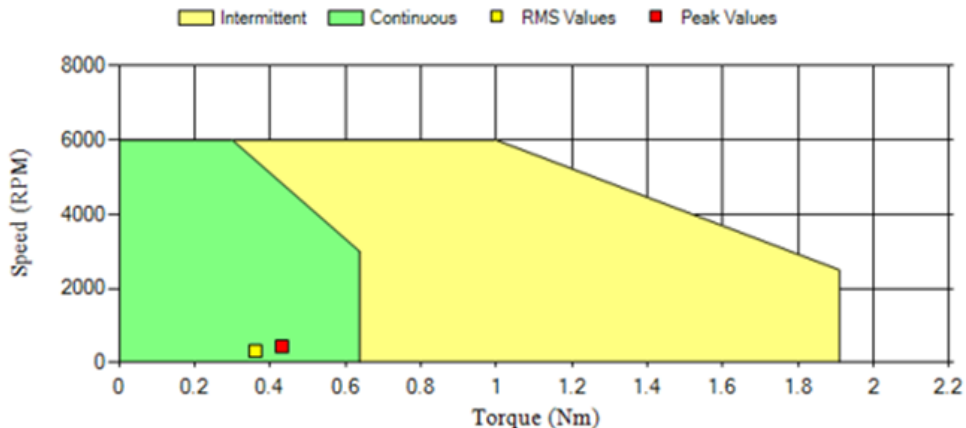


Figure 38: Torque-speed curve for Yaskawa SGMJV-02A*A servomotor

When we reported our selection to Yaskawa, they recommended a slightly different motor, the SGMJV-02A3A6C. Selected pages of the brochure for this motor are in Appendix E.

The only effect of the counterweight was that it increased the motor's inertia, giving us only a 13:1 "application motor inertia ratio" instead of 23:1. According to the Yaskawa engineers, increasing the motor's inertia would help stability, since the motor inertia would more closely match the application's inertia. They also assured us that the ServoBelt system's transverse force on the motor shaft would not pose a problem.

We took our motor sizing results to Bell-Everman, who approved our motor selection for the application. Mike Everman originally told us to use any NEMA-23 or 60-mm motor. Our calculations above resulted in the smallest NEMA-23 motor Yaskawa sells, which confirms that our motor sizing calculations were correct. The torque-speed curve for this motor is shown in Figure 38.

Optional accessories were selected, such as a holding brake, 3-meter cables, 100-VAC power supply, and straight shaft with key cut. Thus, the full model number of the selected motor is

SGMJV-02A3A6C. Selected pages of the brochure for this motor are in Appendix E.

Mechanism Components

In this section we will explain the design process for the components that comprise the mechanism that positions the print head. These are the linear slides, mechanical links, and end effector plate.

Linear slides

The Bell-Everman linear slides play a key role in the success of our printer. Since these slides are purchased parts, we do not have to do detail design beyond specifying how long they need to be and where to tap holes. Many of our other design decisions depended on the linear slides, not the other way around.

The kinematic code and build volume calculations allowed us to determine the necessary amount of linear travel needed and the resulting configuration of the linear slides. The slides selected need to have 840 mm of vertical travel and be offset 120 mm from the bottom plate so we do not have unused travel at the bottom of the slides. Due to these requirements we will need the 1000-mm ServoBelt Light slides with 1120-mm T-slot

extrusion. Refer to Figure 39 to see this offset. The slides will not have linear encoders, and we will rely on the rotary encoders of the Yaskawa servo motors for accuracy. Linear encoders can be installed at a later date if deemed necessary.

The ServoBelt carriages will have two M4 tapped holes in the lower section of the face plate. These holes will house the balls of the magnetic joints. The ball centers will be spaced 50mm to give the arms adequate spacing. The balls will be located at the bottom of the face to ensure clearance for the rods from the motor mount and wires. See Figure 40 for the placement of the balls.

The ServoBelts will be built on a 60-by-60-mm Bosch T-slot, which will act as the vertical supports to our printer. T-slot allows for easy fixation to the top and bottom plates.

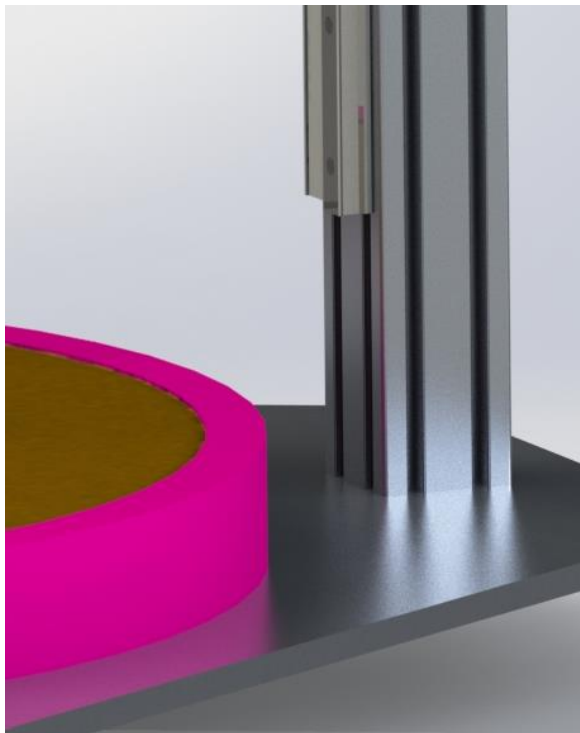


Figure 39: 12-cm vertical offset of linear slide

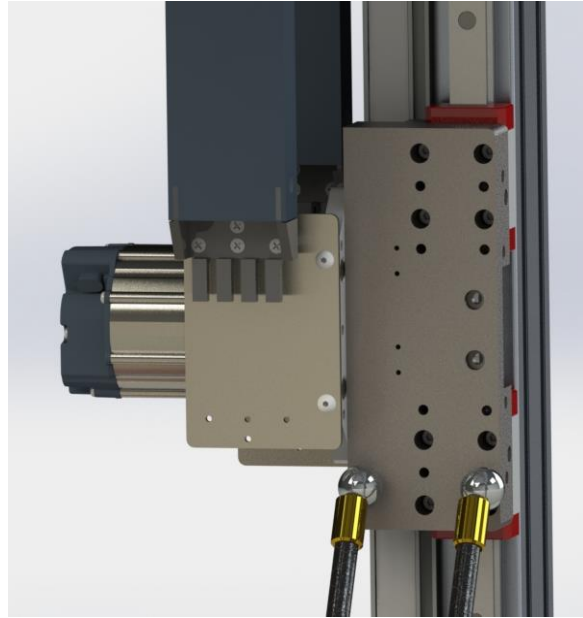


Figure 40: Configuration of chrome balls on ServoBelt Light carriage

Links and fasteners

This section discusses all components that connect the linear slides to the extruder plate, specifically the magnetic ball joints, composite rods, and epoxy adhesive.

Magnetic ball joints

The magnetic ball joints consist of two parts, the cylinder that houses the magnet and the metal ball to which the magnet is attracted. The cylinder housing creates a barrier between the ball and the recessed magnet allowing the ball to move more freely while still having a magnetic force holding it in place. The magnetic cylinder will be epoxied to the carbon fiber rod ends, and the ball will be connected to the end effector and ServoBelt carriage. There will be 12 joints in total, two for each rod.

The magnetic joints are purchased parts, and the metal balls have threaded screws attached to allow for easy installation onto the carriage

and end effector plate. We will be purchasing the parts from TMC Magnetics, a United States-based company.

We have determined that the KD-418 holding force of 49 N will be sufficient for our application. The hand calculations were simple and can be seen in appendix A. The joints cost \$20 each. Several sizes are shown in the TMC Magnetics online catalog. The KD-418 joint can be seen in Figure 41.



Figure 41: KD-418 magnetic ball joint

Composite rods

The arms of our delta mechanism will be unidirectional carbon fiber rods. These rods need to be lightweight and stiff in the axial direction. The major design considerations to be made are what diameter of rod should be used and to what length they should be cut.

The carbon fiber rods will be a purchased part from ACP Composites. We have initially purchased 0.25" and 0.375" rods for testing, to ensure the quality of the company and to choose between the two different sizes.

The MATLAB kinematics simulation dictated that the rods be cut to 460 mm in length. This

length is measured from the face of one magnetic joint cylinder to the face of the one on the other end of the rod. This dimension is shown as L_r in **Error! Reference source not found.** in Appendix A.

The remaining decision, about the diameter of the rods, turned out to be driven more by manufacturing concerns than by weight or stiffness considerations. Neither size presents any issues in terms of weight or stiffness. The vast majority of the weight of our mechanism is in the extruder and motors, so the rods' weight is negligible. Axial forces are not a problem because the magnetic ball joints will come apart long before any appreciable deflection is seen in the rods.

The rods we chose are the 0.375"-diameter, 24"-length Vinyl-Ester Based Matrix carbon fiber rods, whose specifications can be seen in Appendix E. These rods cost \$14 per piece from ACP composites. These larger rods will be easier to interface with the magnetic ball joints, as explained in the following section.

Epoxy adhesive

We plan to adhere the rods to the rod ends via epoxy. To achieve more surface area for the adhesive, we selected the wider, 0.375" cross section. As long as the tensile strength of the epoxy is such that the force required to pull it apart is greater than the maximum holding force of the magnetic joints, the rods will not fail first.

Some brief research on temperature-resistant epoxies suggest that the epoxy best suited for our application is Loctite Hysol E-40HT, which can be purchased for \$18. Its specification sheet is shown in Appendix E. It is heat-resistant, able to handle temperatures over 100 °C, allowing us to use it on the ball

joints that will be in close proximity to the heated bed and the extruder. The holding strength is 30 N/mm^2 . We have surface to surface gluing area of roughly 71 mm^2 so even if our bond strength is only 1 N/mm^2 we still have 71 N of holding force. This holding force is larger than our magnetic holding, so our joints will release before the epoxy comes close to breaking its bond. Both the carbon rods and the brass will have to be treated prior to gluing.

In order to maintain identical rod lengths, the rods will be epoxied in a fixture that holds the lengths constant. The rods will then be measured using a CMM, coordinate measuring machine, to determine the final length. We have purchased a test rod with which to perform measurements of epoxy strength.

End effector plate

The end effector plate is responsible for mounting the proximal extruder and the positioning the chrome balls of the rod ends.

The extruder will be fastened to the plate with the four threaded screws with which it comes, and its tip must be located directly below the center of the plate. The plate must also have internal sections cut out to be able to fit the cooling fan for the hot end.

There will be three sets of chrome balls, one for each rod, and M4 holes must be made in the extruder plate to accommodate these balls. Each pair of holes will be spaced 50 mm apart, as they are in the linear slides, and each of the three sets will be equally spaced from the center of the plate. The orientation of the extruder as it prints is critical, so the positional tolerances on these holes are tight.

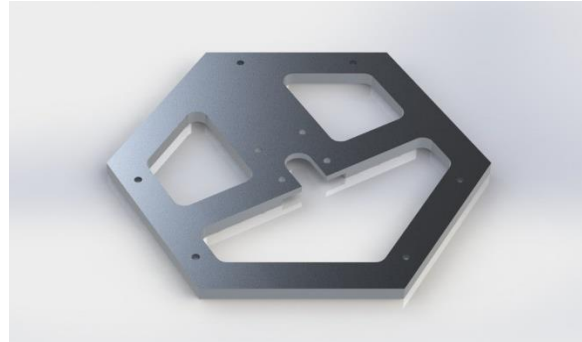


Figure 42: SolidWorks render of extruder plate

A SolidWorks render of the end effector plate is shown in Figure 42. For a material, we decided to use Al 6061-T6, the same material as the top and bottom plate, because of its high stiffness and light weight. We want the end effector plate to be as light as possible, so we will cut out extra interior sections while maintaining an interior structure to hold the extruder. SolidWorks estimates the final mass of the plate to be 0.15 kg.

A render of the plate interfaced with the extruder can be seen in Figure 43. The dimensioned drawing can be seen in Drawing CP002 in Appendix F.



Figure 43: SolidWorks render of whole extruder subassembly

Heated Build Plate

The heated build plate was a late addition to our design considerations. We had thought,

since there were many heated beds available on various 3D printing websites, that this would be an entirely purchased part. However, our design calls for a surface of 60-cm diameter, which is larger than the heated build plates readily available. Thus we will have to assemble one ourselves.

The heated build plate will be made of glass due to its excellent flatness and thermal properties. Aside from the glass, a heating element and insulation system must also be designed for the subsystem.

Glass surface

There are many types of glass suitable for our application. We are primarily concerned with flatness, since an uneven surface can compromise the accuracy of print jobs. It turns out, however, that typical flatness tolerances for glass are well within our requirements.

The first quote we received for a 60-cm-diameter glass surface was from Technical Glass Products. The item was a 0.125"-thick, ground, polished fused-quartz disc and was priced at \$1915. Fused quartz is the strongest glass available and is capable of being ground extremely flat. However, its superior qualities are overkill for our design, and this is reflected in its prohibitive cost.

Our next choice was soda-lime glass, which is commonly used in windows. According to manufacturer Specialty Glass Products, soda-lime glass has an average roughness of 100 Ångströms, or 0.01 µm. This is two orders of magnitude less than our layer thickness. A 60-cm-wide, 2.3-mm-thick disc was quoted at \$350, a more reasonable figure for our project. We will use the soda-lime glass.

Heating element

The temperature of the surface must be hot enough for ABS plastic to stay soft after being laid down by the extruder. There must be a powered heating element that can change the temperature of the glass surface. The resulting problem that must be solved in order to size the components is a three-dimensional, transient heat transfer problem with many variables. To turn this into a soluble problem, we made some assumptions.

First, we assume that the plate has reached steady state at a temperature of 110 °C. This is a valid assumption because the vast majority of the operational time will be spent maintaining this constant temperature. The glass surface will have a resistive temperature device (RTD) in order to provide feedback to the controller of the power supply. This allows us to control surface temperature.

Our next assumption is that, since the diameter of the heated build plate is much larger than its thickness, it can be modeled as a one dimensional composite wall problem. This is a valid assumption as long as the edges of the plate do not transfer significant amounts of heat. Insulating the edges of the build plate would increase the validity of this model, although not by much. As an approximation, this will yield relevant results and allow us to size our components.

Initial design

Our first design was a do-it-yourself heating system in which the heating element was nichrome wire adhered via Kapton tape in the configuration shown in Figure 44. For this system, the heat transferred is a function of the total length of wire in the grid, and the

Kapton tape ensures that this heat is distributed evenly across the glass bed.

The solution to this heat transfer problem was carried out in EES and is shown in Appendix A. The first run was with free air beneath the heater, not foam insulation as in the figure. It quickly became clear that air is not a suitable insulator for our system. The estimated power requirement while using air as insulation was on the order of 1.8 kW. Industrial insulation, such as fiberglass, silicone sponge, or similar, reduced this power input to below 500 W.

With the power requirement determined, the heating component could be sized. Assuming that we used 24-gauge Nichrome 60 wire, a grid of total length 4.7m would be required. Accurately laying out an evenly spaced 4.7-m grid of wire would be a daunting task.

Final design

Fortunately, upon further research, it turned out that there are purchasable components that can fill this role for us. Silicone heating mats are available in various sizes and power densities for relatively low cost. Most of the EES code used for the initial design was recycled for this design.

This pad would eliminate the need for an aluminum plate above the heating element, as the heat is spread evenly across the surface of the silicone mat. Thus, some of the cost of the heating element is immediately offset. The pads have pressure sensitive adhesive, which makes attaching the heater to the glass as simple as peeling and sticking. The product we have selected is on Figure 45.

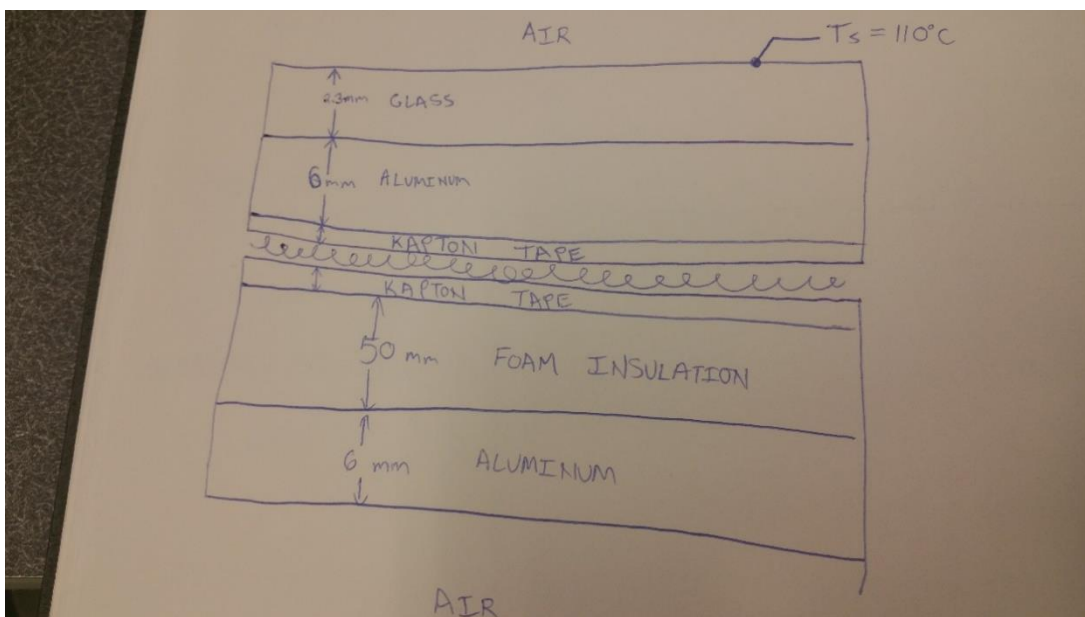


Figure 44: Sketch of one-dimensional heat transfer system for heated build plate



Figure 45: Heating pad for build platform

Insulation

The results of the heat transfer analysis rapidly indicated that air is unsuitable as insulation. Free air convection currents beneath the heater would rapidly cool the bottom of the plate, resulting in less heat reaching the surface and wasted efficiency.

With sufficient insulation, we can set the heated build plate to use less than one-third the power required using air as an insulator. First we considered using fiberglass industrial insulation, like the kind seen in Figure 46. However, exposed fiberglass insulation is hazardous to the lungs.

At the recommendation of Dr. Macedo, we replaced this with two sheets of 3-mm-thick medium density silicone sponge insulation. In order to ensure that this would be adequate insulation for our design, we modified the EES code to account for the change in insulation. The modified EES code is shown in appendix A. Based on this result, we determined the new insulation thickness to be adequate.



Figure 46: Industrial fiberglass insulation

Top and Bottom Plates

The role of the top and bottom plates is to rigidly hold the three columns in alignment while the printer is in motion. In designing the plates we considered material type, geometry, and how to fasten the T-slot extrusions.

Material

We originally decided on using a steel plate because of its good machinability, and high stiffness for a reasonable cost. We changed our mind when we calculated that the weight of a single steel plate would be upwards of 100 lbs.

We then decided to change our material to an aluminum alloy. Three aluminums were considered 6061-T6, 2024, and 1060. When comparing stiffness it was easily determined that Al 1060 was not a valid choice for our high precision design. Both of the other alloys were comparable in terms of stiffness. Al 6061-T6 has an elastic modulus of 69 GPa, and Al-2024 has an elastic modulus of 72 GPa. Since the stiffnesses of the two alloys were so similar,

we decided that the extra 3 GPa wasn't worth the extra cost of Al 2024.

Geometry

The thickness was designed to be 6-mm thick plate, but when we contacted Next Intent, a local private machine shop, they advised us to increase the thickness of the plate to a 12-mm plate in order to help minimize the thermal expansion and hold tighter true hole positions.

The shape of the plates was first determined to be triangular in order to minimize the number of necessary cuts. However, in order to save material cost, the corners of the plates will be cut off. This allows us to use smaller aluminum plate from which to cut. Instead of optimizing each plate, the top and bottom plates will be identical in terms of size and shape to decrease the cost of machine set up.

The flatness tolerance of these plates is paramount, since the linear slides will be mounted on them and need to be properly aligned with one another.

Fastening

Lastly, the holes in the plates needed to be precisely positioned so that each linear slide is the proper distance and direction away from the center of the machine. The hole pattern for the corners of the plates was determined from the cross section of the Bosch 60-mm T-slot seen in Figure 47.

For maximum alignment precision we will be using two 24-mm press fit dowels with an LN fit. These dowels will fit into the square corner holes on the T-slot cross section. By using two dowels we are locking in the position of the vertical column. The two press fit holes will be machined to very high positioning tolerances.

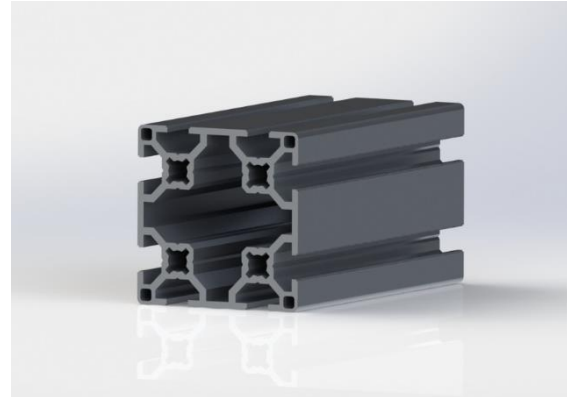


Figure 47: Bosch 60-mm T-slot extrusion

In order to secure the plates tightly to the extrusions we will be using four M8 countersunk sock head screws threaded into the four inside holes of the t-slot cross section. This pattern is illustrated in Figure 48.



Figure 48: Hole pattern for T-slot and plates

The extrusions will be shimmed if determined necessary for a desired alignment. There will also be a 25-mm hole in the center of the plate through which to feed the 3-mm filament. The final plate dimensions can be seen in drawing CP001 in Appendix F.

Enclosure

Our enclosure was a late addition in the design process, after we realized how necessary it

would be. It is required to perform the following main functions:

- To prevent the emission by ABS of toxic acrylonitrile fumes
- To keep the motors between 0 °C and 40 °C ambient temperature while still allowing the glass bed to reach 110 °C
- To keep body parts away from pinch points and hot elements

Enclosing the printer was originally a “nice-to-have” safety feature as far as we could tell, since we thought its main function was to prevent people from touching it during a print job. It wasn’t until we visited Bell-Everman’s facility and experienced acrylonitrile fumes firsthand that we realized we couldn’t avoid enclosing our robot.

Building an enclosure around the printer introduces its own set of concerns. Between the heating pad for the build surface and the three heavy Yaskawa motors, there will be a high amount of heat created inside the enclosure. The ventilation system must therefore also keep the printer cool.

Ventilation system

In order to size the ventilation components, we created an energy balance around the enclosure. That is, the rate of energy entering the control volume is equal to the rate of energy leaving it. The major sources of energy entering the control volume are three 200-W motors, the 680-W heated base, and the 60-W heater on the extruder. Other sources of heat, such as the resistive heating of the energy chain, can be safely neglected. They will be easily offset by the free convection along the enclosure’s exterior walls. The calculation for the heat transfer of the base and the overall

cooling requirements was performed using EES. This calculation is shown in Appendix A.

From the EES code, $CFM_{each} = 146.2 \text{ ft}^3/\text{min}$ is the required rating for each of the two fans in order to cool the enclosure such that the base remains at 110 °C for an ambient temperature of 35 °C and a room temperature of 25 °C.

Upon calculating the CFM rating, we sought guidance from Dr. Jesse Maddren. His first recommendation for keeping the motors cool was to put the motors on the exterior of the enclosure. After we explained that our ServoBelt Light require the motors to be mounted on the moving carriages, he recommended that we mount two or more fans to the top surface of the enclosure. Each of these fans would be pulling air out of the enclosure, resulting in lower than atmospheric pressure inside of the build volume. Air would be pulled in through the gaps and cracks around the edges. This would in turn mean that no air is going to escape the enclosure while the fans were on, except by going through the fans.



Figure 49: Yield Lab charcoal filter
(Source: GrowAce)

If all of the air, and therefore the acrylonitrile fumes, are pulled through the fan, then we can filter the fumes using an inline carbon filter. In Figure 49 is a picture of a 190-CFM fan with inline carbon filter, originally for use in hydroponics. This will be perfect for our application. The factor of safety on the volumetric flowrate provided by these fans, compared to the required volumetric flowrate calculated above, is 1.3.

Acrylic walls

Acrylic is the logical choice for the material of the enclosure walls. It is inexpensive, lightweight, easy to machine, and transparent.

4'-by-8' sheets of acrylic can be bought from the Home Depot for \$98, and we would need two of them to cover all the exposed areas. Attaching the acrylic plates to the aluminum top and bottom plates is simple. Accuracy is not a concern here, so L-brackets and wood screws will suffice. We need to be able to access the enclosure, so we will put hinges on one corner. The opposite end of that sheet of acrylic will have an L-bracket and two magnets to ensure that the door remains closed. This may be outfitted with electronic and/or mechanical stops so that the enclosure cannot be accessed during a print job. All of these small components can be bought from the Home Depot.

Extruder

Here we will discuss the basic considerations in selecting an extruder for our 3D printer. Essentially, the extruder needs to be able to print ABS quickly and with reliable precision.

We initially considered designing our own extruder. That was quickly abandoned, however, as we realized that the thermal

control elements and manufacturing of complex internal parts would be beyond the scope of this project. Attempting to design an extruder would likely result in an extruder with inferior performance to that of a commercially available extruder. So we redirected our efforts toward finding a high-performance extruder that would, above all else, be able to print very quickly.

After some correspondence with various extruder manufacturers, the extruder that we selected is the Micron3DP "All Metal" state of the art 3D printer extruder, in Figure 50. This is the fastest and most accurate 3D printer extruder that is commercially available.

The extruder is by far the most influential component in any 3D printer design, since the speed with which the machine can print ultimately depends on the extruder. Any 3D printer is only as fast as its slowest part, which is invariably the extruder. The extruder will be by far the least accurate of all components in the design.

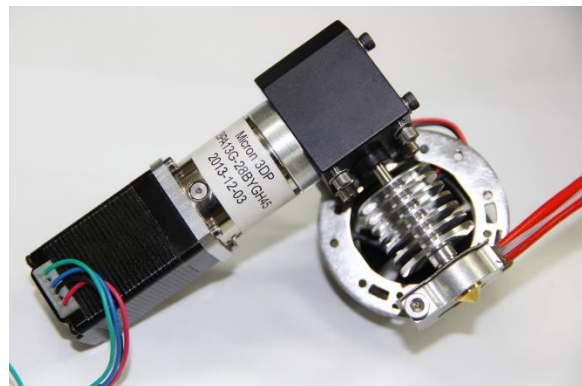


Figure 50: Micron 3DP "All Metal" extruder
(Source: Micron 3DP)

In an email between Justin and Eran Gal-Or, an engineer at Micron3DP, Gal-Or stated "we had managed to print at 400mm/s - ABS - 0.01 layer thickness, but you should be able to print at a higher rate with a rigid machine and a

matching temperature." We are confident that we can achieve a linear speed of greater than 500 mm/s, and we intend to push the limits of the extruder in order to print this fast. How far we can push will be determined after testing.

Electronics Design

The software that we will be working with is Yaskawa's MotionWorks software, which is based on the industry-standard IEC 61131 programming languages for programmable logic controllers (PLCs). The MotionWorks software that we are writing will convert the motion profile of the print head into motion profiles for the three motors connected to the Bell-Everman ServoBelts using the inverse kinematic equations described earlier.

We will have a slicer program running on a PC that converts an STL file to G-code. After converting the file, the program will transfer the G-code to the PLC over a transmission control protocol (TCP) connection. This means that the PLC upon startup and initialization must open a socket and begin listening for TCP requests. The PC will act as a TCP client and will send a request to begin a streaming session with the PLC. They will perform a three-way handshake, and from that point the PC will begin streaming the G-code file to the PLC. The packet size for streaming will be chosen such that the PLC consistently has instructions to be executed in its buffer. Once the file is completely done streaming, the PC will close the socket to let the PLC know it will not be receiving any more instructions.

Mechanism control

This section discusses how the delta mechanism is controlled by the electronics and what hardware is used to do so.

The plan

Our MotionWorks program will consist of three primary tasks running concurrently. Tasks are lines of code execution that will run at different speed cycles and different priorities. A state diagram for this process is shown in Figure

One task will be reading G-code from the TCP socket and storing it in a circular buffer. This will likely be our lowest task in terms of priority and speed.

The second task will be reading commands from the circular buffer and executing them. However, we will be performing movement commands as a special case in order to ensure linear motion within the tolerances we have selected. Since we are using the delta mechanism, gearing the axes together for performing movements would not result in linear movement like it would for a Cartesian mechanism.

In order to overcome this, we will take advantage of a feature in MotionWorks that allows us to create a virtual set of "gantry" axes that can model a Cartesian system for 3 dimensional movement. In this gantry there will be 3 virtual axes/servos with virtual absolute encoders. We will gear these axes together so that they perform movements simultaneously and so they start and stop at the same time. This will ensure that the virtual system will always move in a straight line when it is instructed to do so.

The actual movement commands of physical servos and the use of the inverse kinematics will come into play in the third task. The third task will be running at a much faster rate than the first two tasks and likely at the highest priority. The third task will make use of the

encoders on the virtual gantry system to consistently read the position of the virtual gantry during a move. The system will then perform the inverse kinematics and send the motion commands to the physical servos to move rapidly to the new calculated positions. This process is summarized in Figure 51.

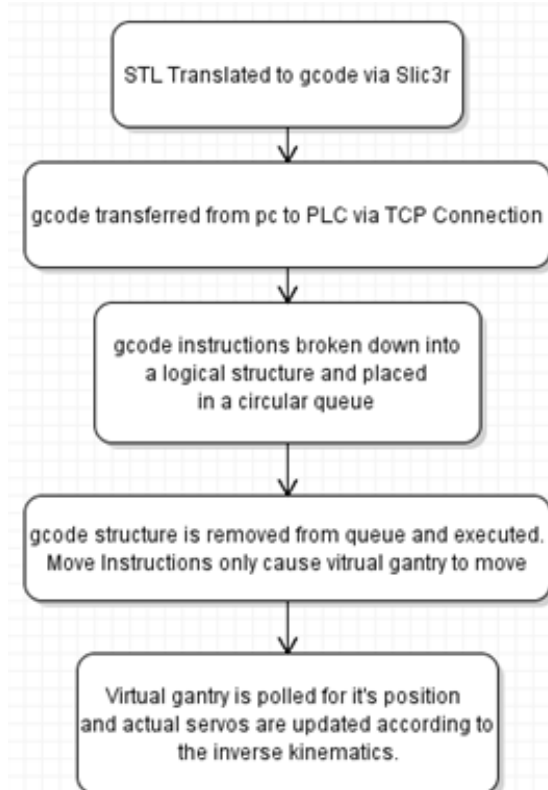


Figure 51: Data processing from STL files

This system should allow the controller to take a linear controlled motion, which will be modeled by the gantry, and break it down into many high-speed incremental movements. By tuning and altering the scan rate of the various tasks, we can make the increments small enough that the error due to the nonlinearity of the extruder's path doesn't cause positional errors that exceed our tolerances.

Final implementation

The electronic assembly involved creating various circuits for interfacing with peripheral devices, wiring the various controllers as a network, and ensuring appropriate power distribution and grounding. A schematic of our design is shown in Appendix C. The assembly consists of the following components:

- MP3300 iec: A Programmable Logic Controller which runs the logic implemented in the Motion Works Project.
- Three Servo Packs: Combined amplifier and controller for individual servos, they are a part of the Mechatrolink 3 network and are slaves to the MP3300.
- Three Regenerative Resistors: These resistors are used by the Servo Packs to dissipate servo momentum as heat.
- Stepper Drive: This device controls the extruder stepper motor; it takes in a pulse train, and a digital value for direction. Every rising edge of the pulse train advances the stepper one increment.
- Two 24V Power Supplies: One supply is used for powering the PLC and the digital control I/O Module, and the other is used for powering the servos' holding brakes and other peripheral devices including the actuated lock, and stepper driver.
- Two 12V Power Supplies: One supply is used for powering the extruder's heating element, the other is for the extruder's fan.
- LI01 Terminal connector and Block: A digital I/O Module consisting of a circuit board installed into the MP3300 and a DIN rail mounted terminal block. This is used for controlling the digital peripherals like

the stepper drive, and door lock. The digital signals from this module are generated by open collector sinking transistors.

- Three CN Servo Pack Terminal Blocks: A digital I/O Module that allows access to the Servo Packs digital control signals specifically the digital outputs used to control the servos' holding brakes.
- Three DC Solid State Relay: Relays used for servo holding brake control. The relays are actuated by the digital outputs of the Servo Pack CN Terminals. Their purpose is to isolate the holding brake power from the PLC and Servo Pack Power.
- VIPA I/O Ethernet Module: A networkable I/O Module that is a slave to the MP3300. This module uses Ethernet Industrial Protocols to read and write analog outputs; it can be upgraded/expanded to handle a wide variety of I/O. In this design the device is used for reading temperature measured by the extruder's thermistor.

Extruder control

The MICRON3DP All Metal Hot-End Extruder contains four primary components that are used in the control of extrusion of plastic. There is a 60-W resistive heating element, which melts the plastic as it is pushed through the nozzle, an NTC 100-K Ω thermistor next to the heater to measure the temperature at the nozzle, a NEMA-11 stepper motor which pulls the plastic through the nozzle via a hobbed gear and a small fan to prevent overheating.

The heating element and thermistor are used together to achieve the appropriate temperature of the nozzle at which the plastic is properly melted and not burned. The recommended temperature to melt and

extrude ABS plastic is about 230 °C. In order to measure this temperature, the voltage divider circuit in Figure 52 below was set up to measure the voltage drop across the thermistor.

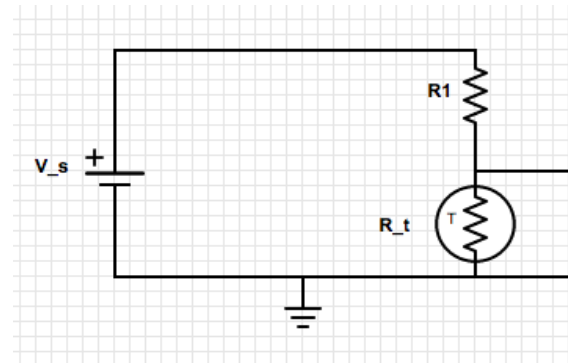


Figure 52: Circuit used to measure thermistor voltage drop

The resistance of the thermistor changes with temperature, so the voltage drop across it will also change as the temperature changes. The resistance can be determined with the following voltage divider relationship, where $V_s = 12.3$ V and $R_1 = 981 \Omega$:

$$V_t = \frac{R_t}{R_t + R_1} V_s$$

With a known resistance of the thermistor, the temperature can be extrapolated from data provided by the manufacturer of the thermistor. The provided data was plotted using Excel and a relationship between resistance and temperature was determined. A plot of this data from 85 °C to 250 °C is shown below in Figure 53, along with the equation relating temperature to resistance.

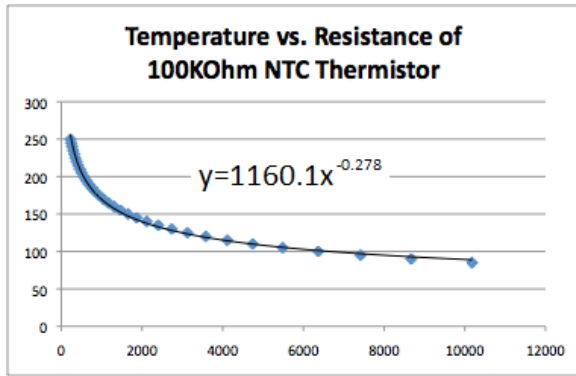


Figure 53: Plot of manufacturer data for extruder temperature calibration

In testing, this relationship was used to find the relationship between the voltage drop across the thermistor and temperature so that this measurement can be directly used in the feedback loop for temperature control. This data can be found in Appendix E. This data should be used to create a lookup table in software so the heater can be turned on and off according to the deviation from the desired temperature.

The heating element is controlled via a sinking switch in the I/O module. Since there is no variation of the voltage supplied to the heater, it is simply switched on to add heat and off to remove heat.

The fan is run at all times so as not to overheat the extruder. There is currently no control loop set up, although that may be desired in the future in the interest of preserving the life of the fan.

The stepper motor is controlled with an AMCII stepper motor driver. The motor driver, as it is currently configured, receives a square wave

and a digital signal for direction to control the speed and direction of the stepper motor. It then outputs the appropriate sequence to the motor. See the AMCII stepper driver reference manual for more information on configuration settings.

The signals sent to the stepper driver (that is, the square wave and the direction signals) are digital signals from the I/O module.

Control of other components

This section describes the plan for control of subsystems in the 3D printer that require control systems.

Motors

The servo motors will be controlled with Yaskawa's MotionWorks IEC software. The means for creating the desired motions are described above.

Heated Build Plate

The heated build plate control system consists of one input and one output: the silicone heating pad and a thermistor on the surface of the bed plate. The point of this control loop is to maintain a steady temperature on the bed.

Ventilation Fans

The ventilation fans will be powered upon system start-up and will run the entire time the system is powered. They have manual speed controllers attached and are not connected to the rest of the electronics.

Table 15: Selected final designs

Parameter	Value
Linear slide travel length	84 cm
Build volume	50-cm diameter, 33-cm height
Motor	Yaskawa SGMJV-02A*A
Rod length	46 cm
Heated build plate diameter	60 cm
Insulation	Fiberglass
Extruder	Micron 3D "All Metal"

Thermal Expansion

For an ME 404 final project, team member Taylor Chris partnered with Andrew Chang to use Abaqus FEA to predict the effect of thermal expansion on the frame of the printer. A copy of the report for this project is included in Appendix A.

Final Design Summary

Our major design selections are summarized in Table 15. See Drawing CP004 in Appendix F. Here we will make some final notes on this design related to accuracy and cost.

Accuracy

As mentioned in the extruder section of this chapter, the limiting factor of the printer is the

extruder. Although we don't have exact numbers, we suspect the inaccuracy associated with the extruder and filament is far higher than simply anyway.

The nozzle top will be well within our positioning accuracy goal, but the material that is extruded will not be. If others were to improve upon our design, the extruder is the logical thing that needs to be replaced.

Cost

The total cost of all components is estimated to be \$4645, over 90% of our budget. Appendix C will contain a final budget spreadsheet once the project is complete.

CHAPTER 6:

MANUFACTURING AND

TESTING PLAN

Introduction

Here we will explain the remaining steps toward completion of our project. We will put forth a manufacturing plan, which explains how we plan to assemble our robot once all parts have arrived. We will then discuss how we will verify that our product and its individual components meet our goals.

In Table 16 we have summarized the key dates for the Delta 3D Printer senior project, as stipulated in the course syllabus. A more detailed schedule in the form of a Gantt chart is given in Appendix B. The Gantt chart puts each phase of the project and its associated critical tasks on the same timeline.

Manufacturing Plan

This section details the processes by which we will manufacture the various components and subassemblies and the final prototype. We are not manufacturing many things ourselves, so this is more of an assembly plan than a manufacturing plan.

Bell-Everman Slides

The linear slides will be assembled and tested at Bell-Everman. We will be assisting in this process, however, to ensure the quality and performance of their slides. We will go to the Bell-Everman site to assemble it with them. We will be constructing one slide with the Yaskawa servomotor and verifying the vertical performance of the motor slide integration. Once we are sure that the motor selected is the correct, we will leave it to Bell-Everman to construct the remaining two slides.

Frame and End Effector Plates

With tight tolerances and large plates, we are unable to manufacture the frame plates in the shops on campus. The construction of the plates will be done by Next Intent, a custom machine shop in San Luis Obispo. The outside of the plates will be water jet cut to the rough shape and the hole patterns will be CNC drilled by Next Intent. The critical holes will have a 0.254-mm (.001") true position tolerance.

Table 16: Key events and deadlines for ME senior design project

Item	Quarter	Week	Date
Project Proposal	Fall	5	10/21/14
Preliminary Design Report	Fall	8	11/14/14
Final Design Report	Winter	4	02/05/15
Critical Design Presentations	Winter	5	02/05/15
Manufacturing and Test Review	Winter	10	03/12/15
Project Update Report	Winter	10	03/12/15
Engineering Project Expo	Spring	9	05/29/15
Final Project Report	Spring	10	06/08/15

Carbon Fiber Rods

To manufacture the carbon fiber rods we will need to design and build a fixture to cut them all to the same length. It is not as important that the slides are exactly 46 cm as it is that the rods are equal in length to one another.

After the rods are cut, they must be epoxied to the magnetic cylinders. A simple solution for this could be to use two table clamps, one to hold each magnet, and a V-block to hold the carbon rod in position. This jig simply needs to hold the magnets onto the carbon fiber rods while the epoxy dries. Once we have assembled a carbon rod with each of its magnetic ends, we will check the overall length using a coordinate measuring machine (CMM) and record this value for modeling and accuracy purposes.

End Effector Assembly

The end effector will be assembled in house. The balls for the magnetic joints will be screwed into the holes, and the end effector will be placed into the center and screws inserted. If need be, the extruder will be shimmed to ensure that it is level with the print bed.

Printer Frame

The frame will be assembled in house. The 4-mm dowel pins will be press fit into the plate first. The slides will then be aligned by putting the dowel pins into the square holes of the vertical slides. Once the slides are aligned, the M8 countersunk socket head screws will be put into the remaining holes. Once tightened, the model will be measured using a laser interferometer to measure the alignment. The slides will be shimmed as needed.

Heated build plate

The heated build plate will be assembled in house. The silicone mat is very easy to affix to the glass plate, because the pressure sensitive adhesive makes it as simple as to peel and stick. The kitchen silicone pads will simply be layered under the heating pad.

Acrylic enclosure

Acrylic panels will be cut to size and affixed to the top and bottom frames. This requires cutting the panels using wood shop tools, such as table saws. Exact sizes will not be helpful—gaps will allow air intake which is needed because of negative internal pressure. For aesthetic purposes, we will want reasonably straight edges and not huge gaps.

Testing Plan

This section contains information about what methods we will employ to confirm that our design is working as intended. We will be testing some parts and subassemblies before the final assembly is built. We also have a plan for what tests to run once the prototype is constructed.

Component testing

There are some parts that we will want to begin evaluating as soon as they arrive. In particular, these are the extruder, composite rods, and linear slides.

Extruder

The maximum print speed that the printer can achieve is ultimately limited by the extruder. The extruder must be able to extrude material at an appropriate speed relative to its linear speed. To find the maximum speed with which

we can move the extruder and achieve an acceptable print, we have devised a test that will move the extruder horizontally along a lead screw track at varying speeds and temperatures. The extruder will be mounted onto a platform driven by a lead screw attached to a servo motor. By varying the linear speed, feedrate, and temperature, we will be able to find the optimum operating point, including the maximum linear velocity that will produce an acceptable print.

Rods

The carbon fiber rods and the magnetic ball joints that hold them to the ServoBelt carriages need to be able to withstand the forces transmitted through them from the movement of the print head. A tensile test will be performed on the rods using the Instron machine in the composites lab. The magnetic joints will be tested with a simple pull test using a tension gauge. We will test the epoxy bond between the magnetic joint cylinder.

The linkages also need to be within strict length tolerances. Once the rods and magnetic joint rings have been epoxied, these sub-assemblies will be placed in a Coordinate Measuring Machine (CMM) in one of Cal Poly's Manufacturing Engineering labs. The CMM will determine the length of the sub-assemblies to within several microns. These lengths will be used in the control software to account for small offsets and inconsistencies.

ServoBelts and servomotors

The linear ServoBelts from Bell-Everman will need to be calibrated via control of the Yaskawa servo motors. This is a simple matter of using one of Cal Poly's laser vision systems to find the position of the motor carriage after sending a motion command, and comparing it to the expected position.

System-level testing

Once the printer is fully assembled, we will need to verify that it can function as intended.

Linear slides and inverse kinematics

By the time the printer is fully built, we should have code written that commands the linear slides to move according to the inverse kinematics of the delta mechanism. This code will be tested and calibrated to match the actual kinematics of the machine, which may differ from the virtual model. The height of the nozzle can be measured using a dial indicator attached to the extruder platform.

Precise extrusion

Once we have verified that the printer moves as intended, we can begin printing shapes. We will begin by printing lines across the glass bed to verify accuracy and tune the feed rate of the extruder according to the velocity of the nozzle. After that, we can begin printing multiple layers and making test parts.

CHAPTER 7:

MANUFACTURING

DETAILS

Introduction

This chapter is a detailed account of our manufacturing process. Most of the events described took place during spring quarter. For assembly, testing, and material storage, we had access to Bldg. 197 (Bonderson), Room 110, conveniently located next to Mustang '60.

Individual Components

In this section we will discuss the production procedure for the components in our design that required us to perform manufacturing processes prior to their inclusion in the full assembly. In particular, these are the plates for the frame and extruder, the carbon fiber arms, and the heated build plate.

Aluminum plates

The machining of the aluminum plates was the most difficult aspect of our manufacturing process and had by far the greatest impact on our overall timeline.

Next Intent

As mentioned in the previous chapter, we had outsourced the manufacture of the aluminum plates to a local machine shop called Next Intent. This plan, however, was abandoned early spring quarter.

During a verbal conversation, Next Intent estimated the plates would take three weeks to arrive and cost about \$2000, with the possibility of a significant student discount. We then received a quote from Next Intent for \$3000 with an eight-week lead time. This was because the top and bottom plates were too large to machine in one pass, even for their equipment, and therefore required further outsourcing to a San Francisco company.

At this point, we started seriously considering the possibility of having the machining performed in house by the Mustang '60 shop. In doing so we would have to compromise our .001" tolerances, but it was necessary because of time constraints.

Mustang '60

The verbal quote Mustang '60 gave us was \$16/hr, plus material costs, and a lead time of one or two weeks, including setup. The formal agreement was for the machining to be done by April 20, giving them three weeks from the beginning of the quarter. This allowed us about a week and a half to achieve full assembly on schedule—by April 29.



Figure 54: IME department's hydraulic shear

We provided the plates and all the necessary tooling. We ordered our 6061-T6 aluminum plate through discountsteel.com, which cost \$460, plus \$192 for shipping. We had Ladd Caine, the IME department's shop technician, help us use the department's large hydraulic shear to cut the edges and corners, leaving one cold-saw-cut edge from which to reference all of the hole positions. The hydraulic shear is shown in Figure 54 above. The extruder plate would be CNC milled from one of the corners

cut off by the shear. The three plates and all required tooling were left in our project room while we waited patiently for Mustang '60 to pick them up and cut them down.

When the deadline was over a week past, we met with them to discuss why we weren't receiving any replies to our requests for status updates. We found out that the student shop technician had been unable to perform the CAM programming due to conflicts with his classes. We were told that if the shop techs had known how much of a "headache" this project would be, they would not have taken it in the first place.

The problem was the sheer size of the plate and the accuracy we wanted for the positional tolerance on the hole patterns. For reference, see the detail drawings in Appendix F. The size of the plate meant that no machine on campus could machine all three hole patterns in one pass. To fix this, Dr. Macedo came up with the solution of using precision locating pins, press fit into holes drilled into both the aluminum plate and the plate on which it would be machined. The first two patterns could be drilled in the VF3 Haas tool room mill, along with the locating pin holes. Then, the center pin could be inserted, and the plate rotated into its new position.

Our new plan became to have the top and bottom frame plates machined in the IME machine shop by Ladd Caine, with assistance from us. Eric Pulse, supervisor of Mustang '60, agreed to still machine the smaller extruder plate in Mustang '60.

Now we will describe the making of the small extruder plate, and the discussion of the top and bottom plates will be continued in the next section. The extruder plate was CNC milled in Mustang '60, the code written by Eric Pulse.

The detail drawing of the part is shown in Appendix F. Below in Figure 55 is a photo of the part after it was removed from the mill.

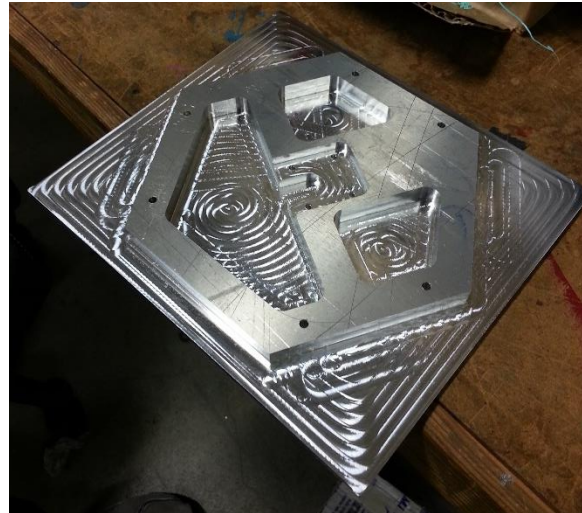


Figure 55: Post-CNC extruder platform

The excess material seen in the picture then needed to be removed. Eric Pulse did this via fly cutting on a manual mill. Unfortunately we neglected to get photos of this process. As the layer of excess material became very thin, the corners began to resonate, creating jagged edges. To fix this, Eric used a band saw to cut the corners closer to the body of the part before fly cutting the rest.

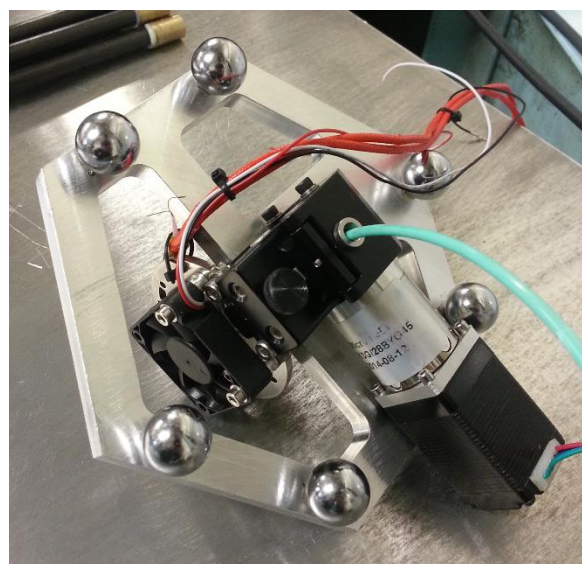


Figure 56: Final assembly of extruder platform

After the fly cutting operation, the part was de-burred, the six outer holes tapped, the magnetic balls threaded through them, and the extruder mounted. Figure 56 is a photo of this finished component.

Ladd Caine's shop

Now we will go over the details of CNC milling the large frame plates with Ladd Caine in his small shop in Bldg. 41. The CNC code was initially written by Eric Pulse but modified by Ladd during setup. All of the machining was done in nearly one week in early- to mid-May. Throughout the process we would take turns visiting him and assisting with setup and whatever else was needed, since none of us has extensive CNC experience.

To accomplish the necessary precision on the top and bottom plates, we worked closely with Ladd. First, we removed the protective sheet

metal siding of his Haas machine, shown in Figure 57, as the plate would not otherwise have fit on it.



Figure 57: Haas protective siding

To begin setup, Ladd used a dial indicator to ensure that the underplate was square to the machine. The dial indicator was run across the entire length of the back edge. Once it was measured to be square to one ten-thousandth of an inch of total runout across that edge, the underplate was fastened down. This process is shown in Figure 58.



Figure 58: Ladd Caine aligning the back edge of the underplate



Figure 59: Aligning and clamping the aluminum plate

The aluminum frame plate was then clamped down loosely on top of the underplate. As shown in Figure 59, we used the dial indicator to ensure that the aluminum plate was square, again to one ten-thousandth of an inch.

Next, we set up all of our tooling, including a center drill, two reamers, a countersink, and three drill bits. Shown in Figure 60 are all of the bits used for the first aluminum plate, laid out on top of the plate.



Figure 60: Tooling used for the first plate

After inserting the tooling, we found the center of the plate by measuring from several points on the edges. Ladd used the center drill to make a small mark at the scribed center and

set that point as the zero of the first operation. We then used an edge finder to make sure that the machine knew exactly where the back edge of the plate was, relative to the center.



Figure 61: Center of plate and edge finder

The first operation on each plate was to drill two of the hole patterns, then cut an L-shaped slot as a reference for the third pattern, which could not be reached in the same operation

due to limitations on the machine's travel. The second operation was simply to finish the final hole pattern.

Ladd began by running the first operation of the drilling process a few inches above the plate to ensure that the tools wouldn't run in to anything we didn't want them to. Our clamps were very close to some of the holes, so extra caution was needed to ensure that no damage would be done to the machine or to us. Ladd let the machine run while we made notes on the line numbers of the G-code at which we were concerned about running into a clamp. After checking those numbers and running through them, he changed some offsets and moves to make sure that nothing would crash.

During the actual operation, we stood by with WD-40 in one hand, to use as coolant for each hole, and the other hand on the stop button, in case of a crash.

One of the acrylic mounting holes was to be center drilled right through the middle of the slot in the clamp. This would have been fine, but one of the Z offsets was set slightly off and the tool ran into the clamp. Fortunately, we were watching carefully and hit the stop button before it went more than a couple of thousandths of an inch, and the tool and clamp were unharmed. The rest of the first operation continued without a hitch.

We took the plate off and removed the burrs from the underside of the plate, which could have otherwise prevented it from sitting flat on the underplate after rotation to the second operation. We cleaned up the underplate, making sure to remove any burrs.

We put the plate back on, clamped loosely, then Ladd indicated the new zero based on the L-shaped slot cut into the aluminum plate

during the first operation. The L-shaped slot can be seen below in Figure 62. We then tightened the plate down for the second operation. This operation went more smoothly, as we were more careful to ensure that the tool did not crash into the clamp.

After completing the second operation to finish the final hole pattern, we used dial indicators to tell us how far off the hole patterns were on their true positioning tolerance. The two hole patterns ended up being very close—within .0007". The third hole, as expected, was off by a bit more since the plate had to be picked up and moved for the second operation. It indicated out to be around .005" off of true position. While this was greater than we might have gotten from Next Intent, it is possible to calibrate for this positional error software-side later. The value of actually getting to work closely with an expert machinist like Ladd was more than worth the effort.

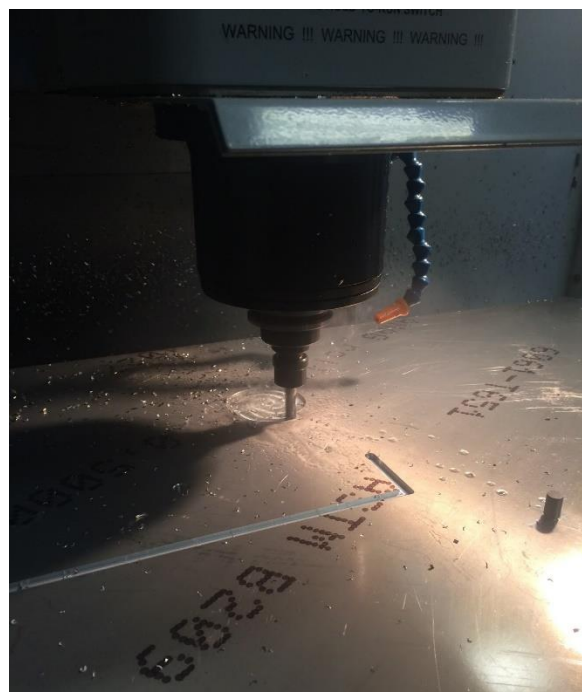


Figure 62: The 4" fan holes being end-milled and the L-shaped datum slot

While we were happy with the tolerances produced for the first plate, we wanted to make some changes to the second plate after discussion with Ladd. The biggest thing was that we wanted to have the 4" diameter fan holes end-milled out rather than trying to use a hole saw as we originally intended. This resulted in a much cleaner cut. Figure 62 is a photo of these holes being milled out.

One thing we found out was that our design's call for precision locating pins was useless, because the four larger diameter countersunk screws would have more pull than the four small corner pins. If the precision pin holes were off from the countersunk screws, the countersunk screws bend either the pins or the t-slot into which it was being screwed. Therefore, we removed the precision pin holes for the second plate and didn't utilize them on the first plate. The rest of the process of machining the second plate went much the same as the first.

After taking our finished plates back to Bonderson, we tapped all the outer holes for the enclosure and sanded down the entire surface of the plates to remove the scratches from shipping and machining.

Carbon rod assembly

To connect the magnetic brass cylinders and the carbon fiber rods end-to-end, we used a high temperature epoxy. The difficulty in manufacturing the rods came from keeping the lengths of the rods the same. The rods were cut to the same 46-cm length by cutting all the rods at the same time on a wet diamond blade tile saw. However, the critical dimension is the distance between the ends of the brass cylinders that contact the ball joints. The distance between ball centers is what forms the "effective arm length" in the kinematics.

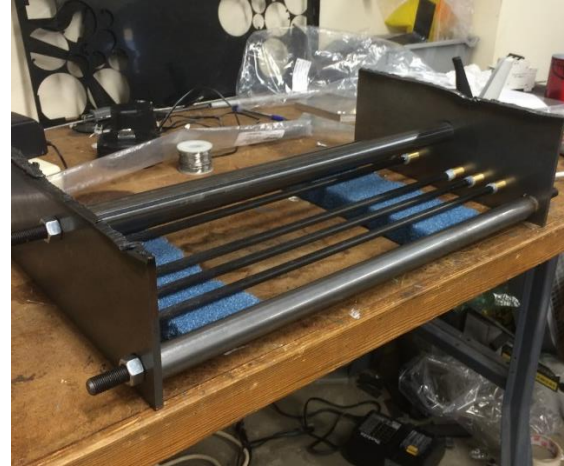


Figure 63: Fixture for arm assembly

To assemble the arms, a fixture was made to keep the length fixed while the epoxy cures, pictured above in Figure 63. Since the brass joints are magnetic, the ends of the fixture were two steel plates to which to stick the magnets. Three $\frac{1}{2}$ " threaded rods were placed through holes in the steel plates. The rods were cut using a chop saw and then grinded and filed down to be the same length. Three steel pipes with an inside diameter larger than that of the threaded rods were used to control the length of the fixture and ensure that the plates were parallel. Between the steel plates, the carbon rods were supported during the curing process using foam, as in the figure. The Loctite epoxy required a special 2:1 mixing gun and an epoxy mixing tip. Once the epoxy was applied, the plates were tightened against the pipes using $\frac{1}{2}$ " nuts.

Heated build plate

In a perfect world, this section would not need to be written. The task of adhering a circular glass plate to a circular silicone heating pad is trivial and unworthy of a detailed narrative. However, we initially ordered the incorrect type of glass for this application, and this produced a significant setback for us.

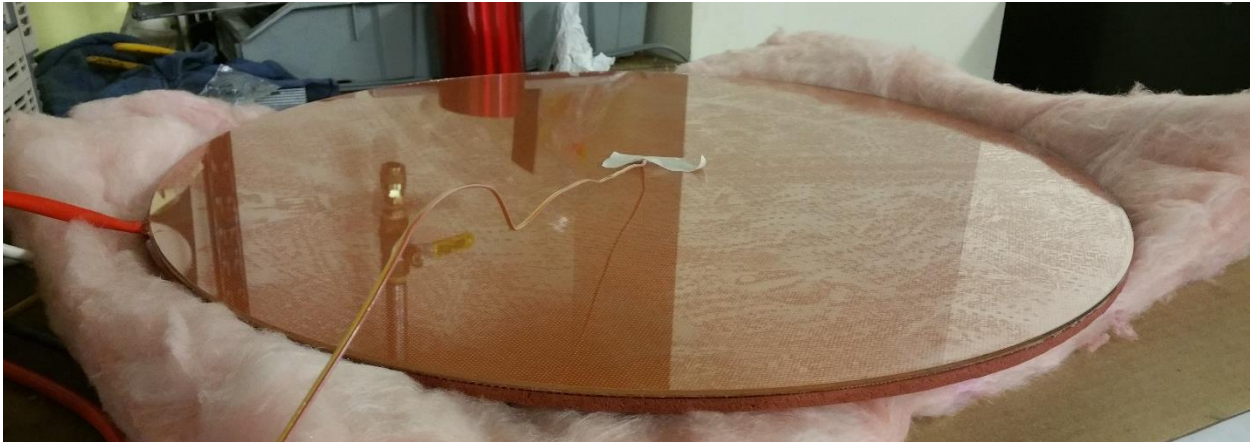


Figure 64: Initial soda lime glass bed temperature test

Initial problems

The soda lime glass that we initially ordered was easy to apply to the heating pad, and we began thermal testing immediately. Figure 64 above shows the initial temperature testing, in which a thermocouple was taped to the glass surface. Once the temperature of the surface reached 85°C , the glass cracked, in the pattern shown below in Figure 65. The heating pad

itself was not damaged, but we needed to apply a new piece of glass.

We now had the task of removing this broken piece of glass from the heating pad so that the new glass could take its place. We also needed to remove the adhesive from the heating pad so that a new adhesive layer could be cleanly applied. This process delayed further progress on the heated bed for several weeks.



Figure 65: Cracked soda lime glass

Recovery

To remove the broken glass plate, we first attempted to freeze the adhesive so that the glass could be removed intact. This rapidly proved impossible, as it was not making it easier to pry the glass from the bed. We then tried WD-40 to loosen up the adhesive as we slowly pried the glass off, which was working, but slowly.

The method that ended up working the best for removing the glass and adhesive was a painstaking process involving a paint scraper and Goo-Gone, which is an acetone-based adhesive solvent. Small fragments of glass would break off at a time, and used this method for the remainder of our efforts. This should never be attempted without gloves and safety goggles.

The next major problem we ran into involved wiring. Unsafe wiring procedures—namely, partly exposed 120-V wires—resulted in a blown breaker in the Mustang '60 shop. In response to this, the shop prohibited us from turning the pad on until we passed relevant electrical safety inspections, further delaying our testing process.

To rectify the wiring problem, we removed the bare solder joints, using insulated wiring connectors inside of a junction box. We also used insulated wire connectors to connect the ground of the pigtail to the ground wire on our frame. We checked all connections using a digital voltage meter. We waited to turn it on again until after passing electrical safety.

The next piece of glass we ordered was the same diameter, 50cm, but it was about twice as thick—.1875", or 4.76 mm. It was also made from tempered glass. Tempered glass is used

for oven doors and is safe to use in 3D printer heated build platforms up to 200 °C.

We asked the manufacturer of the silicone heating pad, Ankland Industries, for a replacement piece of 3M 468MP double-sided, pressure-sensitive adhesive. They supplied the adhesive for just the cost of shipping.

To apply the adhesive, we first degreased the heated pad using a 50/50 mix of water and 99% isopropyl alcohol and then let it dry for a couple of days. We then peeled back the plastic backing on the 3M and applied a small area at a time, using a credit card to apply pressure and smooth out some of the bubbles. Then, we put a large weight on the surface and let it sit for a while. Ankland recommended 12–15 psi, which we were unable to achieve due to time constraints. We filled a box with about 50 pounds of metal and set that on top instead and left it overnight. We peeled back the paper, leaving the adhesive exposed. We degreased the glass using the 99% isopropyl alcohol. Then, we set the glass on top of the adhesive, centering it as well as possible. The adhesive allows for some initial repositioning, meaning that if it had been slightly off center we could lift it off and reapply. Initial testing showed this new tempered glass to be far more resilient than the soda lime glass was at high temperatures.

Linear slide assembly

Bell-Everman performed the assembly of each linear slide in their shop. We mailed them the Yaskawa SGMJV-02A servomotors, and they sent us back the slides with the motors already mounted on the carriages.



Figure 66: Initial orientation of motor

Unfortunately, the motors were mounted in such a way that the main power cable was inaccessible due to the energy chain mount. The image in Figure 66 above shows where the motors were mounted on arrival. In Figure 67 below, the small white rectangular sticker is covering up the power cable plug, which is hidden by the black energy chain in the first photo. In both photos, the encoder cable port is visible near the top of the image.



Figure 67: Repositioned motor

To solve this problem, we needed to remove the motors, rotate them, remount them, and re-tension the belts. The process of mounting and tensioning the belts was done according to instructional videos from the Bell-Everman official website.

The next problem we faced was that the power plugs supplied by Yaskawa did not fit through the energy chain. In order to feed the power cable through, we had to dismantle the plug, carefully feed the cable through the energy chain, then reassemble the plug after pulling the power cable through the other side.



Figure 68: Yaskawa servomotor power plug

Even with this plug removed from the cable, it was impossible to feed the power and encoder cables through unless the chain was stretched out straight. It was a two-person job, with one person feeding the cable through the bottom, and the other using needle-nose pliers to gently work the end of the cable upward through the chain.

Full Assembly

In this section we will discuss the assembly of all components into a working prototype. Due to the aforementioned complications with the aluminum plates, this process did not begin until the middle of May, about two weeks before the expo.

The printer was assembled on top of a steel table given to us by Dr. Macedo. The table was used for a different project in the past and doubled as an electrical cabinet.

Overall frame and mechanism

As soon as all of the aluminum plates were machined, and their holes tapped, the linear slides were fastened on, and the basic frame of the printer was formed. Figure 69 is a photo of this assembly. Also shown in the picture is one of the Ventech fans, as we were testing the size and spacing of the 4" holes in the top plate.



Figure 69: Bell-Everman linear slides attached to top and bottom plates

The next logical step was to attach the arms and extruder to the frame to complete the mechanism. However, the carriages were too low on the columns to do this without the extruder interfering with the bottom plate, and at this point we did not have permission to power on the machine and elevate the carriages. We delayed this step until we met electrical safety requirements.

Acrylic enclosure and door

The next mechanical step in the assembly of our prototype was the attachment of the large acrylic sheets that form the enclosure. We had received donations from Cee Bailey's Aircraft Plastics, where Justin had done a summer internship, for all of the acrylic we would need for the siding. However, the linear slides were slightly longer than we anticipated when we asked for the acrylic, and the panels were too short. We asked Cee Bailey's for more, longer taller sheets, and they happily obliged.

To attach the acrylic sheets to the frame, we used $\frac{3}{4}$ " L-brackets screwed into the holes along the edges of the aluminum plates. Then, we laid the acrylic panels against the side of the printer, marking screw holes and edges. The sheets were cut to their final size on the table saw in Mustang '60, and the holes drilled with a cordless hand drill. The acrylic was screwed onto to each L-bracket with a nut and two washers to distribute the pressure from torqueing the screws.

The front panel had to be further modified so that a lockable door could be installed. Two vertical cuts were made on the table saw, and two hinges fastened to the left-hand side of the middle portion, creating the door. We attached a handle and electronic door lock to the right-hand side of the door, along with a magnet at the top-right to keep the door shut.

Fans and carbon filters

Due to a miscalculation in the manufacturing of our plates, the two fan holes in the top plate were placed too close together, such that the two impeller casings did not have enough clearance to fit side-by-side. We also realized that, if the fans and carbon filters were mounted directly onto the top of the printer as we had planned, the printer would be too tall to fit into the IME automation lab or into the elevator up to the lab.

In order to fix this problem, we decided to place the fans and carbon filters elsewhere and implement a 4"-diameter ducting system to route the airflow from the printer to the fans. There was inadequate space on top of the printer to allow both the fans and the ducting systems in any orientation. We decided to run the fans from the top of the printer to the inside of the cabinet. This helped save space and eliminate the fans from sight. The ducting can be seen in Figure 70.



Figure 70: 4" ducting as seen from above

Two 5"-diameter holes were cut into the sheet metal siding of the cabinet to allow the 4" ducts to pass through. These holes were cut using a hole saw and a drill press. The holes, and the ducting being routed through them, can be seen below in Figure 71.



Figure 71: Ducts and 5" holes into cabinet

Using the mounting brackets that came with the carbon filter fans, the fans were screwed into wooden boards to mount them in the cabinet. Due to the fans being oversized, the head losses due to the ducting will not take us below our necessary flow rates. Small support shelving was put in place to help support the weight of the filters. The mounting inside the cabinet can be seen in Figure 72.



Figure 72: Fans mounted inside table

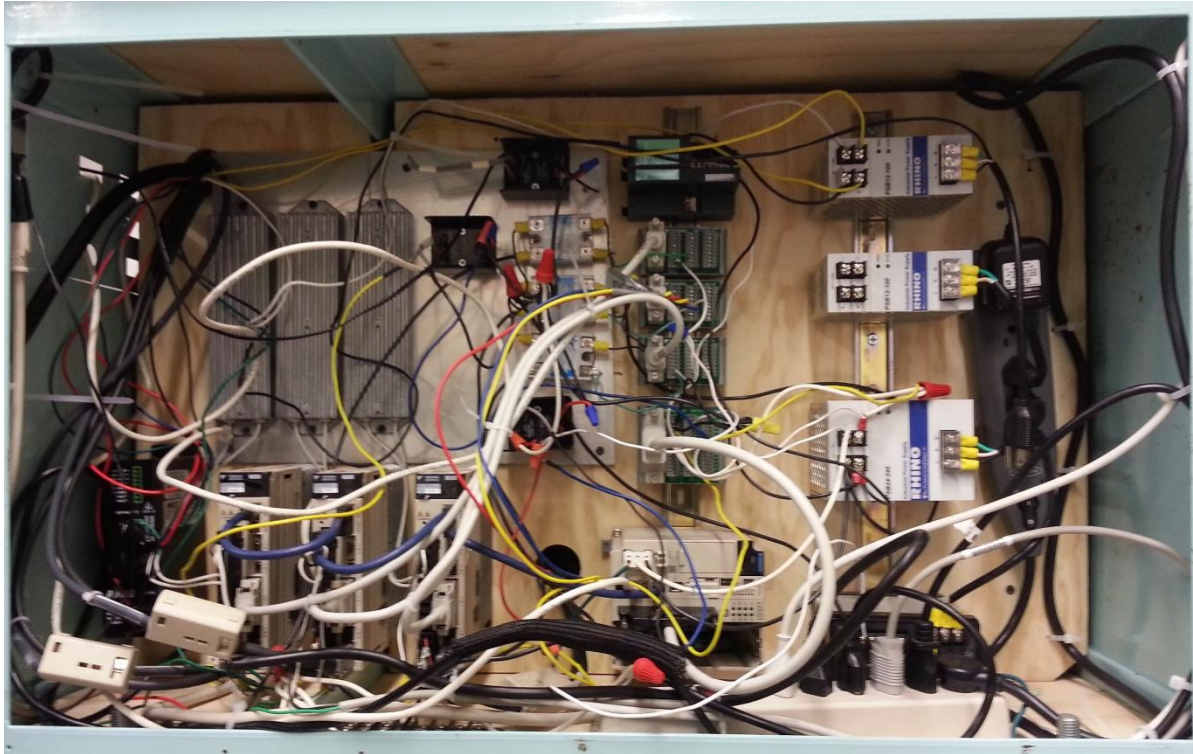


Figure 73: Control system and wiring

Mounting and wiring of electronics

In this section we discuss the process of mounting and connecting all of the electronics safely. As mentioned before, the metal cart was able to act as a base for printer as well as housing for its electronics and HVAC system. Outside of the cabinet, there was also wiring to be done for the extruder.

Control system

During the cabinet electronics mounting, the primary concern was to establish a clean path to ground and ensure that the components needing special care for heat dissipation were handled accordingly. A photo of our hardware under the table is shown above in Figure 73. Clearly, the wiring is a bit messy and ought to be cleaned up.

The PLC, power supplies and I/O terminal blocks were all installed using DIN rails attached to a plywood backing.

The Servo Packs and stepper driver were screwed directly into the plywood back panel. The regenerative resistors and solid state relays were the biggest concern for heat dissipation. Because of this, we mounted them to a steel plate with thermal compound at the point of contact. The plate was then attached to the plywood backing with washers acting as spacers to keep a layer of air between the plate and the plywood.

We established a path to ground by scraping away paint from a bolt connection on the cart. This bolt was then connected to the ground lead from power cable for the PLC's 24 Volt Power Supply. Because of this, the power strips into which the 24-V power supply was plugged now had all grounds linked to the cabinet itself.

Extruder wiring

There were many wires that needed to be routed from the cabinet to the extruder platform, all of which needed to be provided sufficient slack for the extruder to reach all areas within the build volume. Below in Figure 74 is a photo of the mess of wires that run from below the table, to the top of the enclosure, and to the extruder.



Figure 74: Loose extruder wiring

To clean this mess up, we encased the wires a long piece of shrink tubing, which can be seen in Figure 75. Zip ties were used to keep the wires firmly in the shrink tube, the filament tube fastened to the wiring, and the wires routed along one column away from the build volume below.



Figure 75: Extruder wiring in shrink tubing

Glass bed leveling

In order to calibrate the printer for printing the glass print bed needed to be leveled in relation to the bottom plate. The glass plate is sitting on three layers of silicone insulation mat to minimize the amount of heat loss to the aluminum frame. The original design was to have set screws under the plate to level the glass, however this design would be very difficult to accurately level the plate due to the silicone mats being compressible like a sponge.

Our final design for leveling used the compressibility of the silicone mats to our advantage. Instead of leveling the plate by pushing up on the bottom we decided to apply pressure to the top of the glass in three places. We used three high-temperature plastic leveling feet to apply the pressure to the glass to avoid damage to the print bed or melt the feet. These can be seen in Figure 76.

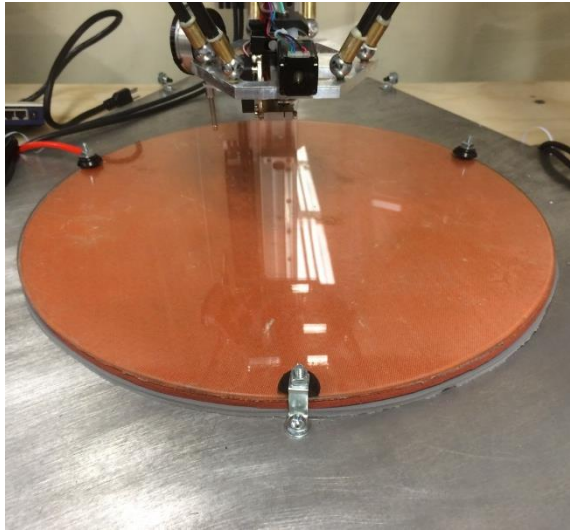


Figure 76: Bed leveling mechanism

The black plastic feet are rated for up to 177°C which is far above our operating temperature. The three leveling feet are connected to the bottom aluminum frame plate by using 1-1/4" Z-brackets. At the location of the Z-brackets, 1/4"-20 holes were drilled and tapped into the aluminum plate.

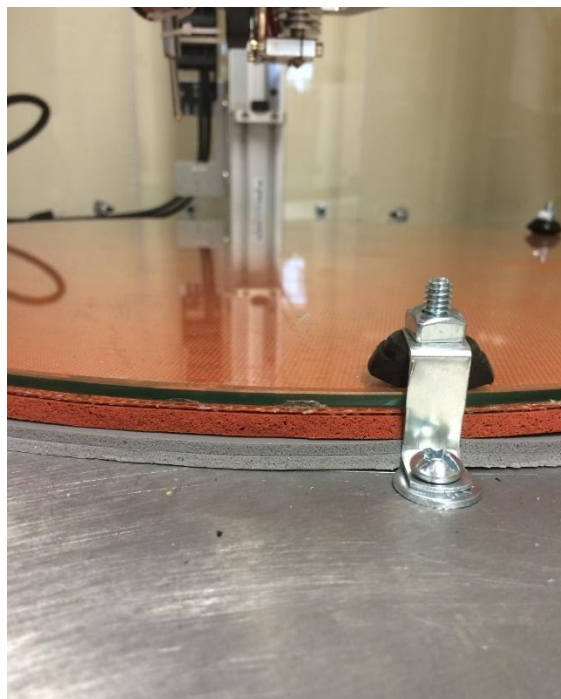


Figure 77: Close-up of a Z-bracket and plastic foot used to level the bed

The high-temperature feet were cut to fit with the Z-brackets using a Dremel and a cutting blade. The feet can be seen in Figure 77. The three Z-brackets are connected to the aluminum plate using 1/4"-20 threaded screws, which are used to adjust the leveling of the plate. Once the leveling feet and Z-brackets were installed the plate was leveled using a caliper to measure the distance from the glass plate to the aluminum plate.

Filament mounting and routing

To mount our filament spool, we purchased a HATCHBOX one-spool mounting rack and placed it on top of the printer. To route the filament to the extruder, we needed to eliminate friction so that the extruder gear could pull the plastic through. To accomplish this, we purchased 4-mm-ID, 6-mm-OD PTFE tubing and fed the 3-mm filament through. The tube was fed through the central hole in the top of the printer and zip-tied to the shrink-tubed wiring, as seen in Figure 75.

CHAPTER 8: DESIGN VERIFICATION

Introduction

Our full assembly and safety checks were not completed until a few days before the expo, so we did not have as much time to complete testing as we would have liked. As of the writing of this report, the printer is able to move but has not been properly calibrated. All of the individual components work as intended, including the extruder, but the full system is little more than a delta positioning robot that happens to extrude plastic, not a working 3D printer.

Heated Bed Calibration

Dialing in the exact temperature we want to set the heater to will be a matter of trial and error to improve print quality. However, we decided to measure the temperature of the glass plate under several conditions.

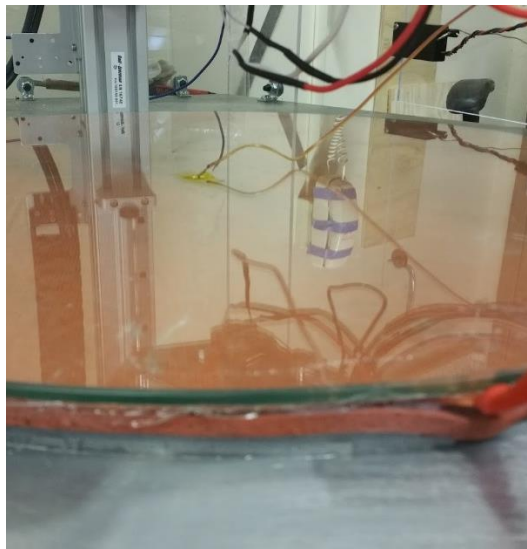


Figure 78: Thermocouple wire taped to glass

Transient response

The first condition was the time-dependent temperature response. The test setup involved using Kapton tape, as seen in Figure 78, to hold down a thermocouple onto the glass surface of

the plate. We then increased the thermostat control of the heating pad to determine the time it would take to get to operating temperature. This turned out to be well within the design requirement of under 30 minutes for warmup. In fact, it was sufficiently hot within five minutes.

The second part of the test was to look at the steady state temperature of the glass printing surface for different heating pad temperature inputs. This is important in determining the heat loss through the glass surface. The results of this test are shown below, in Figure 79.

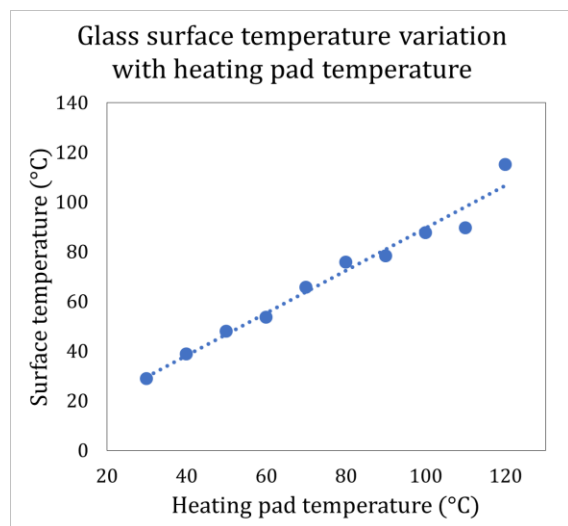


Figure 79: Glass heat loss calibration

The important thing to note is that the temperature range of 90 °C to 110 °C the glass bed should be is easily maintainable by the heating pad. Though the temperature did fluctuate somewhat after reaching steady state, the temperature gradient through the glass was not so huge that the heater would have to be set extremely high. In other words, if the insulation were insufficient, we could have cranked up the heating pad as much as we wanted to. We would never have been able to reach the required temperatures because we would lose too much heat through the bottom and edges.

Speaking of the edges, we also looked at the two-dimensionality of the heat transfer problem. We originally modeled the system as a one-dimensional heat transfer problem with heat generation. The validity of this depends on whether the glass and heater lose a significant amount of heat radially out through the edges. This impacts print quality because if the temperature varied too significantly over the surface of the glass, parts printed near the edge of the build volume would cool too rapidly, resulting in poor layer adhesion in ABS parts. Therefore, we put thermocouples on the surface of the glass in several radial locations and measured the steady state temperatures at each position.

When the center of the heated bed was set to 115 °C, the very edge was as low as 83 °C. However, points nearer to the center were well within the 20 degree “optimum range” for ABS printing, 90 °C to 110 °C. Thus, while parts printed at the very extreme most edges might have some trouble with layer adhesion, it will be minimal because the temperature is not far from the required range. This could be fixed by adding additional insulation around the edges or ordering a larger heater.

In addition, we noticed that the aluminum plate was warm, but not hot, shortly after turning off the heater. This means that the insulation was adequate. It would have been over 100 °C if the insulation was not working.

The final heated build plate test we performed involved using just the center thermocouple. We turned off the heating pad and measured the amount of time for the heated build plate to return to a safe temperature to touch. The glass reached 40 °C after 30 minutes. We would recommend leaving the door locked until 30 minutes after the device powers down to prevent injury.

Extruder Testing

The first extruder test was to verify that the temperature of the hot end could be controlled to reach the desired temperatures. The test data below in Table 17 and

Table 18 confirm that the temperature exceeds melting point of ABS is about 220 °C.

Table 17: Extruder calibration Trial 1

V (V)	R (Ω)	T (°C)
5.7	842	178.3
4.9	646	191.9
4.25	515	204.4
3.75	428	215.2
3.33	363	225.3
3.01	316	234.0
2.76	283	241.5
2.56	257	248.1
2.4	237	253.7
2.25	219	259.4
2.13	205	264.2

Table 18: Extruder calibration Trial 2

V (V)	R (Ω)	T (°C)
12.23	109069	46.1
12.12	54044	56.0
11.7	17934	76.1
10.88	7310	97.7
9.7	3604	119.0
8.38	2076	138.8
7.1	1329	157.1
6	928	173.6
5.2	714	186.7
4.49	561	199.6
3.96	464	210.5
3.51	390	220.9
3.17	339	229.6
2.89	300	237.6

After we verified that the temperatures were sufficient, we verified that the filament could be melted through the nozzle. We were able to extrude small pieces of ABS “spaghetti,” if you will, but that was as far as we were able to get on the extrusion front before expo.

End Effector Positioning

The only system-level testing we have been able to complete until this point is basic end effector positioning. When we moved the carriages according to the inverse kinematics equations, the end effector was able to position surprisingly well. It was far from being within desired tolerances, and the X and Y axes were not in the correct directions, but it did appear to be doing the correct thing to the naked eye. The incorrect orientations of the axes are a result of a mismatch between the carriage numbers in the code and those of the actual machine. Reordering the columns in the kinematics code should solve this problem.

At this point our goal was to get a single test move working, even if we had to use a brute-force method to get the print head to move parallel to the bed. We zip-tied a dial indicator to the extruder plate, as in Figure 80. We commanded the printer to move in a square parallel to the bed—at least, according to the uncalibrated kinematics equations. We then recorded the dial indicator’s reading at various points along the trajectory and offset the test move commands to correct for the error at each point. This is the code we ran at the expo and the extent to which the printer is currently calibrated.



Figure 80: Dial indicator zip-tied to platform

CHAPTER 9: CONCLUSION

Introduction

The small amount of testing that we did took us right into the expo. This chapter discusses that experience and future plans for the project as it gets passed on to other students.

Engineering Project Expo

The 2015 College of Engineering Project Expo took place on Friday, May 29. We exhibited our design in Bonderson, just a few feet away from the room in which we had built the printer. Below in Figure 81 is a photo of all of us at the expo. Mike Everman from sponsor Bell-Everman, Inc., was there, and so were Yaskawa team members Joshua Crayton and Hunter Stofferahn. We were also visited by friends, some by family members. Although we were only able to perform a single test move to show it off, it was gratifying being able to finally see the design working.

Recommendations

Since this is a project whose development will continue in the future, it is important that we give it some direction. There are some things that were never within the scope of a five-man ME senior project, which are the next logical steps to take in producing a competitive 3D printer. In addition, there are some things that we would do differently if we could time-travel back eight months with the knowledge we have now. This is where we will address both of those areas.

Metrology and software calibration

As mentioned in the previous chapter, formal kinematics calibration has not yet been done. The commands we gave the printer during the expo were written with brute-force offsets that only worked for that specific operation and no others.



Figure 81: The team with the final design and poster; from left to right—Stephen Marshall, Taylor Chris, Justin James, Ramon Santos, Paul Maalouf

Actually calibrating the printer will require, at the very least, precisely measuring the actual dimensions of the printer. These can be input to the inverse kinematics code, and other unwanted offsets can hopefully be calibrated out somehow. To verify that the nozzle is actually where it is intended to be, advanced metrology equipment could be used, perhaps alongside the forward kinematics code, which is described in Appendix A.

Extruder

With such high accuracy possible with the inverse kinematics, the extruder's accuracy is what really limits the competitiveness of this design. The one thing that would make the most dramatic impact on the performance of the printer—and this could be a year-long project on its own—is designing a brand-new extruder. We bought the best thing available to us at the time.

Most of the precision lost by FDM extruders comes from the unpredictable volumetric flow rate out of the hot end. In the current extruder, the gear connected to the stepper motor only can be controlled in open loop according to the commands given to it by the firmware, which assumes a constant filament diameter when outputting feed rates. In reality, FDM filament cannot be made to strict diametric tolerances, partly due to the viscoplastic nature of FDM materials such as ABS and PLA.

A more advanced extruder would somehow measure the cross-sectional area of the filament as it enters the extruder and adjust the feed rate in real time to ensure precise volumetric flow rates out of the nozzle. We think this would be easiest with a small servomotor controlled by the same PLC that controls the carriages. This way, all of the

movement commands from the firmware can be coordinated seamlessly.

In addition to more robust feed-rate control, a smaller nozzle diameter could be used. This would allow for more precise features but significantly increase printing times. A balance could be found between precision and printing speed. Or perhaps it could be designed to have multiple options for the user, depending on their requirements. It is also possible that both the feed rate and the translational speed of the nozzle could be increased to very high values. We are not experts in design of FDM extruders, so this last bit has been mere speculation.

Carbon fiber arms

One of our main concerns regarding accuracy on the mechanical side of the project has been the lack of concentricity between the carbon rods and the brass cylinders to which they are epoxied. The fixture we made for this epoxying process, which can be seen in Figure 63 in Chapter 7, did nothing to ensure that the elements were concentric. We “eyeballed” the concentricity and moved the cylinders until they looked good enough. In hindsight, we should have thought about this more before doing it. A quick visual inspection of the rods shows that, although the rod ends are the same distance apart in the axial direction, some of the brass cylinders are not aligned with the axes of their carbon rods. This type of error can cause the extruder platform to rotate slightly instead of strictly translating.

This effect has been untested, so the first step is to determine whether or not it is even a problem. This can be done by predicting it with kinematics and/or measuring it directly. We can see three ways to combat this problem, once it has been measured and confirmed to exist. The first would be to calibrate out the

error in the software. We don't know how difficult that would be. The other two involve redoing the rods entirely.

One way to redo the manufacturing process for the rods is to make a fixture similar to the one that we made but more robust so as to ensure that the rods are actually concentric with their rod ends. This would require buying new rods and magnetic cylinders, unless there is a way to safely dissolve the epoxy.

A second way, which may be easier, is to switch to hollow carbon-fiber tubes, instead of solid rods, and invert the magnetic joints so that the balls rest in the ends of the tubes. The threads on the balls would be unused and sit freely inside the tubes. The brass cylinders would be threaded into the extruder platform and the linear slides. Remanufacturing the arms this way would easily ensure that the elements were concentric. One downside of doing this is that the balls that are currently thread-locked onto the extruder plate and the carriages would have to be removed.

Glass bed leveling

Another source of mechanical inaccuracy is the crude method by which we leveled the glass bed, which was a trial-and-error process of tightening down the screws on the Z-brackets and shimming the bed with more silicone insulation. A more robust method should be employed for this.

Software

The software for this project is incomplete. Improvements that still can be made involve implementing a means for parsing G-code into easily formatted command tuples, breaking command reception and execution into two separate program tasks rather than one, and adding functionality for G-code instructions other than G0 and G1. Also, looking into a means for a smoother transition between movement commands and a better means for syncing the extrusion with the print head movements would be beneficial in achieving cleaner prints. As for hardware, rearranging the wiring so that there is less clutter would be beneficial for enabling faster access to various IO circuitry for modification.

Staying current

The 3D printing industry is very rapidly developing. There were many advances during the course of this project of which we are still unaware. This is partly due to stubbornness on our part—a desire to figure things out on our own. However, if we had done a better job of staying current on 3D printing enthusiasts' websites such as MakerBot and RepRap, our jobs may have been easier, and our product more relevant.

Operator's Manual

We have included in Appendix G a manual for operating the printer. We consider this a working document, as the procedures will evolve as the printer is modified in the future.

APPENDIX A: SUPPORTING ANALYSIS

Kinematics

Error! Reference source not found. on the following page shows one side of our mechanism, along with the relevant dimensions used in these calculations. These dimensions are described in Table 19. Note that all of the values listed in the table are preliminary values based on nominal dimensions. They are close to the actual values that should be used in the positioning code but not exact. Rigorous measurement and testing will be required to obtain the real numbers for these quantities, and they may even vary between the three “identical” sides of the machine.

Table 19: Variable definitions for kinematics computations

Symbol	Value	Description
ϕ	90°, 210°, 330°	Angular position of column counterclockwise from 1 axis
H_c	840 mm	Total travel length of carriage (not pictured)
R_c	400 mm	Radial distance to column
H_t	120 mm	Vertical distance between bottom of slide and aluminum plate
R_t	30 mm	Half-thickness of T-slot extrusion
H_g	60 mm	Height of glass surface above bottom aluminum plate
R_s	47 mm	Radial distance between stage surface and T-slot extrusion
H_s	17 mm	Height of outer rod ends above bottom of carriage
R_n	63 mm	Radial distance between nozzle tip and inner rod ends
H_n	51 mm	Vertical distance between nozzle tip and top of extruder plate
L_j	20 mm	Joint cylinder length
R_j	9 mm	Joint magnetic ball radius
L_r	460 mm	Carbon fiber rod length
θ_m	5°	Minimum angle between rods and horizontal

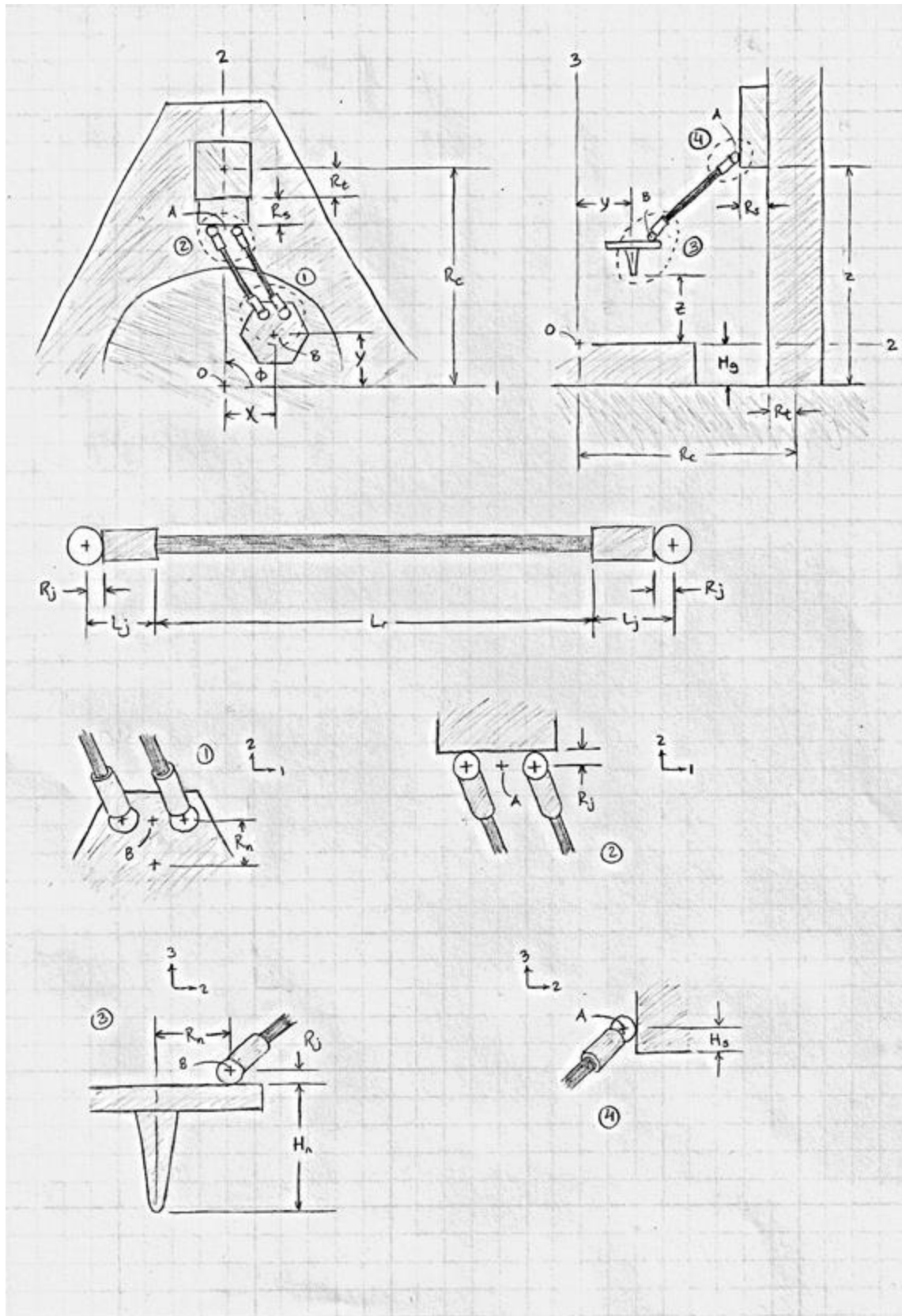


Figure 82: Illustration of variable definitions for kinematics equations

It is not necessary to include calculations for all three sides of the mechanism, since the equations are identical except for the column angle ϕ . To further simplify the analysis, we define the following quantities, where dimensions along the same axis have been lumped into “effective lengths”:

$$\begin{aligned} R_e &= R_c - R_t - R_s - R_n - R_j \\ H_e &= H_s + H_t - H_n - H_g - R_j \\ L_e &= L_r + 2(L_j + R_j) \end{aligned} \quad (\text{A.1})$$

Physically, this is the same as reducing the system to that shown in Figure 83, where offsets due to joints, print head geometry, and carriage size have been eliminated. This formulation will become especially useful when we consider the forward kinematics of the robot.

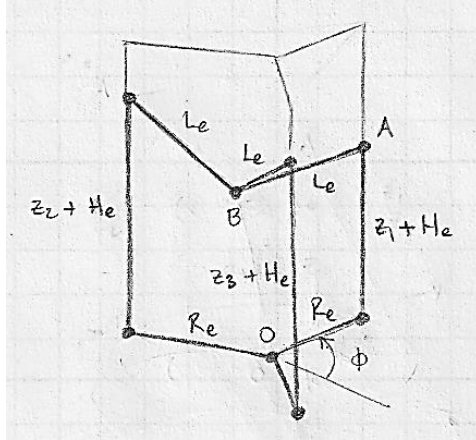


Figure 83: Effective link definition

If the height of a carriage is given by z , then its position, relative to its lowest position, is given by $(R_e \cos \phi, R_e \sin \phi, z + H_p)$. We denote the origin by O and the rod’s endpoints by points A and B , where A is on the carriage and B is on the nozzle tip. We can then define the vectors

$$\begin{aligned} \mathbf{r}_{OA} &= R_e \cos \phi \mathbf{i} + R_e \sin \phi \mathbf{j} + (z + H_e) \mathbf{k} \\ \mathbf{r}_{OB} &= X \mathbf{i} + Y \mathbf{j} + Z \mathbf{k} \end{aligned} \quad (\text{A-2})$$

where \mathbf{i} , \mathbf{j} , and \mathbf{k} are unit vectors in the 1, 2 and 3 directions, respectively. Subtracting \mathbf{r}_{OA} from \mathbf{r}_{OB} yields the following vector representing the member AB :

$$\mathbf{r}_{AB} = (X - R_e \cos \phi) \mathbf{i} + (Y - R_e \sin \phi) \mathbf{j} + (Z - z - H_e) \mathbf{k} \quad (\text{A-3})$$

Since the rod’s length is constant, computing the magnitude of this vector gives the equation:

$$L_r^2 = (X - R_e \cos \phi)^2 + (Y - R_e \sin \phi)^2 + (Z - z - H_e)^2 \quad (\text{A-4})$$

The carriage positions must therefore lie on a sphere originating at the print head’s position.

Inverse kinematics

The inverse kinematics solution can be easily obtained from Eq. A-4. Solving this equation for the carriage height z , we obtain

$$z = Z - H_e \pm \sqrt{L_r^2 - (X - R_e \cos \phi)^2 - (Y - R_e \sin \phi)^2} \quad (\text{A-5})$$

There are thus two possible positions of each carriage for any given print head position. This makes sense because a vertical line (the column) should intersect a sphere in two places (or none). One solution corresponds to the case in which the carriage is above the print head, and for the other solution the carriage is below the print head. Our design places the carriages above the print head, so we choose the greater solution:

$$z = Z - H_e + \sqrt{L_r^2 - (X - R_e \cos \phi)^2 - (Y - R_e \sin \phi)^2} \quad (\text{A-6})$$

These inverse kinematic equations, combined with other geometric constraints, can be used to calculate the exact build volume attainable by the printer. In addition to satisfying Eq. A-6, the configuration of the robot must also satisfy the following conditions.

Obviously, the tip of the extruder nozzle cannot be below the surface of the build plate. This constraint can be written simply as

$$Z \geq 0 \quad (\text{A-7})$$

It must also be true that the carriages do not exceed their maximum travel in either direction. The constraints for the bottom and top of a carriage are, respectively,

$$\begin{aligned} z - H_s + H_g &\geq 0 \\ z &\leq H_c \end{aligned} \quad (\text{A-8})$$

The first of these constraints is trivial, since the mechanism is designed so that the constraint in Eq. A-7 will be compromised first. That is, the print head will crash into the build plate before any of the carriages reach the bottom of their travel.

Next, the rods must point in toward the center of the mechanism so that they do not crash into the carriages. More specifically, the vector \mathbf{r}_{AB} defined in Eq. A-3 must not have a component in the direction away from the 3 axis. This condition is enforced by defining a vector \mathbf{n} normal to the face of the carriage and computing its dot product with \mathbf{r}_{AB} :

$$\begin{aligned} \mathbf{n} &= -\cos \phi \mathbf{i} - \sin \phi \mathbf{j} \\ \mathbf{r}_{AB} \cdot \mathbf{n} &\geq 0 \end{aligned} \quad (\text{A-9})$$

Finally, we intend to impose an angular constraint on the rods so that they do not become too close to the horizontal. This is a safety measure that will be implemented in the control system of the printer. This angle is implemented as follows:

$$\mathbf{r}_{AB} \cdot \mathbf{k} \geq L_e \sin \theta_m \quad (\text{A-10})$$

This constraint does not affect the build volume much. However, it should not be ignored when determining whether the chosen dimensions satisfy the project requirements.

All of the above equations were implemented in a MATLAB script, which is input an end effector position and outputs linear slide positions. The code is documented later in this section and uses the dimensions given in Figure 83 and throughout this section. The script generates plots of the build volume by sampling points in and around the build volume and plotting points that satisfy the requirements in Eqs. A-6 through A-10.

Shown in Figure 84 and Figure 85 on the following pages are the script's output plots, which were used to iteratively size parts and satisfy the build volume requirements. The columns' positions and geometries are plotted for reference.

Forward kinematics

We as of yet have had no use for the forward kinematics equations and haven't written any working code that performs those computations. However, the solution is obtained by trilateration, which is briefly explained here.

Trilateration is a method for finding the intersection between three spheres. A general set of equations for three spheres is

$$\begin{aligned} r_1^2 &= (X - X_1)^2 + (Y - Y_1)^2 + (Z - Z_1)^2 \\ r_2^2 &= (X - X_2)^2 + (Y - Y_2)^2 + (Z - Z_2)^2 \\ r_3^2 &= (X - X_3)^2 + (Y - Y_3)^2 + (Z - Z_3)^2 \end{aligned} \quad (\text{A-11})$$

where XYZ is the Cartesian coordinate system used in the inverse kinematics equations. The solution is obtained by solving this system of equations for X , Y , and Z . However, doing so is difficult, if not impossible. The solution is much simpler if the equations are transformed into an alternate coordinate system xyz , where

- the first sphere lies on the origin,
- the second sphere lies on the x axis, and
- the third sphere lies somewhere in the xy plane.

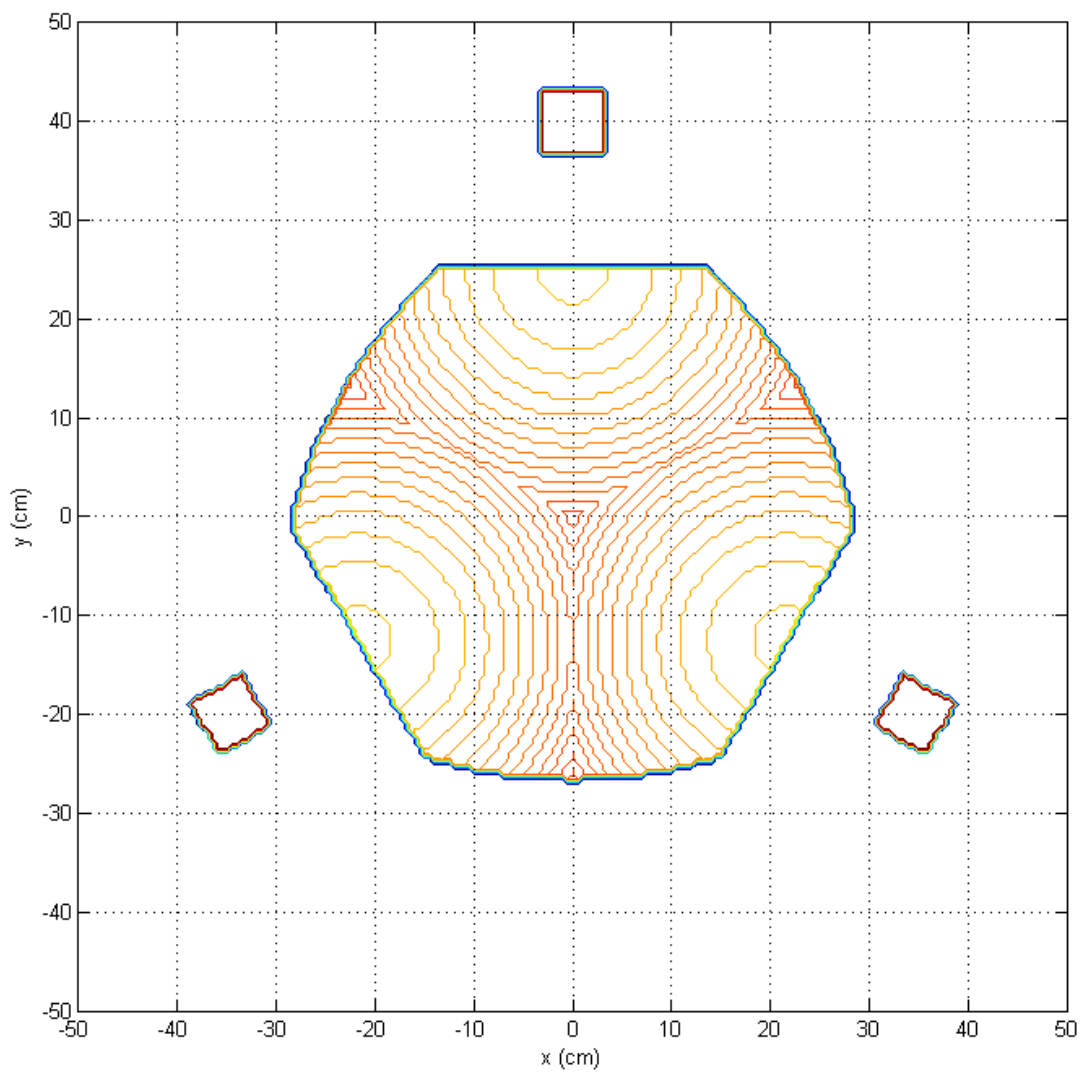


Figure 84: Contour plot of build volume

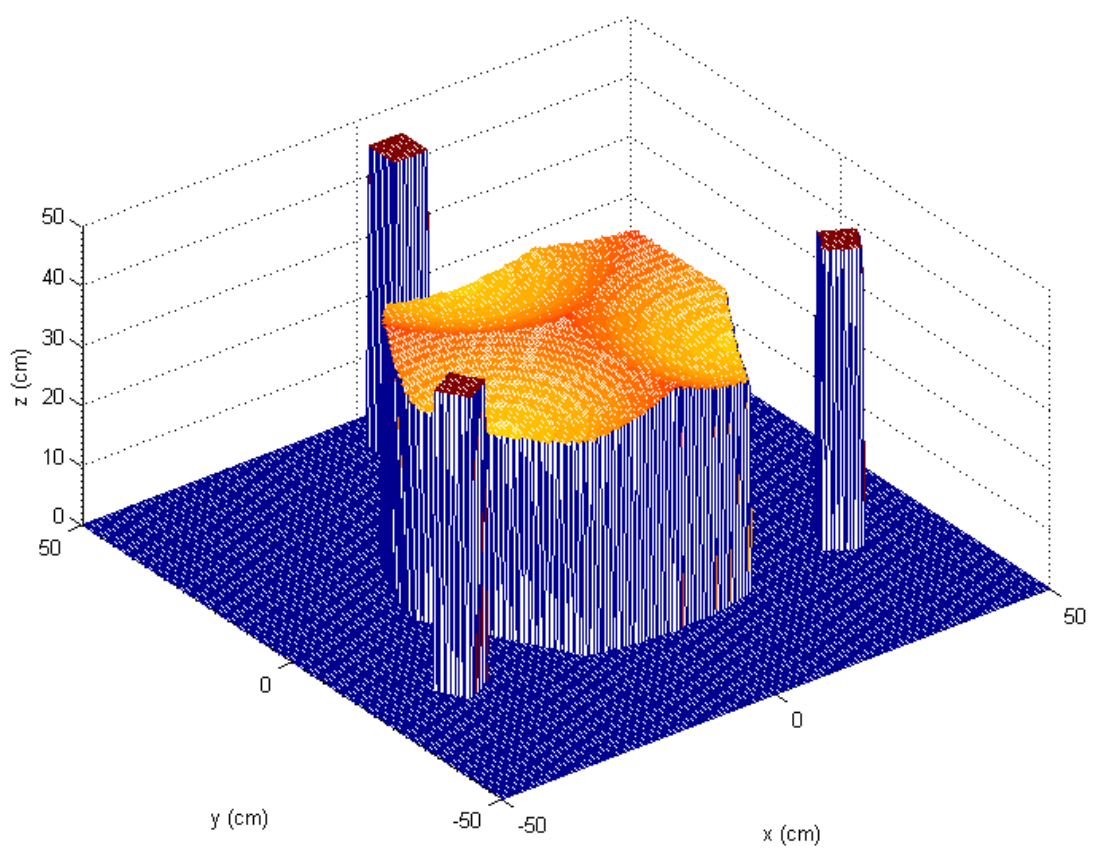


Figure 85: Mesh plot of build volume

In the new coordinate system, the equations look like this:

$$\begin{aligned} r_1^2 &= x^2 + y^2 + z^2 \\ r_2^2 &= (x - x_2)^2 + y^2 + z^2 \\ r_3^2 &= (x - x_3)^2 + (y - y_3)^2 + z^2 \end{aligned} \tag{A-12}$$

Solving these equations is simple. The steps are:

- Subtract the second from the first, expand, and solve for x .
- Subtract the third equation from the first, expand, and solve for y .
- Solve the first equation for z .

Following these steps produces

$$\begin{aligned} x &= \frac{r_1^2 - r_2^2 + x_2^2}{2x_2} \\ y &= \frac{r_1^2 - r_3^2 + y_3^2 + x_3^2 - x_3x}{2y_3} \\ z &= \pm \sqrt{r_1^2 - x^2 - y^2} \end{aligned} \tag{A-13}$$

If all of the spheres have the same radius—that is, if the arms have the same length—this reduces to

$$\begin{aligned} x &= \frac{x_2}{2} \\ y &= \frac{y_3^2 + x_3^2 - x_3x}{2y_3} \\ z &= \pm \sqrt{r^2 - x^2 - y^2} \end{aligned} \tag{A-14}$$

In either solution, the z solution must be chosen so that the print head lies below the carriages.

As for actually defining the coordinate transformation matrix, the following steps should be taken:

- Define a vector from the first carriage to the second, then divide the vector by its magnitude and make it the new **i** vector.
- Define a vector from the first carriage to the third, compute its cross product with the new **i** vector, then divide the result by its magnitude and make this the new **k** vector.
- Cross the new **k** with the new **i** to obtain the new **j** vector.

Beyond this all that is left is to be careful to offset the new coordinate system's origin so that it coincides with the first carriage.

HVAC Systems

Heated build plate

Heating element temperature must not exceed 260 [C], in order to keep kapton from burning

$$T_h = 200 \text{ [K]} + 273 \text{ [K]}$$

Surface temperature of the glass must be 110 [C] to keep ABS from cooling too rapidly

$$T_g = 110 \text{ [K]} + 273 \text{ [K]}$$

Air temperature inside the enclosure- unknown, but somewhere between T_g and room temperature, 25 [C]

$$T_{air} = 80 \text{ [K]} + 273 \text{ [K]}$$

$$h = 20 \text{ [W/m}^2\text{-K]}$$

Surface area of heated build plate

$$A = \pi \cdot 0.6^2 \cdot 0.25 \text{ [m}^2\text{]}$$

Kapton tape thickness

$$t_k = 0.000075 \text{ [m]}$$

Thickness of aluminum plate

$$t_a = 0.006 \text{ [m]}$$

Thickness of glass plate

$$t_g = 0.0023 \text{ [m]}$$

Thickness of insulation

$$t_{ins} = 0.05 \text{ [m]}$$

Thermal Conductivity of Kapton Tape

$$k_k = 0.12 \text{ [W/m-K]}$$

Thermal Conductivity of 6061-T6 Aluminum

$$k_a = 177 \text{ [W/m-K]}$$

Thermal Conductivity of Glass

$$k_g = 1.4 \text{ [W/m-K]}$$

Thermal Conductivity of Insulation (common value for industrial insulation)

$$k_{ins} = 0.05 \text{ [W/m-K]}$$

Atmospheric Pressure

$$P = 101300 \text{ [Pa]}$$

Characteristic Length

$$L = 0.6 \text{ [m]}$$

Heat loss through the base

$$Q_{out} = \frac{T_h - T_{air}}{\frac{1}{A \cdot h} + \frac{t_k}{k_k \cdot A} + \frac{t_{ins}}{k_{ins} \cdot A}}$$

Heat loss up through the glass top

$$q_{out} = \frac{T_n - T_{air}}{\frac{1}{h \cdot A} + \frac{t_k}{k_k \cdot A} + \frac{t_a}{k_a \cdot A} + \frac{t_g}{k_g \cdot A}}$$

Total heat loss

$$q_{in} = q_{outb} + q_{out}$$

Power Equation

$$q_{in} = \frac{V^2}{R}$$

Line Voltage

$$V = 120 \text{ [V]}$$

Total resistance is proportional to wire length

$$R = L_{wire} \cdot \text{resistivity}$$

Resistivity of 24 Gage Nichrome Wire

$$\text{resistivity} = 4.5 \text{ [\Omega/m]}$$

Current from Ohm's Law

$$I = \frac{V}{R}$$

Unit Settings: SI C kPa kJ mass deg

$$A = 0.2827 \text{ [m}^2\text{]}$$

$$h = 20 \text{ [W/m}^2\text{K]}$$

$$I = 5.675 \text{ [Amp]}$$

$$k_g = 177 \text{ [W/m-K]}$$

$$k_g = 1.4 \text{ [W/m-K]}$$

$$k_{ins} = 0.05 \text{ [W/m-K]}$$

$$k_k = 0.12 \text{ [W/m-K]}$$

$$L = 0.6 \text{ [m]}$$

$$L_{wire} = 4.699 \text{ [m]}$$

$$P = 101300 \text{ [Pa]}$$

$$q_{in} = 681 \text{ [W]}$$

$$q_{outb} = 32.29 \text{ [W]}$$

$$q_{out} = 648.7 \text{ [W]}$$

$$R = 21.14 \text{ [\Omega]}$$

$$\text{resistivity} = 4.5 \text{ [\Omega/m]}$$

$$t_g = 0.006 \text{ [m]}$$

$$T_{air} = 353 \text{ [K]}$$

$$t_g = 0.0023 \text{ [m]}$$

$$t_{ins} = 0.05 \text{ [m]}$$

$$t_k = 0.000075 \text{ [m]}$$

$$T_n = 473 \text{ [K]}$$

$$T_s = 383 \text{ [K]}$$

$$V = 120 \text{ [V]}$$

Cooling and ventilation system

Heated base temperature must not exceed 260 [C], in order to keep silicone from melting

$$T_n = 200 \text{ [C]}$$

Surface temperature of the glass must be 110 [C] to keep ABS from cooling too rapidly

$$T_s = 110 \text{ [C]}$$

Air temperature inside the enclosure- unknown, but somewhere between T_s and room temperature, 25 [C]

$$T_{air} = 35 \text{ [C]}$$

External Room Temperature

$$T_{room} = 25 \text{ [C]}$$

$$h = 20 \text{ [W/m}^2\text{-K]}$$

Surface area of heated build plate

$$A = \pi \cdot 0.6^2 \cdot 0.25 \text{ [m}^2]$$

Thickness of aluminum plate

$$t_a = 0.006 \text{ [m]}$$

Thickness of glass plate

$$t_g = 0.0023 \text{ [m]}$$

Thickness of insulation

$$t_{ins} = 0.05 \text{ [m]}$$

Thermal Conductivity of 6061-T6 Aluminum

$$k_a = 177 \text{ [W/m-K]}$$

Thermal Conductivity of Glass

$$k_g = 1.4 \text{ [W/m-K]}$$

Thermal Conductivity of Insulation (common value for industrial insulation)

$$k_{ins} = 0.05 \text{ [W/m-K]}$$

Atmospheric Pressure

$$P = 101300 \text{ [Pa]}$$

Characteristic Length

$$L = 0.6 \text{ [m]}$$

Heat loss through the base is approximately zero, since it will be insulated

$$\dot{q}_{cub_b} = 0$$

Heat loss up through the glass top

$$\dot{q}_{cub_s} = \frac{T_n - T_{air}}{\frac{t_g}{k_g \cdot A} + \frac{1}{h \cdot A}}$$

Total heating required by HBP

$$\dot{q}_{in,b} = \dot{q}_{outb} + \dot{q}_{outs}$$

Heating assuming all 3 motors are converting 200W to heat

$$\dot{q}_{in,m} = 3 \cdot 200 \text{ [W]}$$

Heating from Extruder heater

$$\dot{q}_{in,e} = 60 \text{ [W]}$$

Heating in=Cooling requirement

$$\dot{q}_{cool} = \dot{q}_{in,e} + \dot{q}_{in,b} + \dot{q}_{in,m}$$

To find mass flow rate in, assume all cooling occurs at constant mass flow rate and temperature gradient, & constant properties

$$\dot{q}_{cool} = \dot{m} \cdot c_p \cdot (T_{air} - T_{room})$$

$$c_p = 1005 \text{ [J/kg-C]}$$

$$\text{density} = 1.127 \text{ [kg/m}^3\text{]}$$

Volumetric flowrate

$$\dot{V} = \frac{\dot{m}}{\text{density}}$$

Convert to CFM

$$\text{CFM} = \left| 2118.88 \cdot \frac{\text{ft}^3/\text{min}}{\text{m}^3/\text{s}} \right| \cdot \dot{V}$$

CFM rating for each of two fans

$$\text{CFM}_{\text{each}} = \frac{\text{CFM}}{2}$$

Unit Settings: SI C kPa kJ mass deg

$$A = 0.2827 \text{ [m}^2\text{]}$$

$$\text{CFM} = 292.5 \text{ [ft}^3/\text{min}\text{]}$$

$$\text{CFM}_{\text{each}} = 146.2 \text{ [ft}^3/\text{min}\text{]}$$

$$c_p = 1005 \text{ [J/kg-C]}$$

$$\text{density} = 1.127 \text{ [kg/m}^3\text{]}$$

$$h = 20 \text{ [W/m}^2\text{K}\text{]}$$

$$k_a = 177 \text{ [W/m-K]}$$

$$k_g = 1.4 \text{ [W/m-K]}$$

$$k_{ins} = 0.05 \text{ [W/m-K]}$$

$$L = 0.6 \text{ [m]}$$

$$\dot{m} = 0.1556 \text{ [kg/s]}$$

$$P = 101300 \text{ [Pa]}$$

$$\dot{q}_{cool} = 1563 \text{ [W]}$$

$$\dot{q}_{in,b} = 903.4 \text{ [W]}$$

$$\dot{q}_{in,e} = 60 \text{ [W]}$$

$$\dot{q}_{in,m} = 600 \text{ [W]}$$

$$\dot{q}_{outb} = 0 \text{ [W]}$$

$$\dot{q}_{outs} = 903.4 \text{ [W]}$$

$$t_a = 0.006 \text{ [m]}$$

$$T_{air} = 35 \text{ [C]}$$

$$t_g = 0.0023 \text{ [m]}$$

$$t_{ins} = 0.05 \text{ [m]}$$

$$T_n = 200 \text{ [C]}$$

$$T_{room} = 25 \text{ [C]}$$

$$T_s = 110 \text{ [C]}$$

$$\dot{V} = 0.138 \text{ [m}^3/\text{s}\text{]}$$

Thermal expansion FEA

DEFINING THE PROBLEM

In order to compare to high end printers, the target positioning accuracy for this delta printer is 25 microns. Designing a printer to be accurate to 25 microns amplifies the effects of frame deflections and component deflections dramatically. We wanted to be able to analyze the effects of an internal temperature change during a 3D print. The printer is designed to print at an internal temperature of 35 degrees Celsius, however the design team needs to know how critical it is to maintain this internal temperature.

For a 5 degree increase we will analyze how the thermal expansions of different components changes the position and orientation of the columns. By being able to report the new column position and orientations the design team can use their forward kinematic equations to determine the final position of the extruder tip. By knowing the resulting extruder location the team can determine how accurately the temperature needs to be regulated, as well as being able to account for the resulting locating with the positioning software. We expect the thermal effects will be far higher than the team expects due to the majority of the structure being made out of aluminum.

MODEL

The 3d printer model has been simplified to represents the frame of the printer. The frame consists of three linear rails conjoined to aluminum base plates on the top and bottom. The frame model can be seen below in Figure 1. The rails consist of a steel bar attached to an aluminum T-slot. The T-slot's cross section is complex in shape; this is the only component that has complex geometry. The 3D printer CAD model was stripped down to the bare essentials of the frame. The stripped down assembly consisted of the aluminum t-slot, aluminum plates, and harden steel linear rails. In order to simplify the cross section of the t-slot, the internal M8 threaded holes and corner square holes were filled in. The chamfers and fillets were eliminated to help simplify the part meshes. The cross sectional area was held constant throughout the changes to have the simplified model accurately reflect the actual model.

Once the Cad model was developed in Solidworks, the assembly was saved as a .STEP file and imported as a part into Abaqus. Importing the CAD model created 8 separate parts within the Abaqus model, representing the 3 steel rails, the three t-slot extrusion and the two plates. The benefit of importing the model is that once the parts are instanced the assembly is already aligned. In the Solidworks files all inertias, areas, volumes, masses, and measurements can be taken. The t-slot extrusions are made out of Al-6063, the end effector and plates are made out of Al 6061, and the linear rail is made out of 1.4116 DIN Stainless Steel.

Due to the difficulty of obtaining a quality mesh and the amount of elements needed to model the t-slot cross section it was determined that further simplifications of the model were necessary. By removing the holes in the plate, the remaining assembly could be symmetrically divided into three sections. The model was cut in SolidWorks into three pieces and imported into Abaqus via a .STEP file. The resulting model is now constructed of only 4 parts, all made from solid deformable elements. One piece of the symmetrical frame can be seen below in Figure 2. The symmetry to allows us to reduce the amount of elements by 2/3 and increases the computational speed of the model.



The resulting axis of symmetry do not align with the global coordinate system. For each side of the cut a local coordinate axis was created. In both local coordinates the cuts resulted in using the XSYMM boundary condition that restricts motion in x-axis, and rotation about the y-axis and z-axis. These conditions represent the effect of the rest of the model on the cut out section.

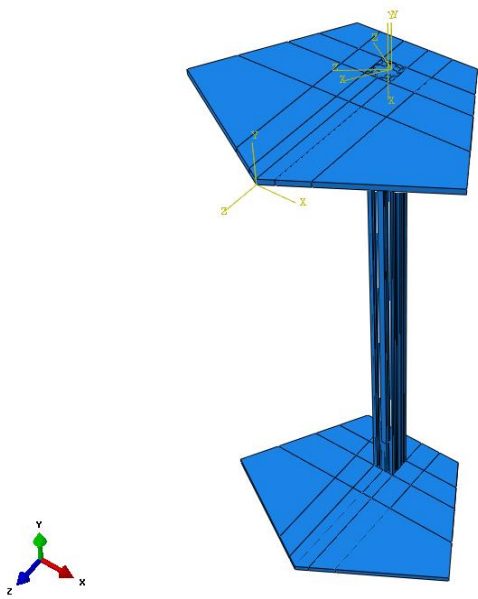


Figure 2. Abaqus assembly model with exploiting symmetry of the printer

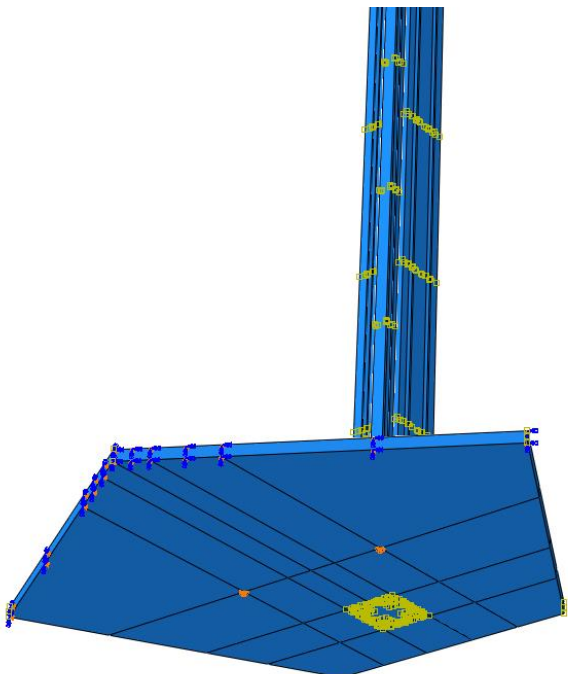


Figure 3. Boundary conditions on lower plate

The printer will be bolting to a rigid table using six bolts two per corner. A boundary condition restricting the movement in x, y, and z what placed at the two node at the bottom of the plate that represent the location of the bolts. The boundary condition for the symmetric sides and table bolts can be seen in Figure 3 below.

To model the screws used in the printer frame, tie constraints were constructed. Four nodes on the plate in the locations of the screws were chosen as the master nodes. The corresponding four points on the t-slot were chosen as the slave nodes. The same was completed for the bottom plate.

The rail is connected to the t-slot extrusion by screws in the channel of the t-slot. The screws were modeled by tying the surface of the t-slot to the nodes of the screw holes on the rail. This is a critical aspect of the analysis because the rail and t-slot are constructed out of steel and aluminum respectively and have different thermal expansion coefficients. The steel rail will attempt to resist the expansion of one side of the t-slot and should result in the bowing of the columns.

MESH

The meshing of this model proved to be the most difficult aspect of the model. The model was made out of linear quad elements with reduced integration. The element used was the C3D8R 8-node linear brick. The mesh quality was evaluated by looking at elements with an aspect ratio greater than 4 and minimum angle smaller than 45 degrees.

The top and bottom plates were partitioned using the cross section of the t-slot to align the nodes of the two interacting parts. This partitioning was done using the “extruded edge” partitioning tool. The rest of the plate was then partitioned using the “define cutting plane” and a point and normal approach to produce a quality mesh on the plate. Partitioning the plate allows for a clean mesh with nodes placed at the critical locations.

Both the rail and the t-slot of the model were not partitioned in the design due to errors when attempting to mesh. The seed size was critical in both of these elements to produce a quality mesh. For the t-slot any mesh size over 5mm produced large aspect ratios, and small minimum angles. Figure 4 below show the t-slot meshed with a 3mm global size element.

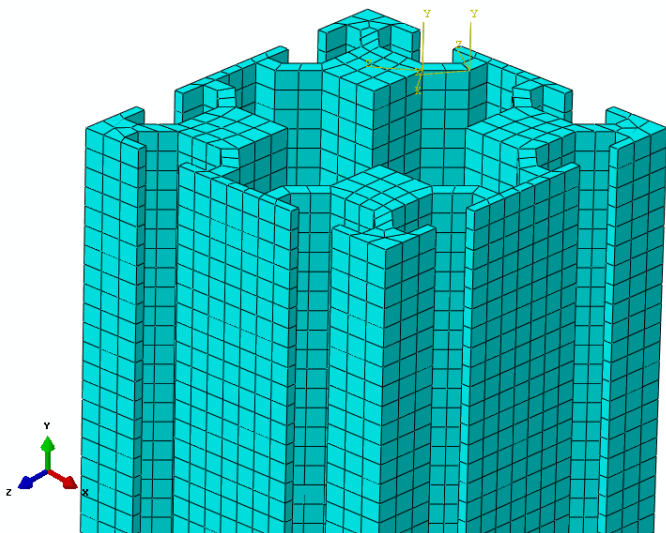


Figure 4. Mesh of t-slot with 3mm seed size.

The convergence study for the model was completed by varying the global mesh size of the entire model. Only 5 sizes were used for the study due to computational abilities of computers on campus. The four global element sizes used were 12mm, 6mm, 3mm, 1.5mm, and 0.75mm elements. The models with 3mm size elements or less produced models with element numbers in the millions. The U3 deflection was used to determine the convergence of the mesh.

The results for the various element sizes shows that the model is converged with the size 3mm global element. These results can be seen in Table 1 and Figure 5 below. From the above study it was determined that the element size of 3 is the point at which the model is converged because there is less than a 2% variance in the deflection.

Table 1. Convergence study of model with different element sizes

Element Size	U3, Deflection in z-axis in mm
12	0.035
6	0.096
3	0.126
1.5	0.130
0.75	0.131

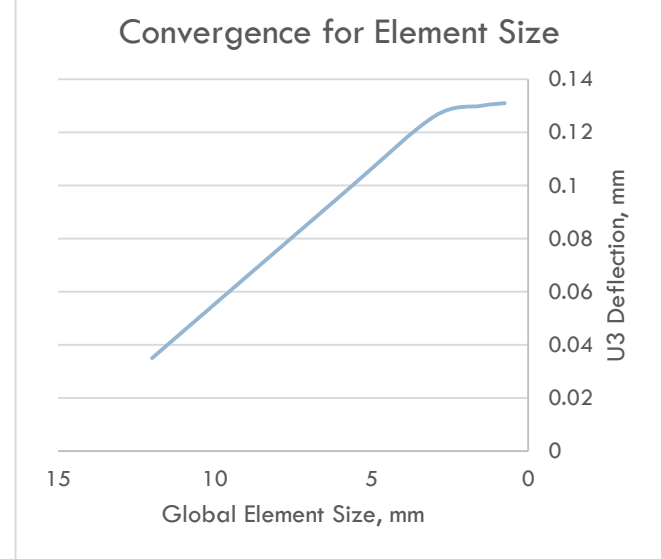


Figure 5. Convergence study for decreasing element size

The final element was determined to be a 3mm global size, C3D8R 8-node linear brick quad element with reduced integration. The quality of the mesh was then measured using the verify mess tool in Abaqus. The quality of mesh was determined by having elements with aspect ratios less than 4, and minimum angles greater than 45 degrees. Table 2 below shows the percent of elements outside this range for the given parts.

Table 2. Quality of mesh analysis results

Part	% of Element with aspect ratio >4	% of elements with minimum angle > 45 degree
Top Plate	0.17%	0.16%
Bottom Plate	0.06	0.15%
T-slot	0.0%	7.90%
Rail	0.0%	0.0%

The quality of mesh is very acceptable with the only concern being the minimum angle for the t-slot elements. When you take a closer look at the problem elements, we can see that the smallest angle below 45 degrees is 42 degrees. This 3 degree difference is acceptable to us and the location of these elements can be seen in Figure 6. on the right.

FE ANALYSIS

A thermal finite element analysis was completed on the model. The frame was subjected to a temperature increase from 313K to 318K as specified by from Deltronic Solutions. The deflection results were then monitored to see the effect of temperature on the overall location of the linear slides.

The model was constructed by imputing an initial temperature of 313K in the predefined field of the initial step. A secondary step was then constructed and a final temperature on 318K was implemented into the predefined field of the second step. With the resulting stress in the system is negligible the field output request was changed to only determine the deflections of the system. The limited field output request allowed for faster computational time of the model.

4 different models had been constructed prior to the final one and all were not used due to errors and difficulty in producing a quality mesh. A full size model was too large to be run on school computers and

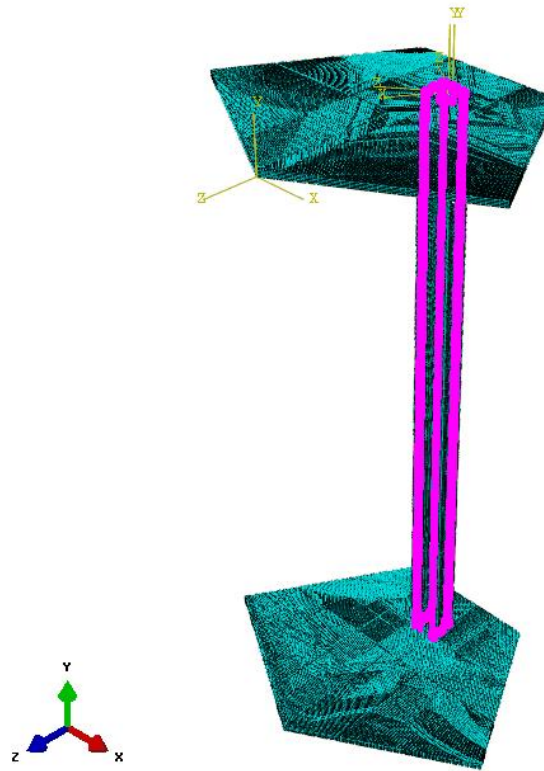


Figure 6. Problem mesh elements with minimum angle less than 45 degrees

would crash the computer when the job was run. The model with a full size plate with holes in it was extremely hard to mesh due to the 9 holes, and odd outside shape. Table 3. Below explains the solutions to the major errors found while attempting the run the final model.

Table 3. Typical Errors and Solutions to Overcome Errors

Error	Reason and Solution
"The following pairs of attributed are applied to overlapping/intersecting/adjoining regions in different coordinate systems"	The boundary conditions made for the symmetry cuts were made on separate coordinate systems but shared a common side. The common side was being defined in both coordinate systems and produced the error. CTRL clicking the common side for one coordinate system solved the problem.
"XXX number of element with zero area"	Global seeding produced poor elements. Fixed by partitioning or changing the element global seed size.
"Job aborted. Check disk space"	Problem trying to run on school computers. Simplify model, reduce number of elements, reduce field output request, and increase disk space.

The models with a high number of elements were extremely difficult to run on the school computers in a reasonable time. To reduce the amount of time, the number of parallel processors was increased. With increasing the processors the computer would crash if the "increase memory allocation" box was not unchecked. Unchecking the box limited the amount of memory Abaqus could pull and would help to minimize crashes.

RESULTS

The main result concern of the senior project team is the deflection of the columns due to a temperature increase. Table 4 below shows the results for a 5 degree increase in overall temperature.

Table 4: Deflection Results for the Model with 3mm Seed Size

Direction	Deflection in mm
U3	0.126
U2	0.088
Magnitude	0.137

As expected the amount of deflection due to a temperature increase is much larger than the team had expected. The results do not seem concerning to a normal project, however the target accuracy for the printer is 25 microns, a deflection of one of the columns by 137 microns becomes a major concern. Figure 7 and Figure 8 show the U2, and magnitude contour plots of the model respectively. Figure 8 shows the model mirrored about the Y-axis to show the entire model.

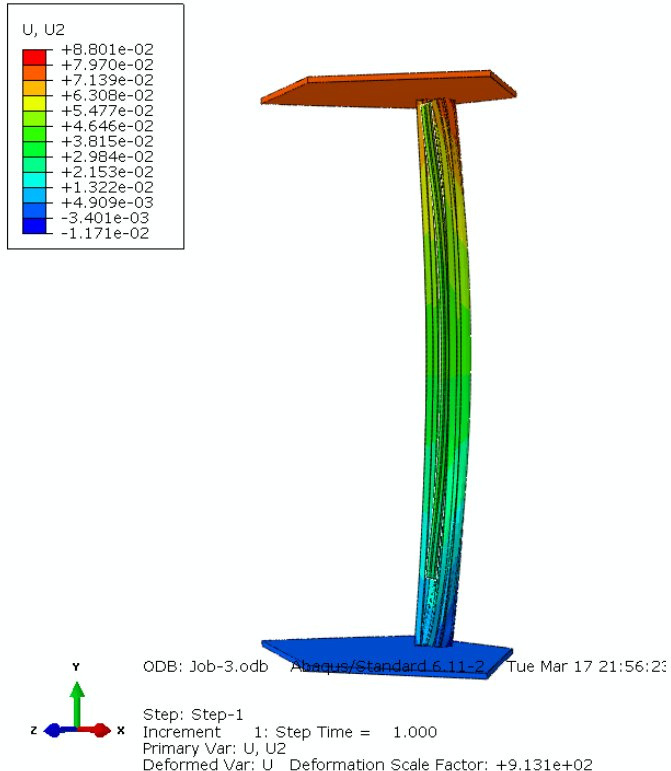


Figure 7. Deflection in y-direction

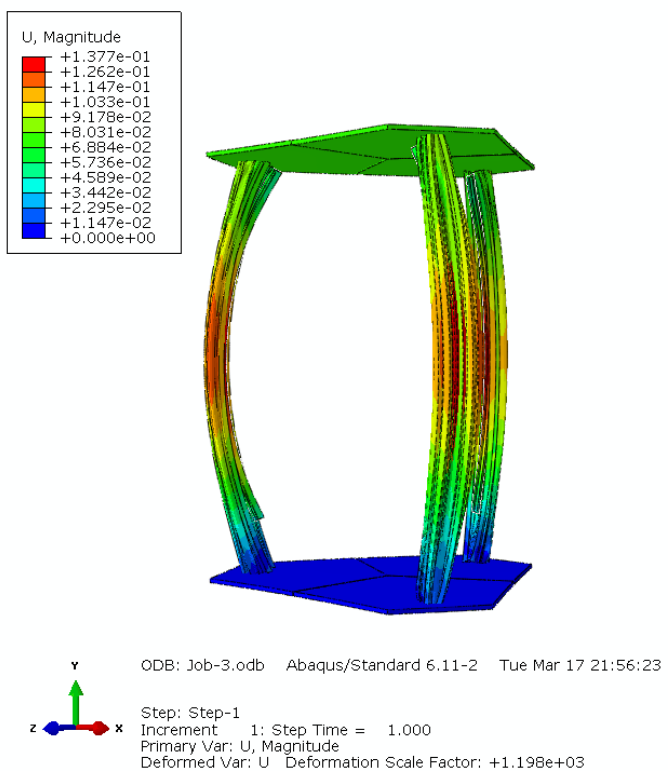


Figure 8. Magnitude of deflection contour plot.

The results from the model compare to the hand calculations of for the deflection of the columns due to the thermal expansion of the plates. The hand calculations for the plates resulting in a column deflection of 0.096 in the U3 direction. The model result of 0.126mm is only a 30 micron difference. However the hand calculations for the elongation of the t-slot did not relate to the model due to the effect of the hardening steel rail distorting the expansion and causing the t-slot to bow. A hand calculation of the column modeled as a composite material would result in relatable results to the model.

Due to the results of the model we recommend that Deltronic solutions closely regulate the internal temperature, and brace the back side of the columns to counteract the effect of the steel rail.

DISCUSSION

The model and hand calculations do not directly compare due to the effect of the rail and t-slot bolts not being considered in the hand calculations. The plate expansion did compare to the deflection of the columns in the z-direction. The results from the plate calculations are not an exact solution only an estimate due to the odd shape and discrepancies in the material. The model resulted in the deflections we were looking for, and modeled the effect of the steel rail on the column as expected.

These results bring about a major concern for the senior project team is the internal temperature fluctuates 5 degrees Kelvin. The expansion properties of Aluminum are not ideal for this application and should be a major consideration for redesign. The bow of the columns results in a very hard calibration of a delta robot and accounting for the error in the output of the motors would be difficult.

We definitely recommend bracing the back side of the columns as well as having temperature control for the chamber. If more time were permitted we would have liked to complete a study possible solutions to the expansion problem, such as bracing the back side of the columns. These results are applicable to any aluminum t-slot frame being used for precision applications and a study on braces to counter act thermal properties would be highly valuable for t-slot users.

APPENDIX B: CODE DOCUMENTATION

Inverse Kinematics MATLAB Script

```
%% deltakinematics.m
% Deltronic Solutions

clear

%% Component Specifications

% Dimensions

% column angles (deg)
phi = [90
        210
        330];

Hc = 0.840; % slide travel length (m)
Rc = 0.400; % column radial distance (m)

Ht = 0.120; % offset of slide from bottom plate (m)
Rt = 0.030; % half-thickness of T-slot extrusion (m)

Hg = 0.060; % offset of glass bed surface from bottom plate (m)

Rs = 0.047; % radial offset of stage from column (m)
Hs = 0.017; % rod end offset from bottom of stage (m)

Rn = 0.063; % radial distance between nozzle and edge of plate (m)
Hn = 0.051; % vertical distance between top of plate and nozzle tip (m)

Lj = 0.020; % rod end cylinder height (m)
Rj = 0.009; % magnetic ball radius

Lr = 0.460; % rod length (m)
Dr = 0.060; % rod diameter (m)

Re = Rc - Rt - Rs - Rn - Rj; % effective column radial distance (m)
He = Hs + Ht - Hn - Hg - Rj; % effective vertical offset (m)
Le = Lr + 2*(Lj + Rj); % effective rod length (m)

%% Nozzle Motion Input

% Displacement (m)

X = 0;
Y = 0;
Z = 0;

% Velocity (m/s)

VX = 0;
VY = 0;
```

```

VZ = 0;

% Acceleration (m/s^2)

AX = 0;
AY = 0;
AZ = 0;

%% Robot Kinematics

% Preallocate matrices

C(1:3) = zeros;
S(1:3) = zeros;
z(1:3) = zeros;
r(1:3,1:3) = zeros;
e(1:3,1:3) = zeros;
v(1:3) = zeros;
vG(1:3,1:3) = zeros;
omega(1:3,1:3) = zeros;
a(1:3) = zeros;
aG(1:3,1:3) = zeros;
alpha(1:3,1:3) = zeros;

for i = 1:3

    % Cosines and sines

    C(i) = cosd(phi(i));
    S(i) = sind(phi(i));

    % Linear slide displacement (m)

    z(i) = Z - He + (Le^2 - (X - Re * C(i))^2 ...
        - (Y - Re * S(i))^2)^{(1/2)}; 

    % Position vector representing rod (m)

    r(i,1:3) = [X - Re * C(i)
                Y - Re * S(i)
                Z - z(i) - He];

end

%% Calculate Build Volume

% enter 1 to skip this calculation
skip = 1;

if skip ~= 1

```

```

% Define axes (m)

%      min   max   step
Xaxis = [-0.5  0.5  0.005];
Yaxis = [-0.5  0.5  0.005];
Zaxis = [0.0   0.5  0.005];

% axis vectors
Xt = Xaxis(1) : Xaxis(3) : Xaxis(2);
Yt = Yaxis(1) : Yaxis(3) : Yaxis(2);
Zt = Zaxis(1) : Zaxis(3) : Zaxis(2);

% number of steps
nX = length(Xt);
nY = length(Yt);
nZ = length(Zt);

% unit vectors perpendicular to columns and toward origin
nt = [-C(1) -S(1) 0
       -C(2) -S(2) 0
       -C(3) -S(3) 0];

% angular limit from vertical/horizontal
AngLim = 5;

% preallocate matrices
zt(1:3) = zeros;
rt(1:3,1:3) = zeros;
Zplot(1:nX,1:nY) = zeros;
zm = Inf;
Rm = Inf;

for i = 1:nX
    for j = 1:nY
        for k = 1:nZ
            for n = 1:3

                % linear slide displacement (m)
                zt(n) = Zt(k) - He + (Le^2 - (Xt(i) ...
                    - Re * C(n))^2 - (Yt(j) - Re * S(n))^2)^{(1/2)};

                % position vector representing rod (m)
                rt(n,1:3) = [Xt(i) - Re * C(n)
                             Yt(j) - Re * S(n)
                             Zt(k) - zt(n) - He];

            end

            % Check that X and Y values satisfy rod length limit
            % carriage heights must be real values

```

```

if isreal(zt) == 1

    % Check that the rods do not intersect the carriages

    % rod position vectors must satisfy limit at carriages
    if sum(dot(rt',nt') > 0) == length(dot(rt',nt') > 0)

        % Test if Z value satisfies column height limit

        % carriage heights must be less than column height
        if sum(zt < Hc) == length(zt < Hc)

            % Implement angle limits on rods

            % rods not too close to horizontal
            if sum(asind(-rt(:,3)/Le) > AngLim) ...
                == length(asind(-rt(:,3)/Le) > AngLim)

                % build volume height (m)
                Zplot(j,i) = Zt(k);

                % check lowest carriage position
                if min(zt(n)) < zm

                    % minimum carriage height (m)
                    zm = min(zt(n));

                end

            end

        end

    end

else

    Zplot(j,i) = 0; % plot build volume height as zero

end

% Plot columns

if Xt(i) >= -Rt && Xt(i) <= Rt ...
&& Yt(j) >= Rc - Rt && Yt(j) <= Rc + Rt

    Zplot(j,i) = max(Zt);

elseif Yt(j) - (Rc + Rt) * S(2) ...
>= -C(2)/S(2) * (Xt(i) - (Rc + Rt) * C(2)) ...
&& Yt(j) - (Rc - Rt) * S(2) ...

```

```

<= -C(2)/S(2) * (Xt(i) - (Rc - Rt) * C(2)) ...
&& Yt(j) - Rt * C(2) ...
>= S(2)/C(2) * (Xt(i) + Rt * S(2)) ...
&& Yt(j) + Rt * C(2) ...
<= S(2)/C(2) * (Xt(i) - Rt * S(2))

Zplot(j,i) = max(Zt);

elseif Yt(j) - (Rc + Rt) * S(3) ...
>= -C(3)/S(3) * (Xt(i) - (Rc + Rt) * C(3)) ...
&& Yt(j) - (Rc - Rt) * S(3) ...
<= -C(3)/S(3) * (Xt(i) - (Rc - Rt) * C(3)) ...
&& Yt(j) + Rt * C(3) ...
>= S(3)/C(3) * (Xt(i) - Rt * S(3)) ...
&& Yt(j) - Rt * C(3) ...
<= S(3)/C(3) * (Xt(i) + Rt * S(3))

Zplot(j,i) = max(Zt);

end

end

Zplotmin = min(nonzeros(Zplot)); % build volume height

% generate mesh plot
figure(1)
mesh(Xt*100,Yt*100,Zplot*100)
xlabel('x (cm)')
ylabel('y (cm)')
zlabel('z (cm)')
title('Surface plot of build volume')
axis equal

% generate contour plot
figure(2)
contour(Xt*100,Yt*100,Zplot*100,Zt*100)
grid on
xlabel('x (cm)')
ylabel('y (cm)')
title('Contour plot of build volume')
axis square

end

```

Machine Software

INITIALIZE

```
(* This Is The Initialization for the Communications Manager*)
(*This code obtains the Controller's IP Address*)
BUF_TO_STRING(
    REQ:=TRUE,
    BUF_FORMAT:=TRUE,
    BUF_OFFSET:=DINT#0,
    BUF_CNT:=DINT#17,
    BUFFER:= Controller.Network.Interface[1].IPAddress,
    DST:=IPAddress
);

Controller.Network.Interface[1].IPAddress:=BUF_TO_STRING.BUFFER;
IF BUF_TO_STRING.DONE THEN
    IPAddress:=BUF_TO_STRING.DST;
END_IF;
ComConfig.CommType:=INT#2;                                (* Ethernet *)
ComConfig.Ethernet.LocalIPAddress:=IPAddress;
ComConfig.Ethernet.LocalPort:=UINT#1206;
ComConfig.BufferSize:=UDINT#0;
(*
CommandBuffer.CmdDelimiters[0]:=BYTE#13;
CommandBuffer.CmdDelimiters[1]:=BYTE#10;*)
CommandBuffer.Size:=INT#8192;
(*****)
Physical_Axis_1.AxisNum := UINT#3;
physical_Axis_2.AxisNum := UINT#4;
physical_Axis_3.AxisNum := UINT#5;
(*****)
(* column angles (deg) *)
DeltaSins[0] := REAL_TO_LREAL(SIN(REAL#1.57079632679));
DeltaSins[1] := REAL_TO_LREAL(SIN(REAL#3.66519143));
```

```

DeltaSins[2] := REAL_TO_LREAL(SIN(REAL#5.75958653));

DeltaCos[0] := REAL_TO_LREAL(COS(REAL#1.57079632679));
DeltaCos[1] := REAL_TO_LREAL(COS(REAL#3.66519143));
DeltaCos[2] := REAL_TO_LREAL(COS(REAL#5.75958653));
(* Component Specifications *)
(* Dimensions *)
slide_travel_length := LREAL#0.840; (*Hc (m)*)
column_radial_distance := LREAL#0.400; (* Rc (m)*)
slide_offset := LREAL#0.120; (* Ht (m)*)
t_slot_half_thickness := LREAL#0.030; (* Rt (m) *)
glass_bed_offset := LREAL#0.060; (* Hg (m) *)
radial_offset := LREAL#0.04815; (* RS radial offset of stage from column (m) *)
rod_end_offset := LREAL#0.017; (* HS rod end offset from bottom of stage (m)*)
radial_dist_nozzle := LREAL#0.063; (* Rn radial distance between nozzle and edge of plate (m)*)
vert_dis_nozzle := LREAL#0.051; (* Hn vertical distance between top of plate and nozzle tip (m)
*)
rod_end_height := LREAL#0.020; (*Lj rod end cylinder height (m) *)
mag_ball_rad := LREAL#0.009; (*Rj magnetic ball radius *)
rod_length := LREAL#0.465; (*Lr rod length (m) *)
rod_diameter := LREAL#0.060; (*Dr rod diameter (m) *)
col_radial_dist := column_radial_distance - t_slot_half_thickness - radial_offset -
radial_dist_nozzle - mag_ball_rad; (*Re effective column radial distance (m) *)
vert_offset := rod_end_offset + slide_offset - vert_dis_nozzle - glass_bed_offset - mag_ball_rad;
(*He effective vertical offset (m) *)
effective_rod_len := rod_length + LREAL#2.0*(rod_end_height + mag_ball_rad); (* Le effective rod
length (m) *)

(*Motor Axis Reference Assignment*)
(*
Servo_Axis_1.AxisNum := UINT#89;
Servo_Axis_2.AxisNum := UINT#90;
Servo_Axis_3.AxisNum := UINT#91;
*)
Servo_Axis_1.AxisNum := UINT#3;
Servo_Axis_2.AxisNum := UINT#4;

```

```
Servo_Axis_3.AxisNum := UINT#5;  
(**)  
Physical_move_Velocity := LREAL#50.0;  
Physical_move_Acceleration := LREAL#50.0;  
Virtual_Axis_1.AxisNum := UINT#86;  
Virtual_Axis_2.AxisNum := UINT#87;  
Virtual_Axis_3.AxisNum := UINT#88;  
Virtual_Extruder_Axis.AxisNum := UINT#92;  
Desired_Position := LREAL#0.0;  
Extruder_Stepper_Position := LREAL#0.0;  
Extruder_Stepper_Inc := LREAL#1.0 / LREAL#73.03;
```

COMMAND_EXEC

```
Move_Print_Head_1(Execute_Virtual_Move:=Execute_Move,X_Pos:=X_Pos,Y_Pos:=Y_Pos,Z_Pos:=Z_Pos,extru
de_pos:=E_Pos, Done:= MOVE_FINISH);
position := Command_Buffer.UsePointer;
p2 := Position + INT#1;
p3 := Position + INT#2;
p4 := Position + INT#3;
p5 := Position + INT#4;
p6 := Position + INT#5;
if(Retrieve_Command) THEN

    if((Command_Buffer.UsePointer <> Command_Buffer.StorePointer) AND position =
Command_Buffer.UsePointer) THEN
        Execute_Move := False;
        command.hasX := BYTE_TO_BOOL(Command_Buffer.Data[Position]);
        command.hasY := BYTE_TO_BOOL(Command_Buffer.Data[p2]);
        command.hasZ := BYTE_TO_BOOL(Command_Buffer.Data[p3]);
        command.hasE := BYTE_TO_BOOL(Command_Buffer.Data[p3]);
        command.hasF := BYTE_TO_BOOL(Command_Buffer.Data[p4]);
        command.hasS := BYTE_TO_BOOL(Command_Buffer.Data[p5]);
        BUF_TO_REAL_1(REQ:= Convert,BUF_FORMAT := True, BUF_OFFSET:=
INT_TO_DINT(Command_Buffer.UsePointer) + DINT#8, BUF_CNT:= DINT#4 ,BUFFER := Command_Buffer.Data
,DST:=command.X);
        X_Done :=BUF_TO_REAL_1.DONE;
        Command_Buffer.Data := BUF_TO_REAL_1.BUFFER;
        command.X :=BUF_TO_REAL_1.DST;
        Err1 := BUF_TO_REAL_1.ERROR;
        Stat1 := BUF_TO_REAL_1.STATUS;

        BUF_TO_REAL_2(REQ:=Convert,BUF_FORMAT :=
True, BUF_OFFSET:=INT_TO_DINT(Command_Buffer.UsePointer) + DINT#12
, BUF_CNT:=DINT#4 ,BUFFER:=Command_Buffer.Data ,DST:=command.Y);
        Y_Done :=BUF_TO_REAL_2.DONE;
        Command_Buffer.Data:=BUF_TO_REAL_2.BUFFER;
        command.Y:=BUF_TO_REAL_2.DST;
```

```

    Err2 := BUF_TO_REAL_2.ERROR;
    Stat2 := BUF_TO_REAL_2.STATUS;

    BUF_TO_REAL_3(REQ:=Convert,BUF_FORMAT :=
True,BUF_OFFSET:=INT_TO_DINT(Command_Buffer.UsePointer) +
DINT#16,BUF_CNT:=DINT#4,BUFFER:=Command_Buffer.Data,DST:=command.Z);
    Z_Done :=BUF_TO_REAL_3.DONE;
    Command_Buffer.Data :=BUF_TO_REAL_3.BUFFER;
    command.Z:=BUF_TO_REAL_3.DST;
    Err3 := BUF_TO_REAL_3.ERROR;
    Stat3 := BUF_TO_REAL_3.STATUS;

    BUF_TO_REAL_4(REQ:=Convert,BUF_FORMAT :=
True,BUF_OFFSET:=INT_TO_DINT(Command_Buffer.UsePointer) +
DINT#20,BUF_CNT:=DINT#4,BUFFER:=Command_Buffer.Data,DST:=command.E);
    E_Done :=BUF_TO_REAL_4.DONE;
    Command_Buffer.Data :=BUF_TO_REAL_4.BUFFER;
    command.E:=BUF_TO_REAL_4.DST;
    Err4 := BUF_TO_REAL_4.ERROR;
    Stat4 := BUF_TO_REAL_4.STATUS;

    BUF_TO_REAL_5(REQ:=Convert,BUF_FORMAT :=
True,BUF_OFFSET:=INT_TO_DINT(Command_Buffer.UsePointer) +
DINT#24,BUF_CNT:=DINT#4,BUFFER:=Command_Buffer.Data,DST:=command.F);
    F_Done := BUF_TO_REAL_5.DONE;
    Command_Buffer.Data:=BUF_TO_REAL_5.BUFFER;
    command.F:=BUF_TO_REAL_5.DST;
    Err5 := BUF_TO_REAL_5.ERROR;
    Stat5 := BUF_TO_REAL_5.STATUS;

    BUF_TO_REAL_6(REQ:=Convert,BUF_FORMAT :=
True,BUF_OFFSET:=INT_TO_DINT(Command_Buffer.UsePointer) +
DINT#28,BUF_CNT:=DINT#4,BUFFER:=Command_Buffer.Data,DST:=command.stops);
    S_Done :=BUF_TO_REAL_6.DONE;
    Command_Buffer.Data:=BUF_TO_REAL_6.BUFFER;
    command.stops :=BUF_TO_REAL_6.DST;
    Err6 := BUF_TO_REAL_6.ERROR;

```

```

Stat6 := BUF_TO_REAL_6.STATUS;
Convert := bool#1;

if X_Done AND Y_Done AND Z_Done AND E_Done AND F_Done AND S_Done THEN
    Convert := False;
    X_Done := False;
    Y_Done := False;
    Z_Done := False;
    E_Done := False;
    F_Done := False;
    S_Done := False;
    Retrieve_Command := False;
    Command_Buffer.UsePointer := Command_Buffer.UsePointer + INT#32;
    if Command_Buffer.UsePointer >= INT#8192 THEN
        Command_Buffer.UsePointer := INT#0;
    END_IF;
    If command.hasX Then
        if(REAL_TO_LREAL(command.X) > LREAL#200.0) THEN
            X_Pos := LREAL#200.0;
        elsif REAL_TO_LREAL(command.X) < LREAL#-200.0 THEN
            X_Pos := LREAL#-200.0;
        else
            X_Pos := REAL_TO_LREAL(command.X);
        END_IF;
    END_IF;
    IF command.hasY Then
        if(REAL_TO_LREAL(command.Y) > LREAL#200.0) THEN
            Y_Pos := LREAL#200.0;
        elsif REAL_TO_LREAL(command.Y) < LREAL#-200.0 THEN
            Y_Pos := LREAL#-200.0;
        else
            Y_Pos := REAL_TO_LREAL(command.Y);
        END_IF;
    END_IF;
    IF command.hasZ THEN
        if(REAL_TO_LREAL(command.Z) > LREAL#200.0) THEN

```

```

        Z_Pos := LREAL#200.0;
    elseif REAL_TO_LREAL(command.Z) < LREAL#-75.0 THEN
        Z_Pos := LREAL#-75.0;
    else
        Z_Pos := REAL_TO_LREAL(command.Z);
    END_IF;
    END_IF;
    IF command.hasE THEN
        E_Pos := REAL_TO_LREAL(command.E);
    END_IF;
    END_IF;
END_IF;
Else
    MOVE_FINISH:=Move_Print_Head_1.Done;
    Execute_Move := NOT Execute_Move;

    IF MOVE_FINISH THEN
        Retrieve_Command := True;
        MOVE_FINISH := bool#0;
        command.hasX := False;
        command.hasY := False;
        command.hasZ := False;
        command.hasE := False;
        command.hasF := False;
        command.hass := False;
    END_IF;

    END_IF;
    return;

```

Inverse_Kinematics

```
(* Robot Kinematics*)
Counter := DINT#0;
x := x/LREAL#1000.0;
y := y/LREAL#1000.0;
z := z/LREAL#1000.0;
while Counter < DINT#3 DO
    Column_Heights[Counter] := (LREAL#1000.0)*(z - vert_offset_arg +
((effective_rod_len_arg)**(LREAL#2.0) - (x - col_radial_dist_arg *
DeltaCos_arg[Counter])**LREAL#2.0
    - (Y - col_radial_dist_arg * DeltaSin_arg[Counter])**LREAL#2.0)**(LREAL#0.5));
    Counter := Counter + DINT#1;
end_while;
```

TCP_Gcode_Command_Stream.py

```
#!/usr/bin/env python
import socket
from collections import namedtuple
from time import *
import struct
TCP_IP = '192.168.1.1'
TCP_PORT = 1206
BUFFER_SIZE = 1024

G1 = namedtuple("G1", "hasX hasY hasZ hasE hasF hasS X Y Z E F S")
format_ = ">?????xxffffff"
sock = socket.socket(socket.AF_INET, socket.SOCK_STREAM)
sock.connect((TCP_IP, TCP_PORT))

def RecycleSocket(s):
    s.shutdown(socket.SHUT_RDWR)
    s.close()
    s = socket.socket(socket.AF_INET, socket.SOCK_STREAM)
    s.connect((TCP_IP, TCP_PORT))
    return s

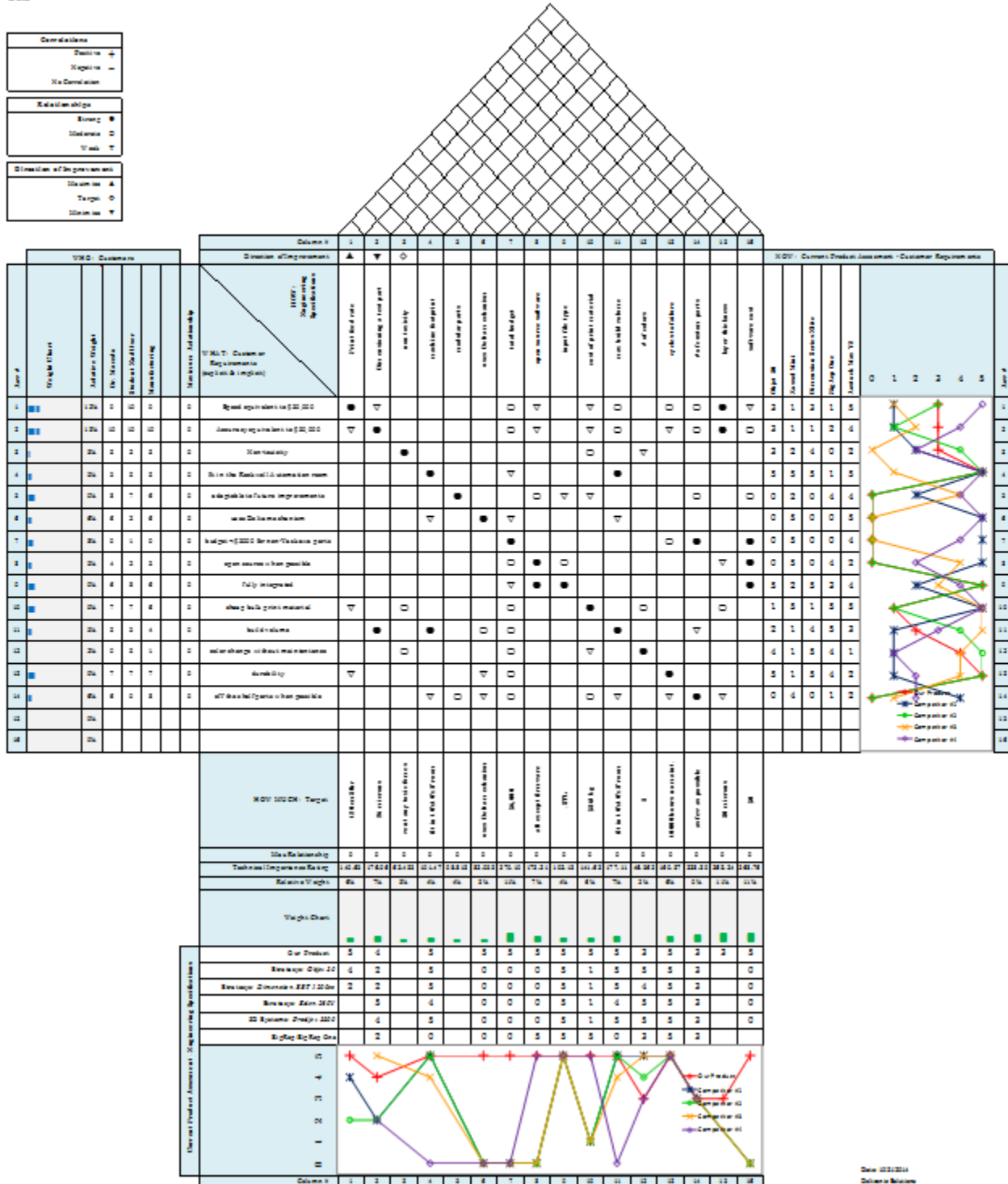
def movexyz(sock,x,y,z,s_time):
    g = G1(True, True, True, False, False, False, x, y, z, 0.0, 0.0, 0.0)
    string_to_send = struct.pack(format_, *g._asdict().values())
    sock.send(string_to_send)
    RESPONSE = sock.recv(BUFFER_SIZE)
    if s_time:
        sleep(s_time)

movexyz(sock, 0, 0, 0, 1)
s.shutdown(socket.SHUT_RDWR)
s.close()
```

APPENDIX C: OTHER FIGURES AND TABLES

QFD House of Quality

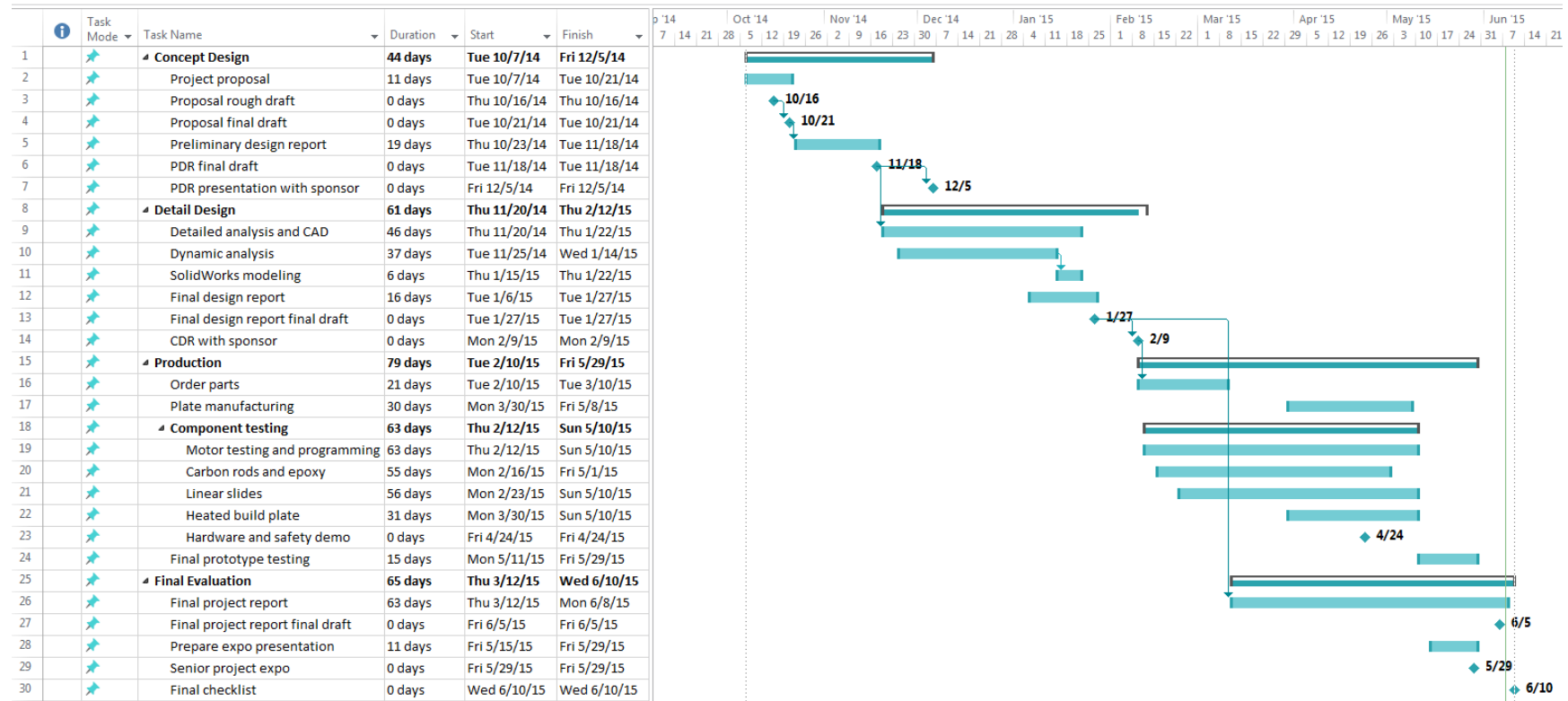
QFD: House of Quality



Preliminary SolidWorks Model



Gantt Chart



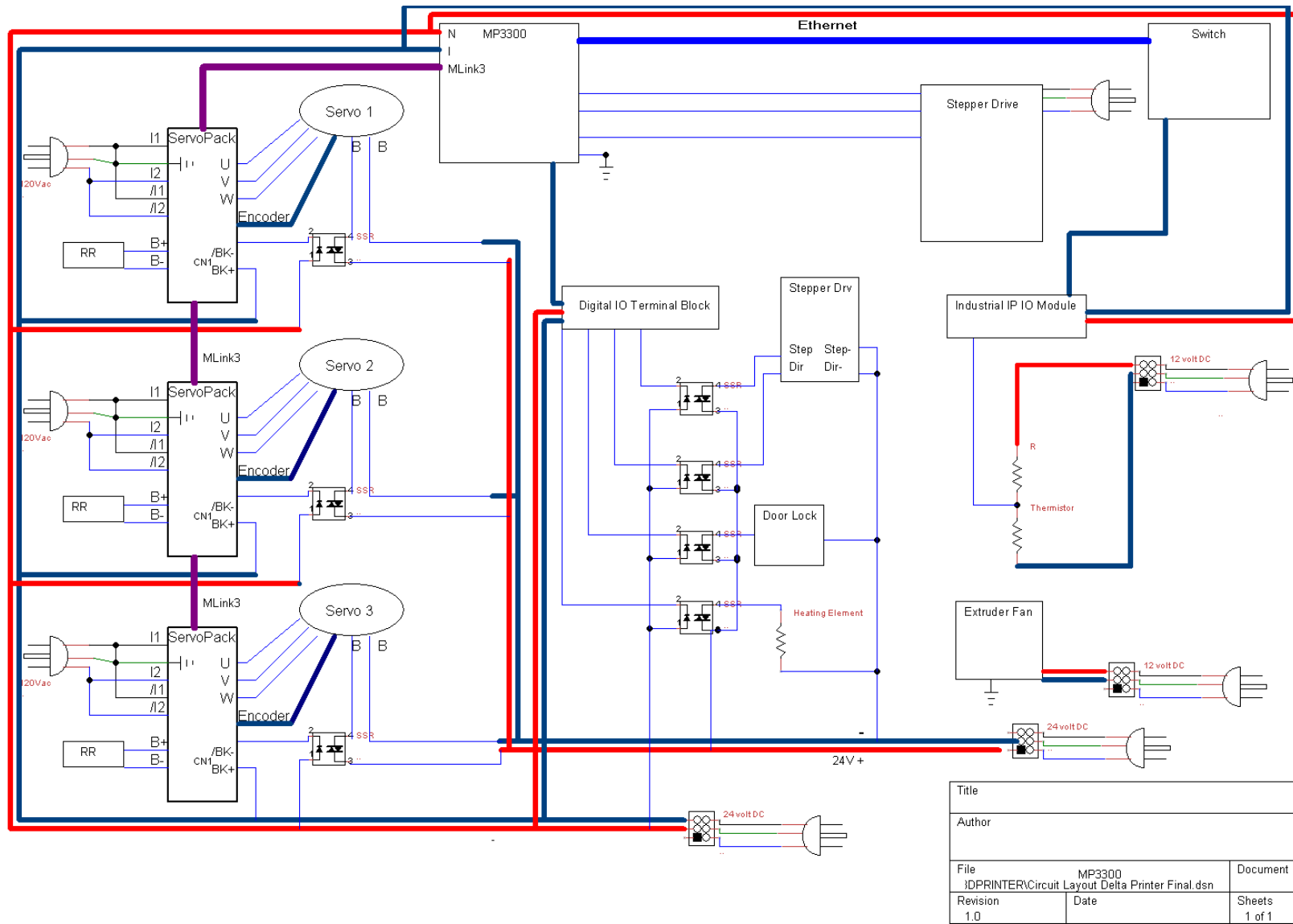
Design Verification Plan and Report (DVP&R)

Report Date		Sponsor							Component/Assembly		REPORTING ENGINEER:				
TEST PLAN												TEST REPORT			
Item No	Specification or Clause Reference	Test Description	Acceptance Criteria	Test Responsi	Test Stage	SAMPLES		TIMING		TEST RESULTS			NOTES		
						Quantity	Type	Start date	Finish date	Test Result	Quantity Pass	Quantity Fail			
1	Volumetric Speed	with max speed settings print 3 cubes with demensions of 5cm x 5cm x 5cm. Measure the time to print each cube. Take an average of the ten measured times.	62.5 mins												
2	Accuracy	with max accuracy settings print 3 cubes with demensions of 5cm x 5cm x 5cm. Measur the lengths of sides using high precision calipers.	30 microns												
3	Non-toxicity	refer to MSDS on plastics that will be printed	non- toxic												
4	machine foot print	use a tape measure to measure demensions of final machine	<3.05m x 3.05 x 2.43m												
5	minimize custom parts	count custom parts	<8												
6	delta mechanism	verify it is a delta mechanism	yes												
7	total budget	total all purchases	<\$5,000												
8	open source	verify software is open source	yes												
9	input file type	input a .stl file and verify it will print	yes												
10	print material cost	purchase bulk plastic spool, record price and mass	<\$35/kg												
11	build volume	print a 30cm x 30cm x 30cm cube shell, verify measurements with a ruler	yes												
12	number of colors	purchase 3 different color spools of bulk plastic, verify all colors can be printed	3												
15	Life	Perform fatigue analysis on joints, structure, and arms. Consult manufacturer on servobelt, motors and extruder	10,000 hours												
16	layer thickness	with maximum accuracy settings print 3 cubes with demensions of 5cm x 5cm x 5cm. Measur the height of cube using high precision calipers. Divide height by the number of layers printed	30 microns												
17	software cost	total software cost	\$0												
18	level print bed	adjust height of rubber feet until bed is level, verify with laser level	<5 deg												
19	horizontal movement of print head	send horizontal movement commands to motors with dial indicator on extruder plate and record deviations in flatness of move	<100 micron over 5 cm												
20	accurate print bed temperature control	measure temperature on surface of print bed and compare to digital reading	within 5 deg C at steady state												

Final Budget

Subsystem	Item	Quantity	Description	Vendor	Estimated	Unit Price	Estimated Total Cost	Actual Cost
Arms	Rod Bearings	12	Magnetic Ball Joints connect the carbon fiber rods to the sliders and extruder	TMC Magnetics	\$18.00		\$216.00	\$250.00
	Rods	6	Carbon Fiber Rods that are the arms of the delta robot.		\$14.00		\$84.00	\$105.47
	Epoxy Gun	1	Dual chamber epoxy gun used to apply epoxy		\$89.00		\$89.00	\$88.66
	Epoxy	1	fastens the CF rods to the ball joints.		\$24.35		\$24.35	\$24.35
	subtotal						\$413.35	\$468.48
Extruder	Extruder	1	melts and extrudes the plastic	Micron 3DP	\$340.00		\$340.00	\$340.35
	Extruder Plate	1	Plate that will hold the extruder in place		\$100.00		\$100.00	\$0.00
	ABS filament	1	3mm printing filament, structural parts		\$30.00		\$30.00	\$43.58
	PLA Filament	0	3mm printing filament, visual parts		\$30.00		\$0.00	\$0.00
							\$470.00	\$383.93
Frame	Top plate	1	12.5mm aluminum plate, machining flat, holes drilled	Discount Steel	\$500.00		\$500.00	\$324.29
	Bottom Plate	1	12.5mm aluminum plate, machining flat, holes drilled		\$500.00		\$500.00	\$324.29
	hardware	24	3/8" socket countersunk head screws		\$1.00		\$24.00	\$27.59
	Manufacturing Cost	7	Cost for set up and manufacturing of top and bottom plate hole patterns		\$60.00		\$420.00	\$0.00
							\$1,024.00	\$676.17
Heated Build Plate	Flexible Silicone Heater	1	Heats the glass surface	keenovo	\$50.00		\$50.00	\$243.50
	Glass Plate	1	Plate that parts are printed on		\$350.00		\$350.00	\$381.95
	Insulation	1	silicone 1/4" insulation mat		\$35.00		\$35.00	\$35.00
	Leveling	3	High Temp Leveling Feet and Z brackets		\$8.54		\$25.63	\$25.63
							\$435.00	\$686.08
Enclosure	Door Lock	1	electronic door lock	Simco	\$85.00		\$85.00	\$98.65
	Fans	2	190 CFM fans with inline carbon filter		\$99.95		\$199.90	\$310.82
	Hardware	10	L brackets		\$0.69		\$6.90	\$6.90
	Hardware	40	Screws		\$0.50		\$20.00	\$20.00
							\$226.80	\$436.37
Electronics Enclosure	Wires	1	16 gage wire	Ace	\$183.56		\$183.56	\$183.56
	relays	4	1 for fans, 3 for brakes, 24V		\$5.00		\$20.00	\$20.00
	relays	2	2 for outlet fans 120V		\$7.00		\$14.00	\$14.00
	Power Supply Unit	1	Power supply		\$150.00		\$150.00	\$150.00
	Wood	2	3'x4' plywood, 2"x4"		\$28.56		\$57.12	\$57.12
	Hardware	40	Screws		\$0.50		\$20.00	\$20.00
							\$444.68	\$444.68
							Total	\$3,096

Electronics Wiring Schematic



APPENDIX D: WORKS CITED

Works Cited

"3D Printer Overview 2013." *3DSystems*. Web. 20 Oct. 2014.

<[http://peakllc.net/main/wp-content/uploads/2013/07/3D-Systems-Printer-Overview 2013 PPS.pdf](http://peakllc.net/main/wp-content/uploads/2013/07/3D-Systems-Printer-Overview%202013%20PPS.pdf)>.

"3D Printer Price Compare." *3Ders*. Web. 9 Oct. 2014.

<<http://www.3ders.org/pricecompare/3dprinters/?tab=Details>>.

"3D Printer Price - Stratasys 3D Printers." *MCAD*. Web. 20 Oct. 2014.

<<http://www.mcad.com/3d-printing/3d-printer-price/>>.

"BigRep Full Scale 3D Printer." *BigRep*. Web. 9 Oct. 2014. <<http://bigrep.com/1/features/>>.

"Cardan Joint." *The Green Book*. Web.

<[http://www.thegreenbook.com/advertiserfiles/productshowcasepictures/main/t/t0735_29862/universal joint tasaro s pore pte ltd.jpg](http://www.thegreenbook.com/advertiserfiles/productshowcasepictures/main/t/t0735_29862/universal_joint_tasaro_s_pore_pte_ltd.jpg)>.

"Dimension 1200es Durability Meets Affordability." *Stratasys*. Web. 9 Oct. 2014.

<<http://www.stratasys.com/3d-printers/design-series/dimension-1200es>>.

"Dimension SST 1200ES." *Amtek Company*. Web. 20 Oct. 2014.

<<http://www.amtekcompany.com/dimension-sst-1200es/>>.

"Dual Head All Metal Extruder." *Micron 3DP*. Web.

<<http://micron3dp.myshopify.com/products/dual-head-all-metal-3d-printer-extruder>>.

"Erik's Bowden Extruder." *RepRap Wiki*. Web. <http://reprap.org/wiki/Erik's_Bowden_Extruder>.

"Fused Deposition Modeling." *Wikipedia*. Web.

<http://en.wikipedia.org/wiki/Fused_deposition_modeling>.

"G-code Generator for 3D Printers." *Slic3r*. Web. 20 Oct. 2014. <<http://slic3r.org/>>.

"Kossel." *RepRapWiki*. Web. 9 Oct. 2014. <<http://reprap.org/wiki/Kossel>>.

"Learn about 3D printing and compare 3D printing products." Anwiaa. Web. 20 October 2014.

<<http://www.aniwaa.com/product/3d-systems-projet-3500/>>

"Linear Slides: ETL Long Travel Series." *Newmark Systems, Inc.* Web.

<<http://www.newmarksystems.com/linear-positioners/etl-series-linear-slide/>>.

"MH3000 - 5 Color/Material 3D Printer With Liquid Cooling - Fully Assembled." *ORD Solutions*.

Web. 9 Oct. 2014. <<http://www.ordsolutions.com/mh3000-5-color-material-3d-printer-with-liquid-cooling-fully-assembled/>>.

"Magnetic Ball Joint Assembly." *Freenergy*. Web.

<<http://www.freenergy.com.au/products/Magnetic-Ball-Joint-Assembly-KD310-%2d-BRASS.html>>.

"Magnetic Ball Joint." *Magnetics China*. Web. <<http://www.magnetics-china.com/wp-content/uploads/2012/09/5208.jpg>>.

"Material Safety Data Sheet -- ABS." Edinburg Plastics, Inc., 2006. Web. 2015.

<http://www.plasticsmadesimple.com/DataSheets/ABS_MSDS_GP.pdf>.

Newman, John. "Objet 30 Pro Unveiled." *Rapid Ready Tech*. 22 May 2012. Web. 20 Oct. 2014. <<http://www.rapidreadytech.com/2012/05/objet30-pro-unveiled/>>.

"Next Gen All Metal 3D Printer Extruder from Micron." *3Ders*. Web. 16 Oct. 2014.

<<http://www.3ders.org/articles/20131231-all-metal-next-gen-3d-printer-extruder-from-micron.html>>.

"Objet30 Pro Desktop 3D Printer." *Stratasys*. Web. 9 Oct. 2014.

<<http://www.stratasys.com/3d-printers/design-series/objet30-pro>>.

"Our Software." *Ultimaker*. Web. 20 Oct. 2014.

<<https://www.ultimaker.com/pages/our-software>>.

"Polyjet Printing." Web.

<https://encrypted-tbn3.gstatic.com/images?q=tbn:ANd9GcRKY4IdQxbqAXeOQmNOBKh-uMX7_OyQNMwpv2ic13H0lqIGMZ26lw>.

"Projet 3500 HDMax." *3DSystems*. Web. 20 Oct. 2014.

<<http://www.3dsystems.com/de/projet3500max>>.

"PSK Precision Modules." *Bosch Rexroth*. Web.

<http://www.boschrexroth.com/country_units/america/united_states/sub_websites/brus_dcl/Products/Linear_Modules_and_Cartesian_Systems/PSK/index.jsp>.

"Sailfish Firmware - Tuning Acceleration." MakerBot. N.p., n.d. Web. 05 Feb. 2015.

<<http://www.makerbot.com/sailfish/tuning/>>.

"SeeMeCNC PartDaddy 4,5 Meter Tall Pellet Fed Delta 3d Printer." *DIY 3D Printing*. 29 July 2014. Web. 6 Oct. 2014. <<http://diy3dprinting.blogspot.com/2014/07/seemecnc-partdaddy-45-meter-tall-pellet.html>>.

"Rapid Prototyping." *M&B Engineering*. Web. 21 Oct. 2014.

<http://www.mandbengineering.com/rapid_prototyping.htm>.

"Rod End Ball Joint." *Danuser*. Web.

<<http://www.danuser.com/sites/all/themes/danuser/images/oem50.jpg>>.

"Rostock MAX™ V2 Desktop 3D Printer Kit." *SeeMeCNC Delta 3D Printers and More*. 29 July 2014. Web. 8 Oct. 2014. <<http://seemecnc.com/products/rostock-max-complete-kit>>.

"Selective Laser Sintering." *Wikipedia*. Web.

<http://en.wikipedia.org/wiki>Selective_Laser_Sintering>.

"ServoBelt Linear Drive." *Bell-Everman Embedded Motion Systems*. Web.

<<http://bell-everman.com/products/linear-positioning/servobelt-linear-sbl>>.

"Single Head All Metal Extruder." *Micron 3DP*. Web.

<<http://micron3dp.myshopify.com/products/all-metal-state-of-the-art-3d-printer-extruder>>.

"Slicers and User Interfaces for 3D Printers." *Edutech Wiki*. Web. 20 Oct. 2014.

<http://edutechwiki.unige.ch/en/Slicers_and_user_interfaces_for_3D_printers>.

"Stereolithography." *Wikipedia*. Web. <<http://en.wikipedia.org/wiki/Stereolithography>>.

"Threaded Fasteners: Mechanics." *DANotes*. Web.

<http://www-mdp.eng.cam.ac.uk/web/library/enginfo/textbooks_dvd_only/DAN/threads/mechanics/mechanics.html>.

Ullman, D. "The Mechanical Design Process." 1992.

"Voyager VB1 Belt Actuator." *Isel Automation*. Web.

<<http://www.techno-isel.com/tic/Catdas/Voyager01.htm>>

"Yield Lab 4 Inch 190 CFM Charcoal Filter and Duct Fan Combo Kit." GrowAce. N.p., n.d.

Web. <<http://growace.com/yield-lab-4-inch-190-cfm-charcoal-filter-and-duct-fan-combo-kit.html>>.

APPENDIX E: SPECIFICATION SHEETS

Below is a short table of contents for this section:

Page Number	Product
138	ACP Composites .375" Carbon Fiber Solid Rod
139	Loctite Hysol E-40HT Epoxy
140	Yaskawa SGMJV Servomotors
142	Epcos NTC Thermistors

.375" Carbon Fiber Solid Rod



Carbon Fiber Solid Rods are manufactured through a process referred to as pultrusion. Continuous fibers combined with a resin matrix are pulled through a heated steel forming die. As the carbon fibers are saturated with the resin mixture and then pulled through a round die, the hardening of the resin is initiated by the heat from the die and a rigid, cured structure is formed in the shape and size of the die. The majority of the fibers are running in the 0 degree direction, along the length of the rod to produce an extremely stiff and lightweight with incredible linear strength, due to the orientation of the carbon fibers, and tight outer diameter (OD) tolerances.

Physical Properties

Diameter	.375" +/- .004"	Test Method-Caliper
Straightness	.050" total indicator runout (TIR) over 24" span	For reference only
Color	Natural dark gray to black	No color match
Surface Finish	Small scratches, surface defects, or blemishes may be apparent.	Mimimum-Visual
Composite Type	0° unidirectional orientation	For reference only
Resin Type	Premium grade bisphenol epoxy vinyl ester	For reference only
Fiber Type	33 to 35 MSI standard modulus carbon fiber	For reference only
Fiber Volume	60%	+/- 5%
Cuts	Rough abrasive cut both ends, small burrs may be apparent.	Mimimum-Visual
Cleaning	Product blown off with dry air, some dust may be apparent.	Mimimum-Visual

Technical Properties

Tensile Strength	250 ksi / 1.72 GPa
Tensile Modulus	20.0 msi / 138 GPa
Ultimate Shear Strength	6.0 ksi / 41.3 Mpa
Ultimate Tensile Strain	1.50%
Flexural Strength	265 ksi / 1.83 GPa
Flexural Modulus	19.0 msi / 131 GPa
CTE	-0.1 ppm/cm ³ / -0.2 ppm/°C
Thermal Properties	150°F maximum
Glass Transition Temp.	100° C
Density	.054 lbs/in ³ / 1.5 g/cm ³

Sample data is measured from a .156" diameter solid rod with standard modulus fibers and Bisphenol Epoxy Vinyl Ester

All the information contained in these properties is believed to be reliable. It is intended for comparison purposes only as each manufactured lot will exhibit variations. The user should evaluate the suitability of each product for their application. We cannot anticipate the variations in all end use and we make no warranties and assume no liability in connection with the use of this information.



Hysol® E-40HT™

April 2008

PRODUCT DESCRIPTION

Hysol® E-40HT™ provides the following product characteristics:

Technology	Epoxy
Chemical Type	Epoxy
Appearance (Resin)	Off-white
Appearance (Hardener)	Amber ^{LMS}
Appearance (Mixed)	Off-white
Components	Two component - requires mixing
Viscosity	Medium
Mix Ratio, by volume - Resin : Hardener	2 : 1
Mix Ratio, by weight - Resin : Hardener	100 : 43
Cure	Room temperature cure after mixing
Application	Bonding

Hysol® E-40HT™ is a high viscosity, industrial grade epoxy adhesive with extended work life. Once mixed, the two component epoxy cures at room temperature to form a tough, off-white bondline with excellent resistance to shear and impact forces. This product offers elevated temperature resistance, excellent mechanical and electrical properties, and withstands exposure to a wide variety of solvents and chemicals. Hysol® E-40HT™ develops strong, tough bonds on aluminum, steel and other metals, as well as glass, ceramics and plastics.

TYPICAL PROPERTIES OF UNCURED MATERIAL

Resin:

Specific Gravity @ 25 °C	1.17
Viscosity, Cone & Plate, mPa·s (cP):	
Cone CP50-1 @ shear rate 100 s ⁻¹	107,000
Flash Point - See MSDS	

Hardener:

Specific Gravity @ 25 °C	1.01
Viscosity, Cone & Plate, mPa·s (cP):	
Cone CP50-1 @ shear rate 100 s ⁻¹	6,200
Flash Point - See MSDS	

Mixed:

Specific Gravity @ 25 °C	1.13
Viscosity, Cone & Plate, mPa·s (cP):	
Cone CP50-1 @ shear rate 100 s ⁻¹	16,000
Flash Point - See MSDS	

TYPICAL CURING PERFORMANCE

Fixture Time

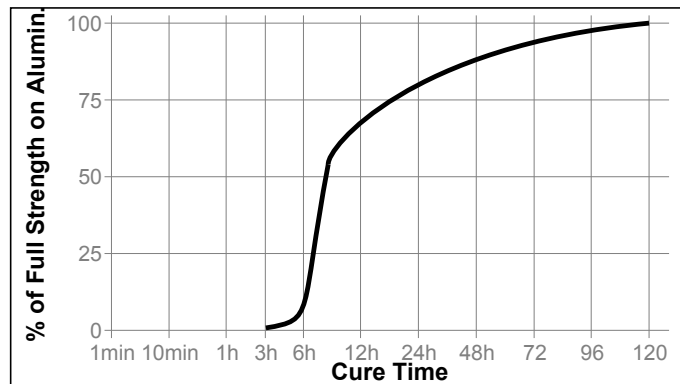
Fixture time is defined as the time to develop a shear strength of 0.1 N/mm².

Fixture Time, ISO 4587, minutes:

Steel (grit blasted), @ 22 °C 165 to 180

Cure Speed vs. Time

The graph below shows shear strength developed with time on abraded, acid etched aluminum lapshears @ 25 °C with an average bondline gap of 0.1 to 0.2 mm and tested according to ISO 4587.



TYPICAL PROPERTIES OF CURED MATERIAL

Cured @ 22 °C for 5 days

Physical Properties:

Glass Transition Temperature (Tg)	57
ISO 11359-2, °C	
Shore Hardness, ISO 868, Durometer D	79

Electrical Properties:

Dielectric Breakdown Strength, IEC 60243-1, KV/mm	33
---	----

Cured @ 22 °C for 3 days

Physical Properties:

Elongation, at break, ISO 527-3, %	2.2
Tensile Strength, at break, ISO 527-3	N/mm ² (psi)
	30 (4,300)
Tensile Modulus, ISO 527-3	N/mm ² (psi)
	1,860 (269,200)

TYPICAL PERFORMANCE OF CURED MATERIAL

Adhesive Properties

Cured for 5 days @ 22 °C and 0.13 mm gap

Lap Shear Strength, ISO 4587:

Steel (grit blasted)	N/mm ² (psi)	28 (4,030)
Aluminum (abraded)	N/mm ² (psi)	26 (3,740)



Ratings and Specifications

Time Rating: Continuous

Vibration Class: V15

Insulation Resistance: 500 VDC, 10 MΩ min.

Ambient Temperature: 0 to 40°C

Excitation: Permanent magnet

Mounting: Flange-mounted

Thermal Class: B

Withstand Voltage: 1500 VAC for one minute

Enclosure: Totally enclosed, self-cooled, IP65

(except for shaft opening)

Ambient Humidity: 20% to 80% (no condensation)

Drive Method: Direct drive

Rotation Direction: Counterclockwise (CCW) with forward run reference when viewed from the load side

Voltage		200 V						
Servomotor Model: SGMJV-□□□		A5A	01A	C2A	02A	04A	06A	08A
Rated Output ^{*1}	W	50	100	150	200	400	600	750
Rated Torque ^{*1, *2}	N·m	0.159	0.318	0.477	0.637	1.27	1.91	2.39
Instantaneous Peak Torque ^{*1}	N·m	0.557	1.11	1.67	2.23	4.46	6.69	8.36
Rated Current ^{*1}	A _{rms}	0.61	0.84	1.6	1.6	2.7	4.2	4.7
Instantaneous Max. Current ^{*1}	A _{rms}	2.1	2.9	5.7	5.8	9.3	14.9	16.9
Rated Speed ^{*1}	min ⁻¹				3000			
Max. Speed ^{*1}	min ⁻¹				6000			
Torque Constant	N·m/A _{rms}	0.285	0.413	0.327	0.435	0.512	0.505	0.544
Rotor Moment of Inertia	×10 ⁻⁴ kg·m ²	0.0414 (0.0561)	0.0665 (0.0812)	0.0883 (0.103)	0.259 (0.323)	0.442 (0.506)	0.667 (0.744)	1.57 (1.74)
Rated Power Rate ^{*1}	kW/s	6.11	15.2	25.8	15.7	36.5	54.7	36.3
Rated Angular Acceleration ^{*1}	rad/s ²	38400	47800	54100	24600	28800	28600	15200
Applicable SERVOPACK	SGDV-□□□□	R70□	R90□	1R6A,2R1F	1R6A,2R1F	2R8□	5R5A	5R5A

*1: These items and torque-motor speed characteristics quoted in combination with an SGDV SERVOPACK are at an armature winding temperature of 100°C. Other values quoted are at 20°C.

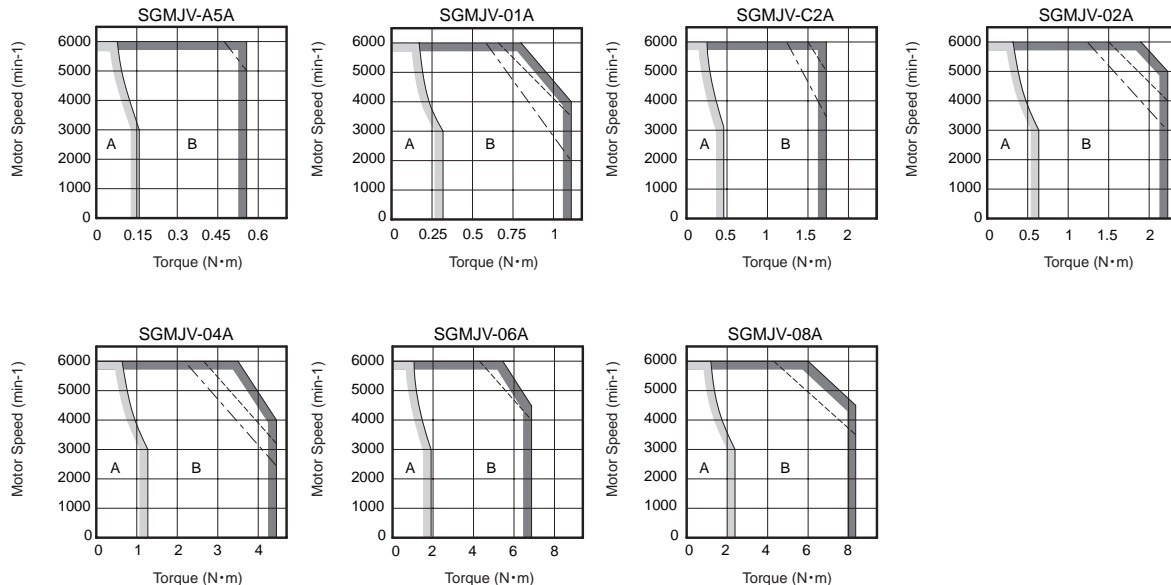
*2: Rated torques are continuous allowable torque values at 40°C with an aluminum heat sink of the following dimensions attached.

SGMJV-A5A, -01A: 200 mm×200 mm×6 mm

SGMJV-02A, -04A, -08A: 250 mm×250 mm×6 mm

Note: The values in parentheses are for servomotors with holding brakes.

●Torque-Motor Speed Characteristics [A] : Continuous Duty Zone [B] : Intermittent Duty Zone^(Note3)



Notes: 1 The solid, dotted, and dashed-dotted lines of the intermittent duty zone indicate the characteristics when a servomotor runs with the following combinations:

- The solid line: With a three-phase 200 V or a single-phase 230 V SERVOPACK
- The dotted line: With a single-phase 200 V SERVOPACK
- The dashed-dotted line: With a single-phase 100 V SERVOPACK

An SGMJV-A5A servomotor has the same characteristics in combination with three-phase 200 V and single-phase 200 V SERVOPACKs.

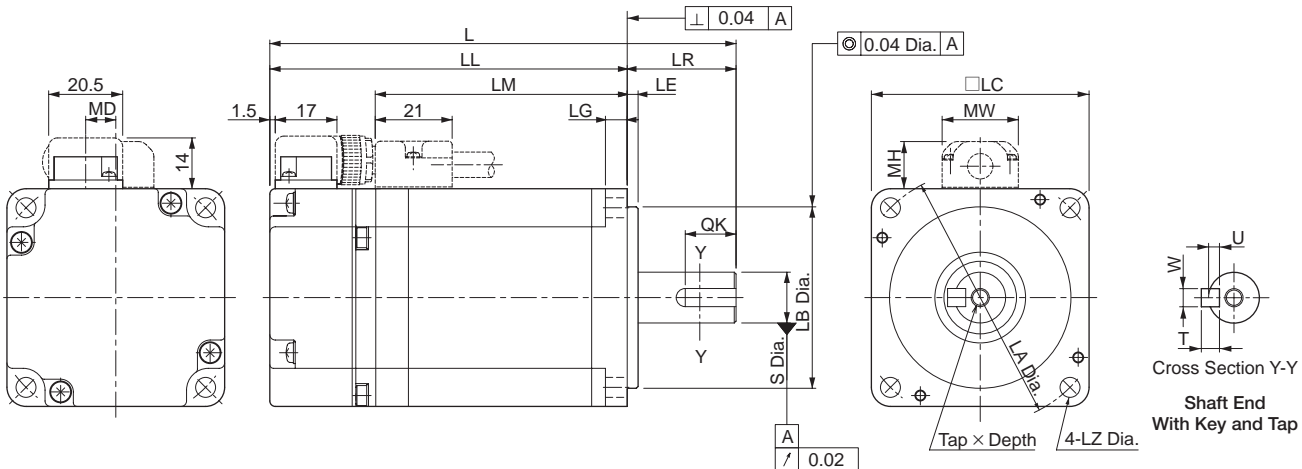
2 The characteristics of the intermittent duty zone differ depending on the supply voltages.

3 When the effective torque during intermittent duty is within the rated torque, the servomotor can be used within the intermittent duty zone.

4 When the main circuit cable length exceeds 20 m, note that the intermittent duty zone of the Torque-Motor Speed Characteristics will shrink as the line-to-line voltage drops.

External Dimensions Units: mm

(2) 200 to 750 W

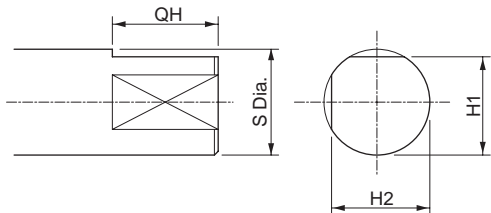


Model SGMJV-	L	LL	LM	Flange Face Dimensions							S	Tap×Depth	Key Dimensions				MD	MW	MH	Approx. Mass kg
				LR	LE	LG	LC	LA	LB	LZ			QK	U	W	T				
02A□A21 (02A□A2C)	110 (150)	80 (120)	51	30	3	6	60	70	50 ⁰ _{-0.025}	5.5	14 ⁰ _{-0.011}	No tap	No key				8.3	21	13	0.9 (1.5)
02A□A61 (02A□A6C)				M5×8L	14	3	5	5				M5×8L	14	3	5	5				
04A□A21 (04A□A2C)	128.5 (168.5)	98.5 (138.5)	69.5	30	3	6	60	70	50 ⁰ _{-0.025}	5.5	14 ⁰ _{-0.011}	No tap	No key				8.3	21	13	1.3 (1.9)
04A□A61 (04A□A6C)				M5×8L	14	3	5	5				M5×8L	14	3	5	5				
06A□A21 (06A□A2C)	154.5 (200.5)	124.5 (170.5)	95.5	30	3	6	60	70	50 ⁰ _{-0.025}	5.5	14 ⁰ _{-0.011}	No tap	No key				8.3	21	13	1.7 (2.4)
06A□A61 (06A□A6C)				M5×8L	14	3	5	5				M5×8L	14	3	5	5				
08A□A21 (08A□A2C)	155 (200)	115 (160)	85	40	3	8	80	90	70 ⁰ _{-0.030}	7	19 ⁰ _{-0.013}	No tap	No key				13.8	27	15	2.7 (3.6)
08A□A61 (08A□A6C)				M6×10L	22	3.5	6	6				M6×10L	22	3.5	6	6				

Note: The models and values in parentheses are for servomotors with holding brakes.

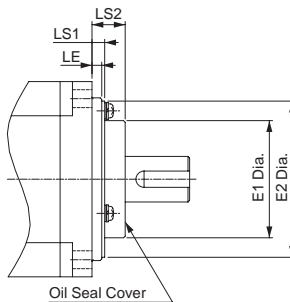
<Shaft End and Other Options>

● With Two Flat Seats



Model SGMJV-	Dimensions of Servomotor with Two Flat Seats mm			
	QH	S	H1	H2
02A□AB□	15	14 ⁰ _{-0.011}	13	13
04A□AB□				
06A□AB□				
08A□AB□	22	19 ⁰ _{-0.013}	18	18

● With an Oil Seal



Model SGMJV-	Dimensions of Servomotor with an Oil Seal			
	E1	E2	LS1	LS2
02A, 04A, 06A	36	48	4	10
08A	49	66	6	11

Notes: 1 The 7th digit of the model designation is "S" or "E."

2 Key dimensions are the same as those in the table above.

Applications

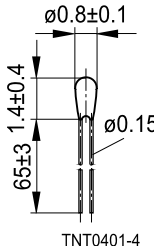
- Automotive electronics
- Industrial electronics
- Home appliances

Features

- Glass-encapsulated, heat-resistive and highly stable
- For temperature measurement up to 250 °C
- Fast response
- Small dimensions
- Leads: dumet wires (copper-clad FeNi)

Options

Leads: nickel-plated dumet wires.

Dimensional drawing


TNT0401-4

Dimensions in mm

Alternative dimensions available on request.

Delivery mode

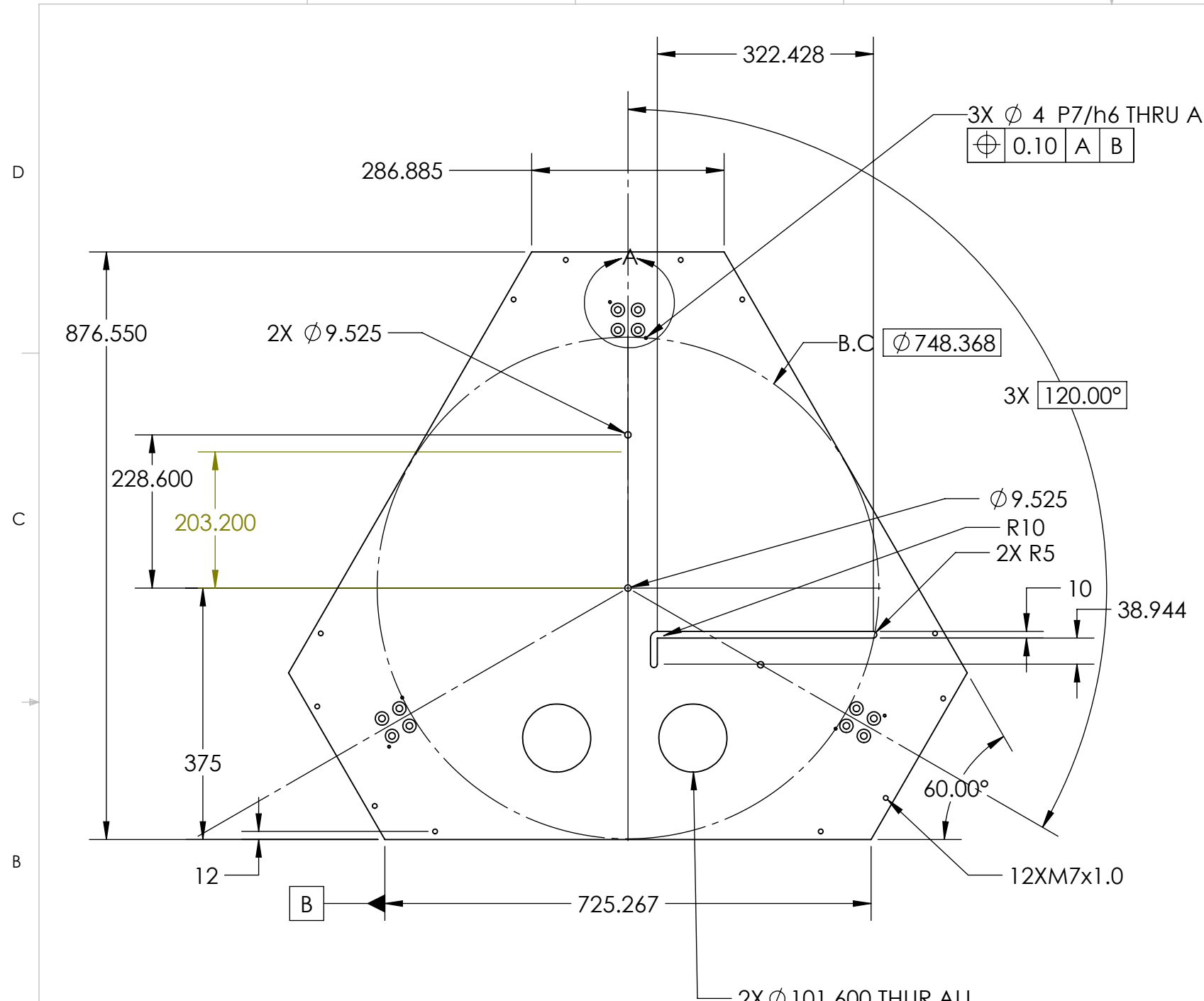
Bulk

General technical data

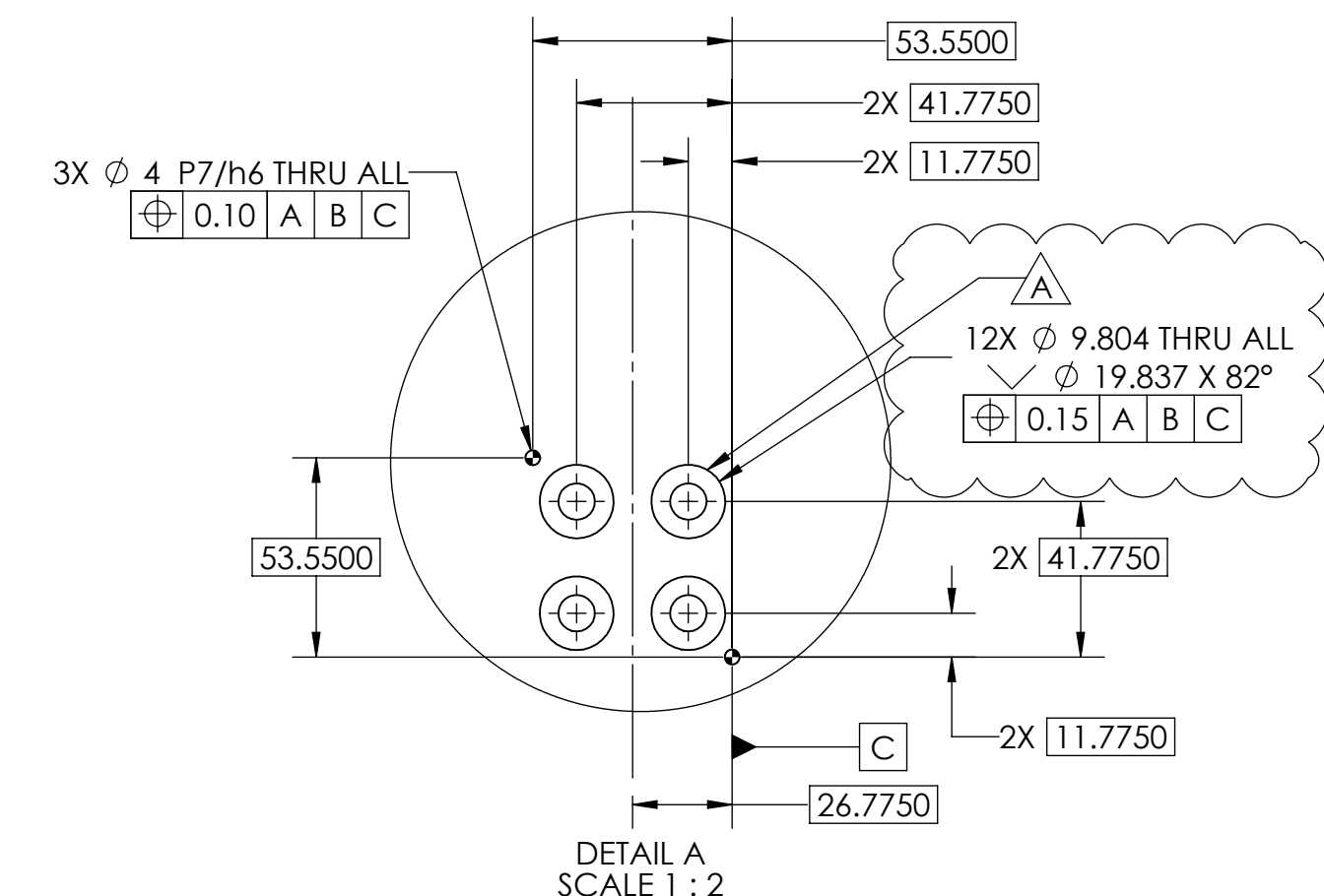
Climatic category	(IEC 60068-1)		55/250/56	
Max. power	(at 25 °C)	P ₂₅	18	mW
Resistance tolerance		ΔR _R /R _R	±1, ±2, ±3, ±5	%
Rated temperature		T _R	25	°C
Dissipation factor	(in air)	δ _{th}	approx. 0.4	mW/K
Thermal cooling time constant	(in air)	τ _c	approx. 3	s
Heat capacity		C _{th}	approx. 1.3	mJ/K

APPENDIX F: DETAIL DRAWINGS

8 7 6 5 4 3 2 1



REVISIONS				
ZONE	REV.	DESCRIPTION	DATE	APPROVED
	A	COUNTERSUNK SOCKET HEAD CAP SCREW CHANGED FROM M8 TO 3/8"-16, METRIC VALUES SHOWN ON DRAWING.	4/29/2015	T.CHRIS



DETAIL A
SCALE 1 : 2

UNLESS OTHERWISE SPECIFIED:		NAME	DATE
DIMENSIONS ARE IN MM	T. CHRIS	2/1/15	
TOLERANCES:			
NO DECIMAL: ± 1			
ONE&TWO PLACE DECIMAL ± 1			
THREE PLACE DECIMAL ± 0.5			
INTERPRET GEOMETRIC			
TOLERANCING PER:			
MATERIAL			
6061-T6 (SS)			
COMMENTS:	THE HOLE PATTERNS ARE CRITICAL, OUTSIDE DIMENSIONS OF PLATE ARE NOT CRITICAL.		
SHEET	DWG. NO.	REV	
B	CP001	A	
SCALE: 1:8	WEIGHT:	SHEET 1 OF 1	

SolidWorks Student Edition.
For Academic Use Only.

PROPRIETARY AND CONFIDENTIAL
THE INFORMATION CONTAINED IN THIS
DRAWING IS THE SOLE PROPERTY OF
DELTRONIC SOLUTIONS. ANY
REPRODUCTION IN PART OR AS A WHOLE
WITHOUT THE WRITTEN PERMISSION OF
DELTRONIC SOLUTIONS IS
PROHIBITED.

CP004

NEXT ASSY

APPLICATION

DO NOT SCALE DRAWING

DELTRONIC SOLUTIONS

TITLE:

FRAME PLATES

SIZE

B

DWG. NO.

CP001

REV

A

SCALE: 1:8

WEIGHT:

SHEET 1 OF 1

D

D

1

1

11

S4

SECTION A-

SolidWorks Student Edition.

For Academic Use Only.

PROPRIETARY AND CONFIDENTIAL
THE INFORMATION CONTAINED IN THIS DRAWING IS THE SOLE PROPERTY OF DELTRONIC SOLUTIONS. ANY REPRODUCTION IN PART OR AS A WHOLE WITHOUT THE WRITTEN PERMISSION OF DELTRONIC SOLUTIONS IS PROHIBITED.

This technical drawing illustrates a mechanical component with the following key dimensions and features:

- Vertical height:** The total vertical height of the part is indicated as 80.83.
- Top surface slope:** The top surface has a 30° angle relative to the horizontal.
- Bottom surface slope:** The bottom surface has a 30° angle relative to the horizontal.
- Bottom width:** The width of the bottom-most flange is specified as 14.
- Outer side finish:** The outer surfaces of the main body are labeled "ALL OUTERSIDES".
- Top hole diameter:** A hole at the top edge is labeled B.C. $\phi 135$.
- Top hole count:** There are two holes located on the top surface.
- Side hole count:** There are three holes located on each of the two side flanges.
- Front hole count:** There are two holes located on the front-most flange.
- Left hole count:** There are two holes located on the left-most flange.
- Top slot width:** A slot at the top edge is labeled 7.
- Top slot depth:** A slot at the top edge is labeled 25.
- Top slot length:** A slot at the top edge is labeled 50.

— 6X M4x0.7

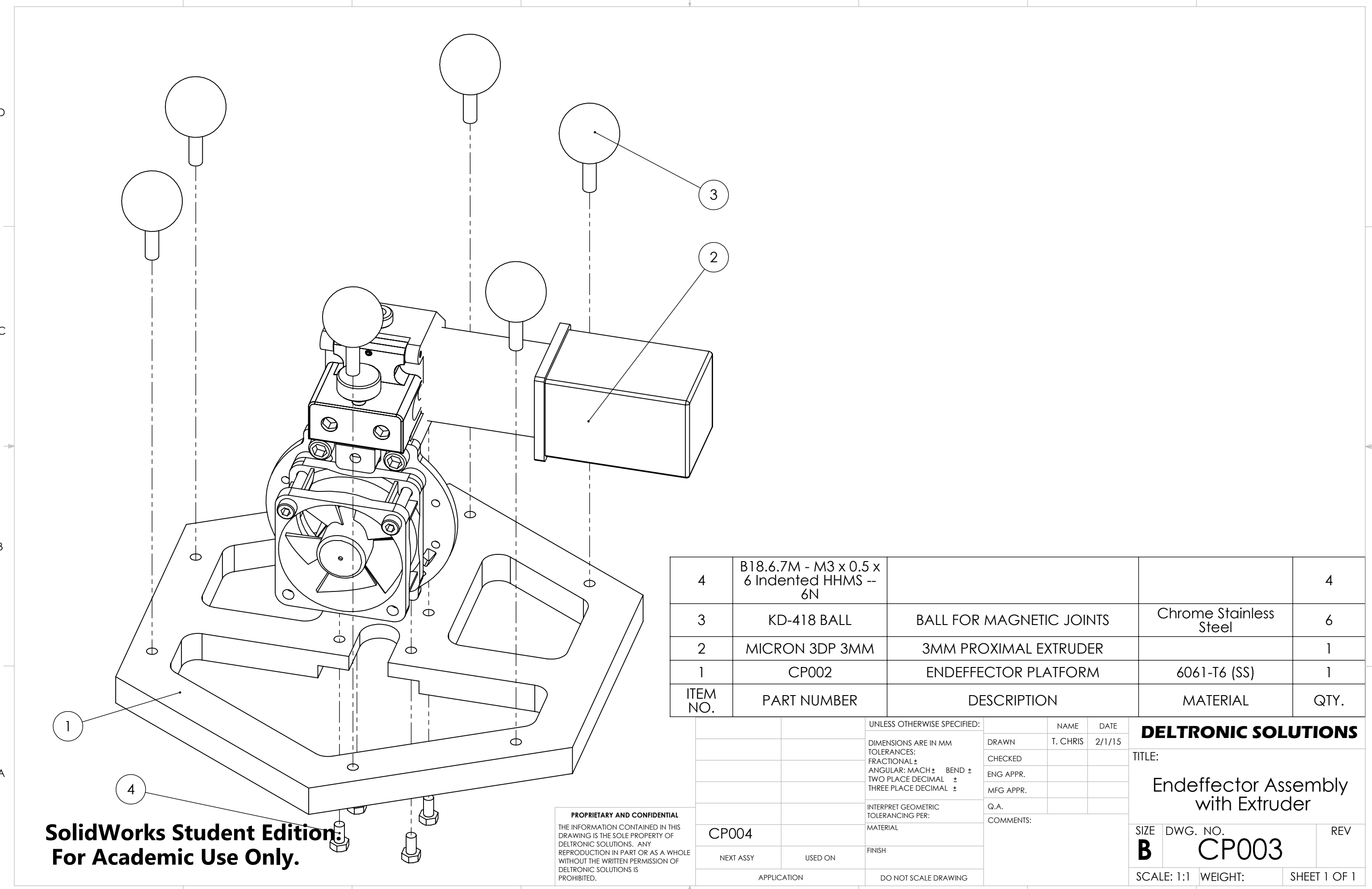
4X M4X0.7 - 6H THRU A

2X 15.2
2X 4.75

A technical drawing showing a vertical profile with various dimensions. The top horizontal dimension is labeled 39. The bottom horizontal dimension is labeled 15.50. The bottom-most dimension is labeled 31. There are two groups of hole locations indicated by dashed lines, each group containing two holes. The left group is labeled 2X11 and the right group is labeled 2X22.

DETAIL B
SCALE 2 : 1.5

		UNLESS OTHERWISE SPECIFIED:		NAME	DATE	DELTRONIC SOLUTIONS TITLE: Endeffector
		DIMENSIONS ARE IN MM	DRAWN	T. CHRIS	2/1/15	
		TOLERANCES: ± 0.152	CHECKED			
			ENG APPR.			
			MFG APPR.			
		INTERPRET GEOMETRIC TOLERANCING PER:	Q.A.			
ITAL THIS OF	CP003	MATERIAL 6061-T6 (SS)	COMMENTS: OUTER M4 HOLE LOCATION IS CRITICAL COMPONENT.			
WHOLE OF	NEXT ASSY	USED ON	FINISH			SIZE DWG. NO. B CP002 REV
	APPLICATION		DO NOT SCALE DRAWING		SCALE: 1:1.5 WEIGHT:	
					SHEET 1 OF 1	



ITEM NO.	PART NUMBER	DESCRIPTION	MATERIAL	Default/QTY.
11	3mm ABS SPOOL	3mm ABS BULK PLASTIC SPOOL		1
10	3mm ABS	3mm ABS PLASTIC	ABS	1
9	CARBON FILTER FAN	OUTLET FAN WITH CARBON FILTER		2
8	KD-418	BALL FOR MAGNETIC JOINTS	Chrome Stainless Steel	12
7	B18.3.5M - 8 x 1.25 x 35 Socket FCHS -- 35C			24
6	4mm DOWEL	4mm PRESSFIT DOWEL FOR COLUMN ALIGNMENT	Plain Carbon Steel	12
5	CP005	CARBON FIBER RODS W/ MAGNET ENDS		6
4	CP006	HEATED BUILD PLATE W/ POWER BOX		1
3	CP003	ENDEFFECTOR W/ MICRON 3mm EXTRUDER		1
2	SBL-L 60X60, NO ENCODER	1000mm SERVOBELT LIGHT SLIDE W/ 120mm OFFSET		3
1	CP001	6mm PLATE FOR SERVOBELT SLIDES	6061-T6 (SS)	2
UNLESS OTHERWISE SPECIFIED: DIMENSIONS ARE IN MM TOLERANCES: FRACTIONAL \pm ANGULAR: MACH \pm BEND \pm TWO PLACE DECIMAL \pm THREE PLACE DECIMAL \pm				
DRAWN T. CHRIS 2/1/15				
CHECKED				
ENG APPR.				
MFG APPR.				
Q.A.				
COMMENTS:				
THE PRESSFIT DOWELS ARE CRITICAL TO THE ALIGNMENT OF THE COLUMNS, INSTALL PRIOR TO M8 SCREWS				
NEXT ASSY		USED ON	FINISH	
APPLICATION		DO NOT SCALE DRAWING		

**SolidWorks Student Edition.
For Academic Use Only.**

PROPRIETARY AND CONFIDENTIAL
THE INFORMATION CONTAINED IN THIS DRAWING IS THE SOLE PROPERTY OF DELTRONIC SOLUTIONS. ANY REPRODUCTION IN PART OR AS A WHOLE WITHOUT THE WRITTEN PERMISSION OF DELTRONIC SOLUTIONS IS PROHIBITED.

DELTRONIC SOLUTIONS

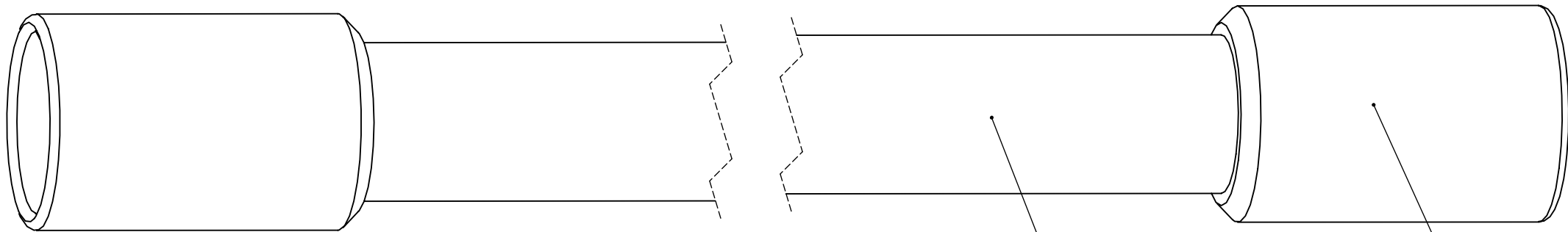
TITLE:
DELTA 3D PRINTER

SIZE **B** DWG. NO. **CP004** REV
SCALE: 1:9 WEIGHT: SHEET 1 OF 1

8 7 6 5 4 3 2 1

D

D



C

C

B

B

A

A

**SolidWorks Student Edition.
For Academic Use Only.**

PROPRIETARY AND CONFIDENTIAL

THE INFORMATION CONTAINED IN THIS DRAWING IS THE SOLE PROPERTY OF DELTRONIC SOLUTIONS. ANY REPRODUCTION IN PART OR AS A WHOLE WITHOUT THE WRITTEN PERMISSION OF DELTRONIC SOLUTIONS IS PROHIBITED.

ITEM NO.	PART NUMBER	DESCRIPTION	MATERIAL	QTY.
2	KD-418 MAGNET	MAGNETIC BALL JOINT BASE	Brass	2
1	CP008	46cm UNIDIRECTIONAL CARBON FIBER 3/8" RODS	Hexcel AS4C (3000 Filaments)	1

		UNLESS OTHERWISE SPECIFIED:		NAME	DATE
		DIMENSIONS ARE IN MM	DRAWN	T. CHRIS	2/1/15
		TOLERANCES:	CHECKED		
		FRACTIONAL \pm	ENG APPR.		
		ANGULAR: MACH \pm	MFG APPR.		
		BEND \pm			
		TWO PLACE DECIMAL \pm			
		THREE PLACE DECIMAL \pm			
		INTERPRET GEOMETRIC TOLERANCING PER:	Q.A.		
		MATERIAL	COMMENTS:		
CP004			KD-418 MAGNET ENDS FIXED TO CARBON RODS WITH ADHESIVE		
NEXT ASSY	USED ON	FINISH			
		APPLICATION	DO NOT SCALE DRAWING		

DELTRONIC SOLUTIONS

TITLE:

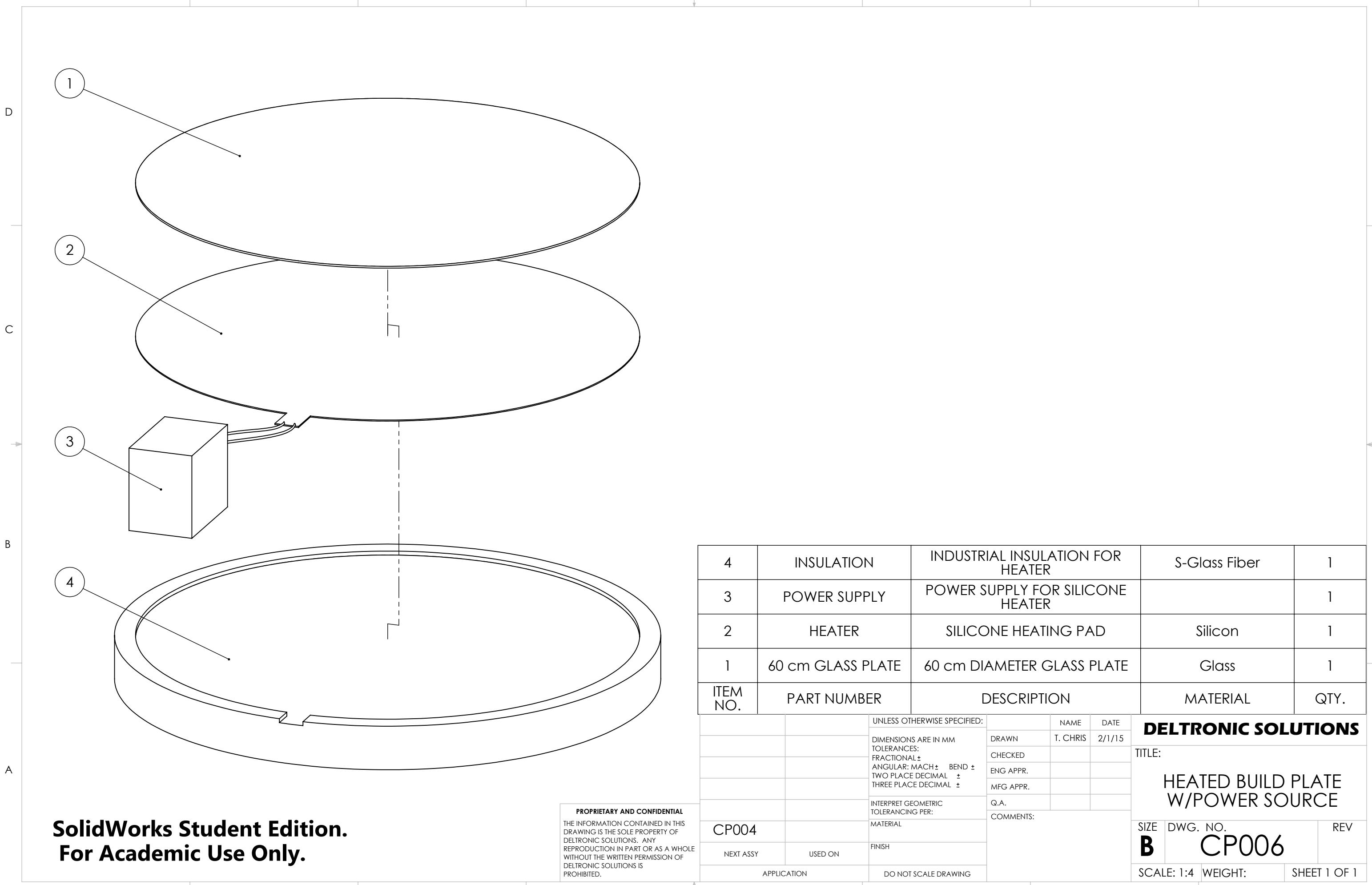
**CARBON ROD
ASSEMBLY**

SIZE DWG. NO. REV

B CP005

SCALE: 3:1 WEIGHT: SHEET 1 OF 1

8 7 6 5 4 3 2 1



8

7

6

5

4

3

2

1

D

D

C

C

B

B

A

A

460±0.0254

3/8" CARBON FIBER UNIDIRECTIONAL RODS



**SolidWorks Student Edition.
For Academic Use Only.**

PROPRIETARY AND CONFIDENTIAL
THE INFORMATION CONTAINED IN THIS
DRAWING IS THE SOLE PROPERTY OF
<INSERT COMPANY NAME HERE>. ANY
REPRODUCTION IN PART OR AS A WHOLE
WITHOUT THE WRITTEN PERMISSION OF
<INSERT COMPANY NAME HERE> IS
PROHIBITED.

		UNLESS OTHERWISE SPECIFIED:		DRAWN T. CHRIS 2/1/15 CHECKED ENG APPR. MFG APPR.	NAME T. CHRIS DATE 2/1/15 Q.A. COMMENTS:		
		DIMENSIONS ARE IN MM TOLERANCES: FRACTIONAL ± ANGULAR: MACH ± BEND ± TWO PLACE DECIMAL ± THREE PLACE DECIMAL ±					
		INTERPRET GEOMETRIC TOLERANCING PER: MATERIAL Hexcel AS4C (3000 Filaments)					
CP004		NEXT ASSY	USED ON				
			APPLICATION		DO NOT SCALE DRAWING		

DELTRONIC SOLUTIONS

CARBON FIBER RODS

B	DWG. NO. CP007	REV
SCALE: 1:2	WEIGHT:	SHEET 1 OF 1

APPENDIX G: OPERATOR'S MANUAL

Instructions for Safe Operation of Delta 3D Printer

Before powering on:

- Check filament to ensure that it is engaged in the extruder. Use only tight diametral tolerance 3mm ABS filament with the settings provided in the guide.
 - Other types of filament are not supported at this time.
- Plug in both exhaust vent fans. Set rocker switches to full.
- Check ground connections between each servopack, power supply, the bottom frame plate, and the metal electronics enclosure with ohmmeter.
- Ensure power cables to ServoPacks are snug.
- Check that stop button is set to stop.
- Connect laptop via ethernet cable.
- CAUTION: Close door and ensure that lock is engaged. The door must remain closed and locked for the duration of the print. The motors may move quickly and unexpectedly enough to cause a pinch hazard.
- If the door lock power off control is disconnected, then the mechanical override must be left inside the enclosure during printing to ensure it is not accidentally opened during a print.

Before printing:

- Press the green Start button to provide power to the printer.
- Turn on ventilation fans. They will be audible when turned on.
- Turn on heated build plate. Set temperature to 120 degrees C. Wait at least 5 minutes for build plate to reach steady state temperature.
- Visually check that the power strip switches are set to on and the ground light is lit.
- Visually check that all electronics are powered. The PLC, ServoPacks, stepper motor driver and power sources all have lights indicating that they are on. Be aware of fault indications as on the stepper driver and ServoPacks. Refer to device manuals for troubleshooting.
- When the heater is powered, the fan on the extruder should be spinning.
- CAUTION: Do not touch the extruder tip or heated build plate to avoid burns. As stated in the before the print section, do not open the enclosure door while the device is printing. The build plate will remain hot for 30 minutes after it is turned off!
- CAUTION: Do not modify any parameters in the firmware if you are familiar with Motionworks IEC 3. After making any changes to the firmware, ALWAYS run test moves

on the virtual gantry before enabling the physical axes. This can result in damage to the printer!

- To enable the virtual axes, comment out the section of firmware code in the initialize block with axes 1, 2, and 3. Remove the commenting around the block for axes 89, 90, and 91.

To begin a print:

- Open Slic3r software. Select your CAD file to be printed. Set parameters as desired. Note: some parameters may be controlled by the MotionWorks software or manually, such as the heated build plate temperature.
- CAUTION: After making any changes to the firmware, save the project, rebuild it, then open up the project dialog box. Next, press download and wait for the bar to reach 100% to download the firmware to the PLC. Press stop, then warm to initialize the motors in warm start mode. Finally, press run to disengage the brakes.
- To manually set the positions for individual moves, use the movexyz command in a python file. Movexyz takes four arguments- the first is desired x position, then desired y position, then desired z position. The final argument for movexyz is s, the time to sleep or wait between starting one move and starting the next one.

During a print:

- CAUTION: Only operate while under the direct supervision of at least one person familiar with the operation of the device.
- Press the large stop button if anything appears about to crash, if an error occurs, or power is interrupted for any reason.
- Listen for the large exhaust fan sounds. If for any reason they shut down, ie due to overheating or clogging, press the big red button.
- If any unusual sounds occur, press the stop button.
 - If the start button did not turn the device off, unplug the internal power strip from the wall. Leave the exhaust fans powered on to ensure that any potentially harmful acrylonitrile fumes are filtered by the carbon filters.
- If any of the lights on the PLC, ServoPacks, stepper motor driver or power sources turns off, press the red button.

After a print:

- Let the python code finish running. Visually check that the servomotors return the carriages to the home position at the end of the code.

- Set the heated bed thermostat to 20 degrees C.
- Press the large red stop button.
- Do not turn off the exhaust fans for 30 minutes.
 - This ensures that the build plate will cool quickly enough to be safe to touch after this amount of time.
 - It also guarantees that all potentially harmful fumes will have been collected by the filter.
- Do not open the door for 30 minutes. This allows the build plate to cool slowly to 40C, perfect for ABS and safe for the user's hands. It also allows any remaining fumes to be captured by the stepper driver.